AN ABSTRACT OF THE THESIS OF

LEROY CRAWFORD LEWIS (Name) for the Ph. D. (Degree)

in CHEMISTRY (Major) presented on _____ (Date)

Title: AN INVESTIGATION OF THE CRYSTAL GROWTH OF HEAVY SULFIDES IN SUPERCRITICAL HYDROGEN SULFIDE

Abstract approved Redacted for privacy
Dr. William J. Fredericks

Solubility studies on the heavy metal sulfides in liquid hydrogen sulfide at room temperature were carried out using the isopiestic method. The results were compared with earlier work and with a theoretical result based on Raoult's Law. A relative order for the solubilities of sulfur and the sulfides of tin, lead, mercury, iron, zinc, antimony, arsenic, silver, and cadmium was determined and found to agree with the theoretical result.

Hydrogen sulfide is a strong enough oxidizing agent to oxidize stannous sulfide to stannic sulfide in neutral or basic solution (with triethylamine added). In basic solution antimony trisulfide is oxidized to antimony pentasulfide. In basic solution cadmium sulfide apparently forms a bisulfide complex in which three moles of bisulfide ion are bonded to one mole of cadmium sulfide.

Measurements were made extending the range over which the volumetric properties of hydrogen sulfide have been investigated to

220°C and 2000 atm. A virial expression in density was used to represent the data. Good agreement, over the entire range investigated, between the virial expressions, earlier work, and the theorem of corresponding states was found.

Electrical measurements were made on supercritical hydrogen sulfide over the density range of 10-24 moles per liter and at temperatures from the critical temperature to 220°C. Dielectric constant measurements were represented by a dielectric virial expression. Conductivity measurements were made on pure hydrogen sulfide and on solutions containing, respectively, stannic sulfide, lead sulfide, and triethylammonium chloride. The conductivity of the solutions of stannic sulfide and lead sulfide showed slight increases over the conductivity of the pure solvent. Triethylammonium chloride solutions exhibited a conductivity that was over a thousand times that of the pure hydrogen sulfide at the same density.

Virial coefficients derived from both compressibility data and dielectric constant measurements showed evidence of very little $(H_2S)_x$ polymer formation. Conductivity measurements indicate a very small solubility for the metal sulfides in hydrogen sulfide, which itself is very slightly ionized. Solutions of triethylammonium chloride are ionized extensively.

Crystal growth experiments were undertaken to demonstrate the feasibility of the solution growth of crystals of cadmium sulfide,

lead sulfide, silver sulfide, and stannic sulfide from pure supercritical hydrogen sulfide. It was shown that stannic sulfide, lead sulfide, and silver sulfide could be grown from these solutions. Growth rates were extremely slow.

An Investigation of the Crystal Growth of the Heavy Metal Sulfides in Supercritical Hydrogen Sulfide

by

Leroy Crawford Lewis

A THESIS

submitted to

Oregon State University

in partial fulfillment of
the requirements for the
degree of

Doctor of Philosophy

June 1968

APPROVED:

Redacted for privacy

Professor of Chemistry
in charge of major

Redacted for privacy

Chairman of Department of Chemistry

Redacted for privacy

Dean of Graduate School

Date thesis is presented January 29, 1968

Typed by Marion F. Palmateer for Leroy Crawford Lewis

ACKNOWLEDGMENTS

The author wishes to express his sincere thanks to Dr. William J. Fredericks for the numerous suggestions, the valuable criticisms, and the discussions during the course of this investigation.

Material support from the Air Force Office of Scientific Research and National Defense Education Act is gratefully acknowledged.

To the graduate students in chemistry, I am particularly indebted for the short term loan of equipment, advice, and suggestions offered by them at some time or another during my stay at Oregon State University.

I wish to thank Dr. K. W. Hedberg, Dr. B. D. Sharma, Dr. T. H. Norris, and Dr. J. T. Yoke for the valuable discussions on some of the phases of this investigation.

Especial thanks are due to Mr. C. D. Woods whose help in converting an idea into practical reality was invaluable.

To Mr. J. C. Looney I am indebted for the use of equipment in his laboratory and to Mr. W. Johnson for his help in stopping the leak in the electrode vessel.

During the course of an investigation of this type, a large number of people contribute to the successful completion of a project. To these people go my sincere thanks for their seemingly small, but significant, contribution.

Finally, I wish to express my heartfelt thanks to my wife, Catherine, for her encouragement and aid throughout this investigation.

DEDICATION

To my father,

Lester L. Lewis

TABLE OF CONTENTS

LIST OF FIGURES

LIST OF TABLES

I. GENERAL INTRODUCTION

The properties of crystals have fascinated man since he became cognizant of the physical world about him. This fascination has led to the discovery and exploitation of many of the interesting and useful properties of crystals.

A consequence of this demand for crystals has led to the development of many different techniques for the production of crystals. One of the oldest techniques used is the growth of crystals from a supersaturated solution. Commonly, when this method is used, the growth vessel is placed in a thermal gradient such that the region containing the nutrient material is at the higher temperature. A convection current carries the saturated solution into a cooler region of the vessel where it deposits on seed crystals.

During the Second World War, the needs of the military for quartz oscillator plates led to the development of a method that could be used for the growth of crystals of difficultly soluble materials that could not be grown by other methods. The increase in solubility due to increased temperature permitted the growth of these crystals. It was necessary, however, to increase the temperature far above the normal liquid range of the solvent. This necessitated the use of apparatus capable of containing the pressures needed to maintain the system at a density sufficient to permit a reasonably fast rate of

crystal growth to take place. Thus, using these high temperature-high pressure systems, both sides made significant progress during the war toward demonstrating the feasibility of quartz crystal growth under conditions that were both practical and economical.

The growth of crystals of difficultly soluble materials from supercritical solutions occurs widely in nature. Hydrothermal deposits of quartz and other pegmatite minerals attesting to this fact are found scattered throughout the world. These deposits were formed under conditions of high temperature and high pressure that are readily attainable under the proper geologic conditions.

Since the growth of crystals from supercritical solutions is geologically important, much of the Pre-World War II work was done to demonstrate that supercritical solutions were capable of dissolving sufficient quantities of a mineral such as quartz, which could then be redeposited in the form in which it is ultimately found in the earth's crust.

After the feasibility of growing crystals by this technique was demonstrated, much work was done to elucidate the system made up of the various phases of silica in either neutral or basic aqueous solutions. However, other work that met with some success was aimed at producing crystals of the heavy metal oxides from supercritical aqueous solutions.

The heavy metal sulfide crystals, as they are usually produced,

are non-stoichiometric. At the very high temperatures required to produce melt-grown crystals, one or the other of the elements present in the compound vaporizes leaving the melt rich in the other element. Thus, one further advantage in using a high pressure system is that the temperatures required are low enough that the stoichiometry of the compound is not affected to the extent that it would be at the temperatures required for melt-grown crystals. For solid state studies of these compounds, crystals that are as nearly perfect as possible are desirable.

The heavy metal sulfides are the sulfur analogs of the heavy metal oxides. To examine crystal growth processes for the heavy metal sulfides under analogous conditions for which success in growing heavy metal oxides was attained, it is desirable to use the analogous solvent, hydrogen sulfide. Hydrogen sulfide as a solvent has been given only a cursory examination. Thus, while the chemistry of substances in liquid hydrogen sulfide is relatively unexplored, the chemistry of high density hydrogen sulfide at high temperatures and high pressures is almost totally unknown.

The purpose of this investigation is twofold. Studies on pure hydrogen sulfide were extended into temperature and pressure regions not previously examined and the solution chemistry of the heavy metal sulfides dissolved in hydrogen sulfide both in the subcritical state and the supercritical state was examined.

The successes met with aqueous supercritical crystal growth systems and the known ability of gases in the supercritical state to dissolve and transport solids led to experiments on the solution crystal growth of the difficultly soluble heavy metal sulfides in high density, supercritical hydrogen sulfide.

As in all work in which a new field is explored, a large proportion of the investigation was devoted to laying the basic ground work. Since very little is known regarding the chemistry of liquid hydrogen sulfide solutions, methods had to be developed to observe the effects of liquid hydrogen sulfide on the various structural materials used in the apparatus and on the behavior of the inorganic compounds under investigation. In the ensuing sections, various aspects of the inorganic and physical chemistry of the solutions of liquid hydrogen sulfide in both sealed glass tubes at room temperature and in high pressure, stainless steel reactors at temperatures above the critical point of hydrogen sulfide are discussed.

II. PRELIMINARY EXPERIMENTS

Liquid hydrogen sulfide is relatively unexplored as a solvent. Experimentation done in the earlier part of this century, particularly by the members of Wilkinson's (102) research group at Iowa State College, indicated that liquid hydrogen sulfide is a poor solvent for inorganic materials and only a slightly better solvent for ogranic compounds. There has been little interest in hydrogen sulfide as a solvent because of its lack of useful properties under the low temperature conditions that were used during the earlier experiments.

The behavior of hydrogen sulfide toward some of the more recently developed materials that are convenient for the construction of apparatus of the type required during this investigation was unknown. For this reason some experiments at room temperature were designed to eliminate any materials that would react with the hydrogen sulfide and to ascertain that all of the salts of interest in this investigation would not behave in an unexpected manner.

Tantalum, according to Wortley (104), owes its extremely corrosion resistant properties to a very adherent and stable oxide film that protects the metal in both oxidizing and reducing conditions. Free sulfur trioxide and hydrofluoric acid attack the metal at room temperature and hot caustic alkalis dissolve the slightly acidic oxide film which leaves the metal unprotected. According to Hampel (40)

tantalum reacts with sulfur and hydrogen sulfide at red heat. Farber and Ehrenburg (32) quantitatively measured the corrosion rate of tantalum in the presence of hydrogen sulfide in the neighborhood of 1000° K, and found that tantalum is very resistant to corrosion in a reducing atmosphere but much less resistant in an oxidizing atmosphere.

In order to check the behavior of tantalum in liquid hydrogen sulfide, "test tube-like" ampoules were prepared from heavy-wall capillary tubing ten millimeters in outside diameter, three millimeters in inside diameter, and 20 cm in length. Each tube contained a weighed piece of tantalum and was partially filled with liquid hydrogen sulfide or with a mixture of hydrogen sulfide and triethylamine.

A small vacuum line was used to provide a pure, dry gas sample for these experiments. The hydrogen sulfide was filtered through a column of Fiberglas and then successively condensed into two U-tubes with liquid nitrogen. From the U-tubes it passed into the manifold where three sample tubes could be filled at the same time. The evacuated tubes were filled, at liquid nitrogen temperature, with enough hydrogen sulfide to provide a liquid phase at room temperature. Any hydrogen sulfide left in the line was pumped into one of the cold traps then, while still frozen in liquid nitrogen, the sample tube was sealed off and carefully annealed with a torch.

The vacuum line is shown in Figure 2. 1. It was used to fill all

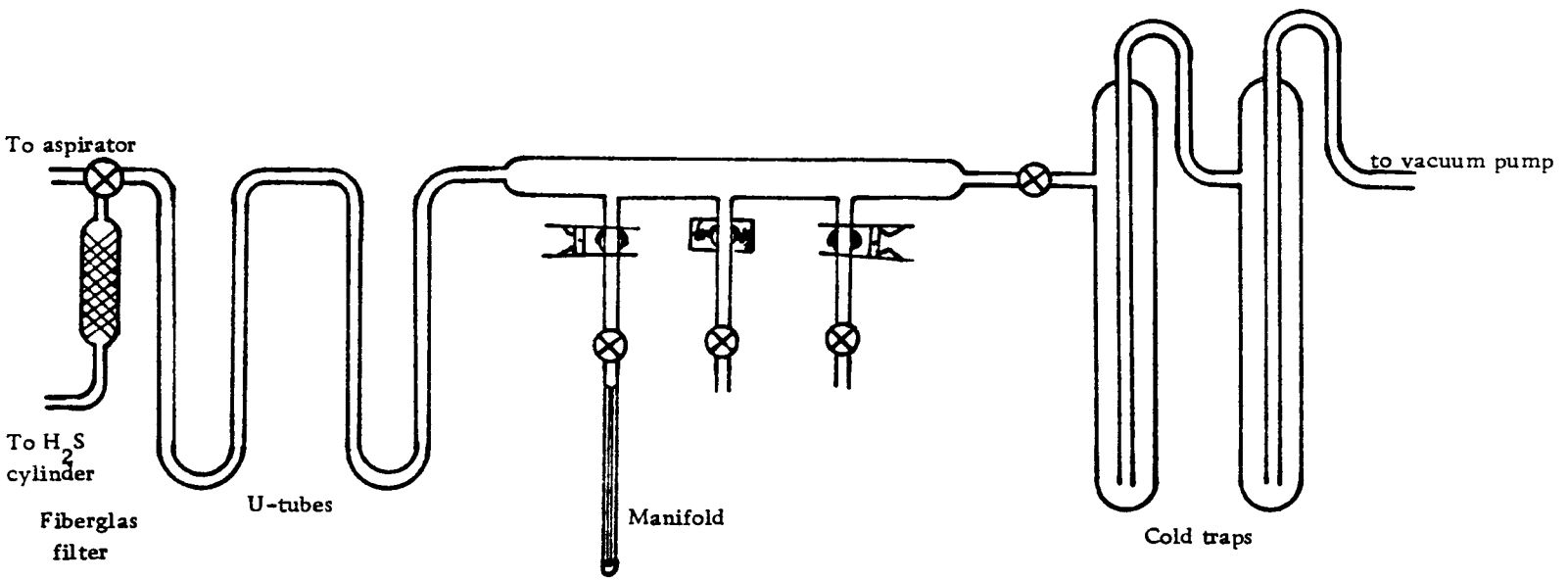

Figure 2. 1. Vacuum system used for the purification of hydrogen sulfide and for filling the "test-tubes" and the "H-tubes".

of the tubes for the preliminary experiments and most of the tubes used during the solubility experiments. The rest of the tubes used during the solubility experiments were filled on the stainless steel system used to fill the high pressure vessels.

All of the tubes were left undisturbed for a week before being opened and the tantalum examined for any pitting, loss of luster, or other change in its physical appearance. Reweighing the piece of tantalum checked for a possible weight loss due to dissolution.

Using the criteria listed above, there was no apparent corrosion of the tantalum due to either the pure hydrogen sulfide or the basic triethylamine-hydrogen sulfide mixture at room temperature.

Teflon, 316 stainless steel, and 304 stainless steel were examined in the triethylamine-hydrogen sulfide solutions. None of these materials showed any evidence of attack by the basic solutions.

The second phase of these preliminary experiments involved investigating the stabilities of the heavy metal sulfides in pure, liquid hydrogen sulfide and in the basic triethylamine-hydrogen sulfide mixtures. "Test-tube" experiments were set up with cadmium sulfide, stannous sulfide, silver sulfide, antimony trisulfide, lead sulfide, zinc sulfide, and manganous chloride. All of these salts were reagent grade salts except for the zinc sulfide and cadmium sulfide used in the experiments with the triethylamine-hydrogen sulfide mixture. In these two experiments, General Electric electronic

grade salts were used.

Oven drying of the salts and the tubes at 110°C preceded the deposition of the salt in the bottom of the tubes. Approximately ten milligrams of salt was used in each experiment. After the tubes were sealed to the vacuum system, they were held under vacuum for at least 12 hours before filling.

In the presence of pure hydrogen sulfide, only one of the salts underwent any noticeable change. Stannous sulfide undergoes a complete conversion from the dark brown stannous sulfide to the light gold colored salt of stannic sulfide according to the reaction

$$SnS + H_2S \longrightarrow H_2 + SnS_2. \qquad (2.1)$$

Verification that the product formed was stannic sulfide was made by comparing an X-ray powder diffraction pattern of the product with the published pattern in the A. S. T. M. card file (card number 1-1010). There was agreement between 18 of the 21 lines published.

In a Dry Ice-acetone bath the reaction between the stannous sulfide and hydrogen sulfide took more than one day to go to completion. At room temperature the rate of the reaction was limited by the rate at which the solvent could diffuse into the salt.

Quam (74) who investigated a large number of substances in the presence of liquid hydrogen sulfide, noted a reaction between stannous chloride and liquid hydrogen sulfide in which stannous chloride was

"reactive and soluble". Later, Ralston and Wilkinson (77) noted the formation of a small amount of stannic sulfide after allowing stannic chloride to remain in contact with liquid hydrogen sulfide at room temperature for a period of two weeks.

A much more reactive system results when a small quantity of triethylamine is added to the hydrogen sulfide to make a basic solution of liquid hydrogen sulfide. According to Cady and Elsey's (22) solvent systems concept of acid-base theory, hydrogen sulfide dissociates in the following manner:

$$H_2S + H_2S \rightleftharpoons H_3S^+ + SH^-. \qquad (2.2)$$

Any chemical that is capable of producing the hydrosulfide ion, SH^-, in liquid hydrogen sulfide is designated a base in that solvent. Hydrogen sulfide reacts with triethylamine to form the tertiary ammonium hydrosulfide in the following manner:

$$H_2S + (C_2H_5)_3N \longrightarrow [(C_2H_5)_3NH]^+SH^-, \qquad (2.3)$$

which can then dissociate into the tertiary ammonium ion and the hydrosulfide ion

$$[(C_2H_5)_3NH]^+SH^- \rightleftharpoons (C_2H_5)_3NH^+ + SH^-. \qquad (2.4)$$

Triethylammonium hydrosulfide was prepared and examined by Achterhof, Conaway, and Boord (1) during their study of the thiolysis

of the simple amines. The extent of the ionization of this compound in liquid hydrogen sulfide, as indicated by equation 2. 4, is not known.

A definite increase in the solubility of various salts in a mixture of triethylamine and hydrogen sulfide was noted by Smith (88).

The same type of "test-tube" experiments were used to investigate the behavior of the heavy metal sulfides in the presence of a mixture of liquid hydrogen sulfide and triethylamine. Pure triethylamine was obtained from reagent grade triethylamine by distillation under vacuum in which the middle third of the distillate was retained.

Pre-drying of the tubes and salts was carried out as described earlier. Addition of the triethylamine took place just prior to filling with hydrogen sulfide. The tube was removed from the vacuum line and a small quantity of triethylamine from a medicine dropper was placed on top of the salt. After replacing the tube on the vacuum manifold, it was frozen with liquid nitrogen, evacuated, then filled with hydrogen sulfide and sealed off.

Table 2. 1 gives the results of the interactions of the heavy metal sulfides with the triethylamine-hydrogen sulfide mixture. A blank in which only triethylamine and hydrogen sulfide were present is also shown.

Table 2. 1. Reaction of triethylamine-hydrogen sulfide with various sulfides.

Material	Reaction	Solubility	Color of Solution	Clarity
CdS	yes	very soluble	yellow green	clear
Ag_2S	possibly	partially soluble	yellow green	clear
Sb_2S_3	yes	orange solid not soluble	brown-black	opaque
PbS	possibly	partially soluble	black	opaque
SnS	yes	product partially soluble	yellow green	clear
ZnS	possibly	partially soluble	yellow green	clear
blank	--	--	yellow green	clear

Several of the tubes, particularly those in which there was a larger ratio of triethylamine to hydrogen sulfide relative to the other tubes, produced needle-like, colorless crystals. The melting point of the crystals was determined by slowly warming the sealed, heavy-wall capillary tube containing the crystals in a well-stirred water bath. These crystals were in equilibrium with the liquid in which they were formed. A sharp melting point of 36°C was obtained with four different samples. A two phase system consisting of a colorless liquid on top of the more viscous green liquid was formed at the melting point. As the temperature was increased, the

fraction of colorless liquid in the tube decreased as it dissolved in the green liquid.

Attempts in this laboratory to measure the melting point in an open tube at atmospheric pressure failed because of the rapid decomposition of the crystals. Achterhof, Conaway, and Boord (1) were able to obtain an open tube melting point of 27°C for the triethylammonium sulfide. They note that extensive and rapid decomposition of the compound took place during this measurement. A closed tube melting point was not listed for this compound. For other amine-hydrogen sulfide reaction products that they studied, and for which they listed both sealed tube and open tube melting point determinations, the melting point in the sealed tube was always higher than that in the open tube.

The stability of triethylammonium sulfide is dependent upon the maintenance of a protective atmosphere above the crystals. Achterhof, Conaway, and Boord (1) note that oxygen or water decomposes the compound.

Cadmium sulfide completely dissolves under the right conditions in the triethylamine-hydrogen sulfide mixtures. The possible utilization of this property of the triethylamine-hydrogen sulfide mixed solvent for the growth of cadmium sulfide crystals led to a more intensive study of the triethylamine-hydrogen sulfide-cadmium sulfide system.

The nature of the compound formed in the triethylamine-hydrogen sulfide-cadmium sulfide system was examined. The assumption behind this series of experiments was that any cadmium sulfide that was not complexed would also be insoluble.

"Test-tubes" were prepared with the stoichiometric ratios of triethylamine to cadmium sulfide of 6:1, 5:1, 4:1, 3:1, and 2:1. After the cadmium sulfide was weighed into the tubes, a stopcock and ball joint combination was sealed onto each tube. Triethylamine was quantitatively measured into the tubes from a 0. 25 cc medical syringe. A long funnel, that passed through the stopcock, permitted the deposition of the triethylamine on top of the salt.

The tubes were attached to the vacuum system manifold, frozen with liquid nitrogen, and then evacuated. Hydrogen sulfide, purified as described earlier, was condensed into the tubes with liquid nitrogen. While still frozen, the tubes were sealed off under a vacuum. A blank tube containing only triethylamine and cadmium sulfide was also prepared.

After filling, the tubes were taped to a turntable which slowly rotated the tubes in a vertical plane producing a stirring action.

In all of the tubes having stoichiometric ratios of triethylamine to cadmium sulfide greater than or equal to three to one, the salt completely dissolved. However, in the tubes having a ratio of two to one, there remained a visible quantity of salt in the bottom of

the tube.

The most likely formulation for this compound is one in which bisulfide ions form three of the ligands on the cadmium atom. Conductivity measurements of triethylamine solutions indicate that the bisulfide ion is present in high concentrations. The bisulfide ion reacts with the cadmium sulfide forming a compound of the form

$$[(C_2H_5)_3NH^+]_3 \left[\begin{array}{c} SH \\ | \\ SH - Cd - S \\ | \\ SH \end{array} \right]^{=} .$$

This formulation accounts for the solubility of all of the tubes having molar ratios of three to one.

There is a definite visible reaction taking place when the hydrogen sulfide and triethylamine interact at the surface of the salt. In this region, a visible turbulence coupled with a change in the refractive index of the liquid as the two solvents mix with the cadmium sulfide is observed. During this process, the cadmium sulfide breaks up into very finely divided free-flowing particles as compared with the large lumps that are present in the pure hydrogen sulfide or in the pure triethylamine blanks.

The contents of these tubes have low melting points. Three tubes were held in an n-pentane slush at -154° C without solidifying. All of the tubes solidified when immersed in liquid nitrogen. An

attempt to isolate crystals of the compound by pouring off the supernatant liquid failed because of the viscosity of the supernatant liquid.

A complex compound of divalent cadmium with triethylamine in liquid hydrogen sulfide definitely exists. A melting point below -154° C is too far below the melting point of triethylamine (-115° C) or hydrogen sulfide (-83° C) to be attributed to freezing point depression due to dissolved species. Because the predominant coordination number of cadmium is four in the complexes of cadmium that are known, and because the coordination number of cadmium in the cadmium-ammonia complex is four, it is probable that the coordination number of cadmium in the cadmium-triethylamine complex is also four. The exact stoichiometry of the complex is unknown, however.

Stannous sulfide and antimony trisulfide are both oxidized to the sulfides of the higher valence state. The stannous sulfide reaction proceeds much more slowly in the solution containing triethylamine than in the pure hydrogen sulfide. Antimony trisulfide, however, does not undergo a similar reaction in pure hydrogen sulfide.

The silver sulfide tubes produced unexpected results. Silver sulfide was placed in the tubes as a finely divided, dull gray solid. In a week's time, small, black crystals had replaced the original salt. When the tubes were opened and the hydrogen sulfide released, there was an immediate precipitation of finely divided silver sulfide

indicating that a significant fraction of the silver sulfide originally present had gone into solution.

An X-ray powder diffraction photograph of the larger crystals matched perfectly with a photo taken earlier of the original salt and corresponded to 30 of the first 33 lines published in the A. S. T. M. card file (card number 14-72) for silver sulfide.

III. SOLUBILITY STUDIES

Introduction

Due to the small amount of information available regarding the solutions formed by the heavy metal sulfides in liquid hydrogen sulfide, a portion of this investigation was devoted to elucidating some of the properties of hydrogen sulfide as a solvent. The literature generally classes the compounds, for which the solubility in liquid hydrogen sulfide has been investigated, as either soluble or insoluble. Seldom has anyone attempted to estimate an absolute solubility or even a relative solubility for any of these heavy metal sulfides in liquid hydrogen sulfide.

In order to evaluate the various heavy metal sulfides, with respect to their potentialities as crystal growth nutrients, a method was developed from which the relative solubilities of two different solutes could be compared. The difficulties encountered in working with solvents that have a boiling point considerably below room temperature severely limits the methods that can be used for determining solubility. A method that is readily adaptable to use in a sealed, pressure containing system is the isopiestic method for the determination of solubilities. The method, based on Raoult's Law, depends upon the formation of two solutions that are at the same vapor

pressure. If tubes are constructed that maintain two separate solutions at the same vapor pressure and at the same temperature--such that one of the solutes is common to all of the tubes and the other solute is different for each tube, then the relative solubilities of all of the salts, with respect to the one salt common to each tube, can be determined. By systematically carrying out this process with a different "common" salt, a series of salts going from the most soluble to the least soluble in that particular solvent can be developed.

Theoretical

If two non-volatile solutes A and B form solutions 1 and 2 respectively, with the same volatile solvent, then the vapor pressure P above each solution will be given by Raoult's Law when the solution is ideal or when it is extremely dilute.

$$P_1 = P^o X_{1\ \text{solvent}} = P^o[1 - X_A(1)]$$
$$P_2 = P^o X_{2\ \text{solvent}} = P^o[1 - X_B(2)] \qquad (3.1)$$

where P^o is the vapor pressure of the pure solvent, $X_{1\ \text{solvent}}$ and $X_{2\ \text{solvent}}$ is the mole fraction of the solvent in solutions 1 and 2, $X_A(1)$ is the mole fraction of solute A in solution 1, and $X_B(2)$ is the mole fraction of solute B in solution 2.

If the solutions are arranged in a vessel that separates the

solutions but allows the vapor above the solutions to be common to both solutions, P_1 must equal P_2 and

$$\frac{P_1}{P^o} = \frac{P_2}{P^o} = 1 - X_A(1) = 1 - X_B(2). \qquad (3.2)$$

Thus, when the system has equilibrated

$$X_A(1) = X_B(2). \qquad (3.3)$$

This may be expressed conveniently as

$$\frac{g_s(2)}{g_s(1)} = \frac{g_B \cdot M_A}{g_A \cdot M_B} \quad , \qquad (3.4)$$

where $g_s(1)$, $g_s(2)$, g_A, and g_B represent the weights of solvent in solution 1 and 2, of solute A in solution 1 and solute B in solution 2 respectively. M_A and M_B are the molecular weight of the two solutes.

If the two solutions are contained in tubes of equal and uniform bore connected such that the vapor above each solution is common to both, then solvent will transfer through the vapor until $X_A(1) = X_B(2)$. A convenient measure of X_A and X_B is the amount of solution in the respective tubes.

If the solutions are dilute, the partial molar volume of the solute will be small and the densities of the two solutions and the

pure solvent will be very nearly equal,

$$\rho_{\text{solvent}} \cong \rho_{\text{solution}}(1) \cong \rho_{\text{solution}}(2).$$

Then

$$\begin{aligned} g_s(1) &= \rho_{\text{solvent}}\, \pi r^2 h(1) \\ g_s(2) &= \rho_{\text{solvent}}\, \pi r^2 h(2), \end{aligned} \tag{3.5}$$

where r is the radius of the solution tube and h is the height of the solution in the tube. Thus, a convenient measure of the relative concentrations of salt in each solution is

$$\frac{g_s(1)}{g_s(2)} = \frac{h(1)}{h(2)} = \frac{g_A/M_A}{g_B/M_B} \ . \tag{3.6}$$

The relative amount of vapor pressure lowering can be estimated if the foregoing assumptions are correct. Consider the reaction

$$A_{(\text{solid})} \rightleftharpoons A_{(\text{dissolved in saturated solution})},$$

then

$$f_A^i(s) = X_A^i f_A^i(l) \tag{3.7}$$

where f_A^i is the fugacity of pure component A in the designated state (solid or liquid) at the same temperature for both states and X_A^i is the mole fraction of component A in solution i.

Rewriting equation 3.7 using natural logarithms and then taking

the partial derivative of the resulting equation with respect to temperature with pressure held constant yields

$$\left(\frac{\partial \ln f_A^i(s)}{\partial T}\right)_P = \left(\frac{\partial \ln f_A^i(l)}{\partial T}\right)_P + \left(\frac{\partial \ln X_A}{\partial T}\right)_P . \tag{3.8}$$

By definition

$$\bar{G} = \bar{G}^o + RT \ln f \tag{3.9}$$

where $\bar{G}$ is the partial molar free energy, $\bar{G}^o$ is the standard free energy, and f is the fugacity.

Utilizing the Gibbs-Helmholtz equation in the form

$$\left(\frac{\partial \bar{G}/T}{\partial T}\right)_P = \frac{-\bar{H}}{T^2} \tag{3.10}$$

where $\bar{H}$ is the partial molar enthalpy, it is possible to calculate the temperature coefficient of the fugacity in the following manner.

Dividing equation 3.9 by T and then taking the partial derivative with respect to temperature at constant pressure, the result is

$$\frac{1}{R}\left[\left(\frac{\partial \bar{G}/T}{\partial T}\right)_P - \left(\frac{\partial \bar{G}^o/T}{\partial T}\right)_P\right] = \left(\frac{\partial \ln f}{\partial T}\right)_P . \tag{3.11}$$

With equation 3.10 the temperature coefficient of the fugacity in equation 3.11 can be expressed as a function of enthalpy

$$\left(\frac{\partial \ln f}{\partial T}\right)_P = \frac{1}{R}\left[\frac{-\bar{H}}{T^2} + \frac{\bar{H}^o}{T^2}\right] = \frac{-\bar{H} + \bar{H}^o}{RT^2} . \tag{3.12}$$

Therefore, from equation 3.8

$$\left(\frac{\partial \ln f_A^i(s)}{\partial T}\right)_P - \left(\frac{\partial \ln f_A^i(l)}{\partial T}\right)_P = \frac{-\bar{H}_A^i(s) + \bar{H}_A^o}{RT^2} - \frac{-\bar{H}_A^i(l) + \bar{H}_A^o}{RT^2} \tag{3.13}$$

and

$$\left(\frac{\partial \ln X_A}{\partial T}\right)_P = \left(\frac{\partial \ln f_A^i(s)}{\partial T}\right)_P - \left(\frac{\partial \ln f_A^i(l)}{\partial T}\right)_P = \frac{\bar{H}_A^i(l) - \bar{H}_A^i(s)}{RT^2}.$$

The expression $\bar{H}_A(l) - \bar{H}_A(s)$ can be equated to the heat of fusion, ΔH_f, for the process $A_{(s)} \rightarrow A_{(l)}$.

If equation 3.13 is integrated over the temperature limits from $T = T_{ambient}$ to $T = T_{melt}$ and over the mole fraction limits from $X_A = X_A$ to $X_A = 1$, under the assumption that the heat of fusion is constant over the range of integration, then the result is

$$\ln X_A = \frac{\Delta H_f}{R}\left(\frac{1}{T_m} - \frac{1}{T}\right). \tag{3.14}$$

From equation 3.6 it is obvious that the height of the liquid column is directly proportional to the number of moles of solute that go into solution. It is a good approximation, at low concentrations, to say that the number of moles of solute in solution is proportional to the molarity of the solution and, under the same assumption, that the molarity is proportional to the mole fraction of solute dissolved in the solution.

Utilizing equation 3.14 and the data contained in Table 3.1, one

can calculate a series of numbers to determine the order of magnitude of the effect to be observed, as well as to specify an order of solubility for a series of salts.

Table 3. 1. Theoretical order of solubilities in H_2S.

Salt[a]	Temperature of fusion	Heat of fusion Kcal/mole	ln X_A
ZnS	1918° K (47)	9. 10 (47)	-12. 73
Sb_2S_3	819° K (47)	5. 60 (47)	- 5. 86
PbS	1387° K (47)	4. 20 (47)	- 5. 45
SnS[b]	1153° K (48)	7. 55 (48)	- 9. 24
Ag_2S	1115° K (47)	3. 36 (47)	- 4. 06
FeS	1468° K (47)	5. 50 (47)	- 6. 58
S (monoclinic)	392° K (48)	0. 335 (48)	- 0. 13

[a]There is no data available for cadmium sulfide, stannic sulfide, mercuric sulfide, or arsenic sulfide.

[b]Stannous sulfide is unstable in liquid hydrogen sulfide.

The order of solubility as calculated is

$$S > Ag_2S > PbS > Sb_2S_3 > FeS > SnS > ZnS.$$

A number proportional to the relative order of magnitude of the ratio of the heights of the liquid in the arms of the tube can be calculated by subtracting the value of ln X_A from the value of ln X_B and then taking the anti-logarithm.

Equation 3. 14 provides a convenient means of examining the temperature dependence of the solubility of any compound in a solvent

for which Raoult's Law is applicable. In an isopiestic experiment, in which two solutions are coupled through the vapor phase, a temperature can be calculated for which the solubility of component A is identical to that of component B. This condition is met, in terms of Raoult's Law, when

$$X_A = X_B \tag{3.15}$$

or, from equation 3.14,

$$\left(\frac{\Delta H_f(A)}{R}\right)\left(\frac{1}{T_m(A)} - \frac{1}{T}\right) = \left(\frac{\Delta H_f(B)}{R}\right)\left(\frac{1}{T_m(B)} - \frac{1}{T}\right). \tag{3.16}$$

Solving this expression for the temperature at which the solubilities of the two components are equal yields the "cross-over" temperature

$$T = \frac{\dfrac{\Delta H_f(A)}{\Delta H_f(B)} - 1}{\left(\dfrac{\Delta H_f(A)}{\Delta H_f(B)}\right)\left(\dfrac{1}{T_m(A)}\right) - \dfrac{1}{T_m(B)}}. \tag{3.17}$$

The value of the "cross-over" temperature for adjacent salt couples in the calculated solubility series is tabulated in Table 3.2.

Table 3. 2. "Cross-over" temperatures for adjacent salt couples in the calculated solubility series.

Couple	Temperature °K
PbS - Ag_2S	5.8×10^4
PbS - Sb_2S_3	3.67×10^2
FeS - Sb_2S_3	1.75×10^2
FeS - ZnS	3.1×10^3
S mono - Ag_2S	1.4×10^2

Sheffer (85, p. 41) points out that the use of the isopiestic method for the measurement of solubilities is capable of producing very accurate results. He also makes the statement: "The contents of the dishes are equilibrated to equal vapor pressure at which time the first dish contains a saturated solution in equilibrium with excess solute and the second dish must now also contain a saturated solution (with no excess solute present). . . ". However, it is shown that only one of the solutions can be saturated and that the other must be unsaturated.

Let S_A be the number of moles of A that will saturate one mole of solvent and S_B be the number of moles of B that will saturate one mole of solvent at a designated temperature. Then nS_A and $n'S_B$ are the number of moles of solute that will saturate n and n' moles of solvent, respectively. Thus, the mole fractions of the saturated solutions can be written as

$$X_A = \frac{nS_A}{nS_A + n} = \frac{S_A}{1 + S_A}$$

$$X_B = \frac{n'S_B}{n'S_B + n'} = \frac{S_B}{1 + S_B} \quad . \tag{3.18}$$

From equation 3. 3 it is seen that at equilibrium the mole fraction of A must be equal to the mole fraction of B. Therefore, if both A and B are saturated at the same temperature, then the two expressions in equation 3. 18 are equal and

$$S_A = S_B. \tag{3.19}$$

Equation 3. 19 implies that in any solvent at a given temperature exactly S_A moles of any salt will saturate one mole of solvent. Obviously an erroneous assumption was made in deriving equation 3. 19. However, the only assumption made was that both solutions had to be saturated. This implies that only one of the solutions can be saturated while the other solution cannot be saturated.

Experimental

The metallic sulfides are so sparingly soluble and the amount of solvent available is so limited, that one cannot prepare an unsaturated solution of a metal sulfide in liquid hydrogen sulfide with any confidence in the value of the concentration. However, the

sulfides are soluble to a slight extent as indicated by the presence of faint "rings" on the walls of the tube when the solvent is distilled from one arm of the tube to the other.

Although the solutions were always prepared in the presence of a large excess of the solid salt, it is possible to use these "H-tubes" to extract qualitative data from this type of experiment. The more soluble of the two salts will tend to decrease its concentration, at the expense of the solvent from the other solution, until the condition expressed by equation 3. 3 is met. By putting together various combinations of the salts, a "solubility series" can be developed that should correspond to the calculated series if Raoult's Law holds for this system.

In order to provide a system that is maintained at a constant vapor pressure throughout, an H-shaped tube was used for the determination of the solubilities of the heavy metal sulfides in liquid hydrogen sulfide. A tube having this shape is capable of maintaining two separate solutions that are in contact only through the vapor phase while under pressures greater than one atmosphere.

Consistent results were obtained from "H-tubes" prepared from thick-walled Pyrex capillary tubing having an outside diameter of 10 mm and an inside diameter of 3 mm. Figure 3. 1 shows the construction of these "H-tubes".

Two styles of "H-tubes" were used in these experiments. In

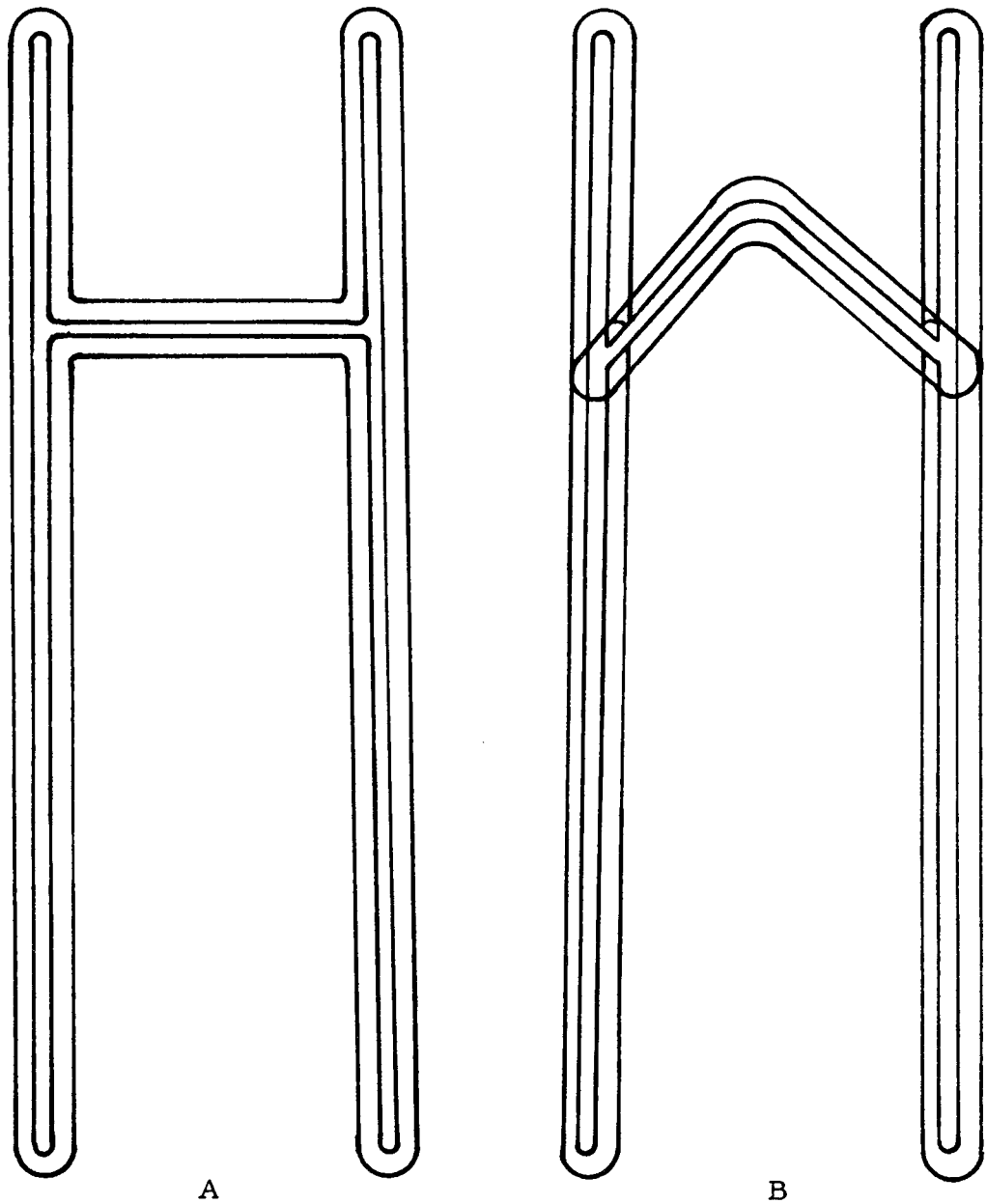

Figure 3. 1. H-tubes. A) regular straight H-tube. B) H-tube designed for rotation on the turntable.

the first style, two pieces of tubing eight inches in length were connected three-fourths of the way along their length by a piece of tubing two inches long which contained a small wad of Fiberglas. These tubes, shown in Figure 3. 1A, were mounted vertically in a water bath and allowed to come to equilibrium.

After it became apparent that long periods of time would be required for the tubes to come to equilibrium and that small variations in temperature would not affect the results, a second style of tube was designed to permit the solutions to be stirred.

When a tube is rotated in the plane 45° to the horizontal, good stirring action is obtained as the liquid flows from one end of the tube to the other. This required certain modifications to the "H-tubes" in order to prevent the two solutions from mixing, as they would if the first model "H-tube" were used. The modifications consisted of doubling the length of the cross-bar and bending it in the middle at a 60° angle. The bent cross-bar was then sealed onto the parallel side tubes at a point three-fourths of the way along the length of the side tubes and at right angles to them. These tubes are shown in Figure 3. 1B.

The first series of experiments using the modified "H-tubes" indicated there were still problems associated with their use that had not been anticipated through previous experiments. Liquid, flowing past the opening to the cross-bar as the tube was being

rotated, would be drawn up into the cross-bar by capillary action and held there by surface tension. Eventually so much liquid would accumulate that it would spill over into the other arm.

Capillary action came about because the opening to the cross-bar was constricted either physically when the cross-bar was sealed onto the side tube or by the wad of Fiberglas put into the tube to keep the salts from mixing when the tube was evacuated on the vacuum system. The first problem was alleviated by carefully enlarging the opening into the cross-bar. Removing the Fiberglas filter took care of the second cause of mixing of the solutions in the side tubes. Evacuating the tubes in small increments eliminated the problem caused by the movement of salt when air trapped in the powder is released. This was done by pumping out the upper part of the manifold with the vacuum pump, closing off the valve to the vacuum pump, and then slowly opening the valve to the "H-tube". Continued repetition of this operation, until the pressure in the manifold and that in the "H-tube" were equal, prevented any visible transfer of salt.

All of the tubes were handled in the same manner. Salt was deposited in the tube by a long, thin funnel that extended into the tube below the opening to the cross-bar. After placing a small quantity of salt in each arm of the "H-tube", one arm was sealed off and the other arm was sealed to a stopcock fitted with a ball of a ball-and-socket joint. Careful evacuation of the tubes was followed by filling

with hydrogen sulfide while the tube was immersed in a Dry Ice-acetone cold bath. The stopcock was closed and the contents were frozen with liquid nitrogen during the final sealing off and annealing. Partially thawing the tube in a Dry Ice-acetone cold bath prevented the violent bubbling and consequent mixing of the solutions that takes place when the tube is allowed to warm to room temperature from liquid nitrogen temperature.

The first style of "H-tube" was set into a water bath built from an aquarium and held undisturbed at 30°C for long periods of time. The transparent sides of the aquarium allowed observation without having to disturb the tube. Attainment of equilibrium took a long time due to the slowness of the processes of diffusion and dissolution. Some of the tubes were held undisturbed for over a year before the quasi-equilibrium state, in which all of the solvent is condensed in one of the side tubes, was attained.

The second style of "H-tube" was taped, with masking tape, to the inclined turntable and rotated at a rate of six revolutions per minute. All experiments with this style "H-tube" were performed at room temperature behind a Lucite barricade.

One of the major difficulties inherent with the "H-tube" experiments is the failure of the sealed tube due to the vapor pressure of hydrogen sulfide (about 20 atm at room temperature). When failure of a tube occurred, it failed, except once, at the end of the tube

where the final seal was made. In the one instance in which failure was not on the end of the tube, the side tube separated from the cross-bar at the point where the seal had been made. The only solution to this problem was to anneal all seals slowly and evenly. One tube in ten seemed to fail in spite of all the precautions taken to prevent it.

Salt purity proved to have a very significant effect on these experiments. General Electric company's luminescent grade zinc sulfide and cadmium sulfide gave consistent results as did the 99.999% pure sulfur obtained from K and K Laboratories, Incorporated. Reagent grade lead sulfide and antimony trisulfide were found to be contaminated with sulfur as was the practical grade arsenic trisulfide. Purification of the antimony trisulfide and arsenic trisulfide was accomplished by washing them with several changes of carbon disulfide followed by washings with absolute ethyl alcohol until no odor of carbon disulfide could be discerned. These salts were allowed to air dry before being dried under vacuum. Hydrogen sulfide was bubbled through an aqueous solution of reagent grade lead nitrate. This sulfur-free lead sulfide was then filtered and dried under a vacuum.

Silver sulfide was obtained commercially from the City Chemical Corporation and by bubbling hydrogen sulfide through aqueous reagent grade silver nitrate. There was no difference in the solubility characteristics of the silver sulfide from the two

different sources.

Stannic sulfide was formed in two ways also. Hydrogen sulfide was bubbled through aqueous stannic nitrate. The yellow precipitate was slurried into centrifuge tubes and separated from the solvent by centrifugation. Several washes with distilled water were made in the same manner. It was finally rinsed with absolute ethyl alcohol and dried under a vacuum. Stannic sulfide was also prepared by the reaction of stannous sulfide with hydrogen sulfide in the presence of liquid hydrogen sulfide at room temperature. Both methods of preparation gave the same results in these experiments.

Mercuric sulfide and ferrous sulfide were reagent grade salts and were used without any subsequent purification.

Since this type of experiment depends upon the kind and number of dissolved species present, accurate and consistent results depended upon the use of a pure salt. If, during the pumping out phase, the more soluble salt is carried into the arm of the less soluble salt, then equilibrium will be attained with the ratio of the heights of the two columns of solvent in a constant ratio to each other. The ratio of the heights of the liquid above the more soluble salt to that above the less soluble salt will always be greater than or equal to one. Ideally, all of the solvent will condense in the side of the "H-tube" that contains the more soluble salt.

Discussion

The solubility of sulfur in liquid hydrogen sulfide has been investigated previously. The literature reports several conflicting opinions regarding the solubility of sulfur in liquid hydrogen sulfide. According to Quam (74) sulfur is soluble and non-reactive. Smith (88, p. 34) estimated the solubility of sulfur in liquid hydrogen sulfide to be between 10 and 20 mg per 1000 mg of solvent. Mickelson (69, p. 32), basing his conclusions on the fact that the half-time for the exchange of radioactive sulfur with liquid hydrogen sulfide was found to be several years, concludes that hydrogen sulfide acts as an inert solvent for sulfur. Mickelson, Norris, and Smith (70) estimate the solubility of sulfur in liquid hydrogen sulfide to be $\sim$ 0.4 g per 100 g of solvent and state that it forms a colorless solution for which the half-time for radioactive sulfur to exchange with the sulfur in hydrogen sulfide is greater than nine years. Zelvenskiĭ, Shalygin, and Bantysh (106) report the preparation of H_2S^{35} by a sulfur-hydrogen sulfide exchange reaction taking place in a stainless steel ampoule above the boiling point of hydrogen sulfide.

On the other hand, Beckmann and Waentig (9), using cryoscopic and direct current conductivity measurements, concluded sulfur is insoluble in liquid hydrogen sulfide. Cotton and Waddington (28) asserted that, because there were no color changes or conductivity

changes, sulfur is insoluble.

Experiments in this laboratory indicate that sulfur is soluble and non-reactive. Experimentally, it has also been demonstrated here that sulfur is more soluble than any of the inorganic sulfides.

The solubility of arsenic trisulfide was investigated by Quam (74), who noted it to be soluble and non-reactive, and by Biltz and Keunecke (13), who found it to be insoluble. Arsenic trisulfide was found, during this investigation, to be one of the more soluble sulfides. Its solubility is less than lead sulfide but greater than antimony trisulfide.

Quam (74) reported that antimony trisulfide is soluble and non-reactive. It was found during this investigation to be less soluble than arsenic trisulfide but more soluble than ferrous sulfide.

Lead sulfide was investigated by Quam (74) who found it to be insoluble and non-reactive. In this investigation lead sulfide was found to be more soluble than either arsenic trisulfide or antimony trisulfide. It was less soluble than silver sulfide.

Quam (74) also investigated ferrous sulfide and classed it as insoluble and non-reactive. Ferrous sulfide was found to be one of the less soluble sulfides investigated. Its solubility is less than antimony trisulfide but greater than cadmium sulfide.

Mercuric sulfide was found to go into solution much more rapidly than any of the salts it was paired with. However, after two

or three days of rotation on the turntable, the solvent would begin to shift to the other side of the "H-tube", and by the end of a week most of the solvent would be gone from above the mercuric sulfide. Mercuric sulfide was the more rapidly soluble of the two salts, but ultimately the solubility of the other salt was greater than that for the mercuric sulfide.

With stannous sulfide, a definite reaction with the solvent takes place in which stannous ion is oxidized to stannic by the reaction

$$SnS + H_2S \longrightarrow SnS_2 + H_2. \qquad (3.\ 20)$$

All attempts to use stannous sulfide in these experiments ended with this result.

Biltz and Keunecke (13) reported that stannic sulfide is insoluble. It was found during these experiments that stannic sulfide, prepared by reaction 3. 20 and by reacting stannic nitrate with gaseous hydrogen sulfide, was more soluble than any of the other heavy metal sulfides investigated. It was less soluble than elemental sulfur.

Experiments that were conducted by Smith (87) lend support to the observed order of solubility of lead sulfide and zinc sulfide. He found, during experiments in which an aqueous sodium sulfide solution containing both lead sulfide and zinc sulfide was cooled, that the zinc sulfide crystallized out at a higher temperature than the lead sulfide. This agrees with the order of deposition observed in

naturally occurring sphalerite and galena deposits.

Agreement with the result calculated from equation 3. 14 was found for the heavy metal sulfides that are stable in liquid hydrogen sulfide and for which heat of fusion and temperature of fusion data are available. The solubility series as observed from these experiments is

$$S > SnS_2 > Ag_2S > PbS > As_2S_3 > Sb_2S_3 > FeS > CdS > ZnS > HgS.$$

Agreement with the calculated result implies that, at these temperatures and at these dilutions, hydrogen sulfide is an "ideal solvent" with respect to Raoult's Law. Ideal solutions, in the sense of Raoult's Law, have been reported by Steele and Bagster (92) who found that the vapor pressure of mixtures of hydrogen sulfide and hydrogen iodide in all proportions obeyed Raoult's Law at low temperatures.

IV. THE GAS PURIFICATION AND FILLING SYSTEM

Because a higher quality hydrogen sulfide supply than is commercially available was required, an all-metal purification and metering system was designed. It consists of a hydrogen sulfide tank, supplied by the Matheson Company, Incorporated and equipped with a regulator with a one-way check valve and needle valve, two stainless steel cryogenic traps, a drying tube filled with desiccant, a Millipore gas filter, a flow meter, a metering valve, and a small manifold. Figure 4.1 shows the construction of the gas purification system.

The cryogenic traps are constructed with baffles which present a large cold surface to the gas as it passes through the traps. A chlorobenzene slush is made up inside the traps. It maintains the trap temperature at -45°C. At this temperature, the vapor pressure of hydrogen sulfide is two atmospheres. Thus, any flow pressure up to two atmospheres may be used for filling the vessels without any hydrogen sulfide condensing in the traps.

Two drying agents were tested. Phosphorus pentoxide, being a very efficient desiccant, was the first choice for a drying agent. However, it reacted with the hydrogen sulfide forming polymeric phosphorus-oxygen-sulfur compounds which were carried in small amounts over into the vessel during filling. Silica gel, although not as efficient as phosphorus pentoxide, proved to be satisfactory for

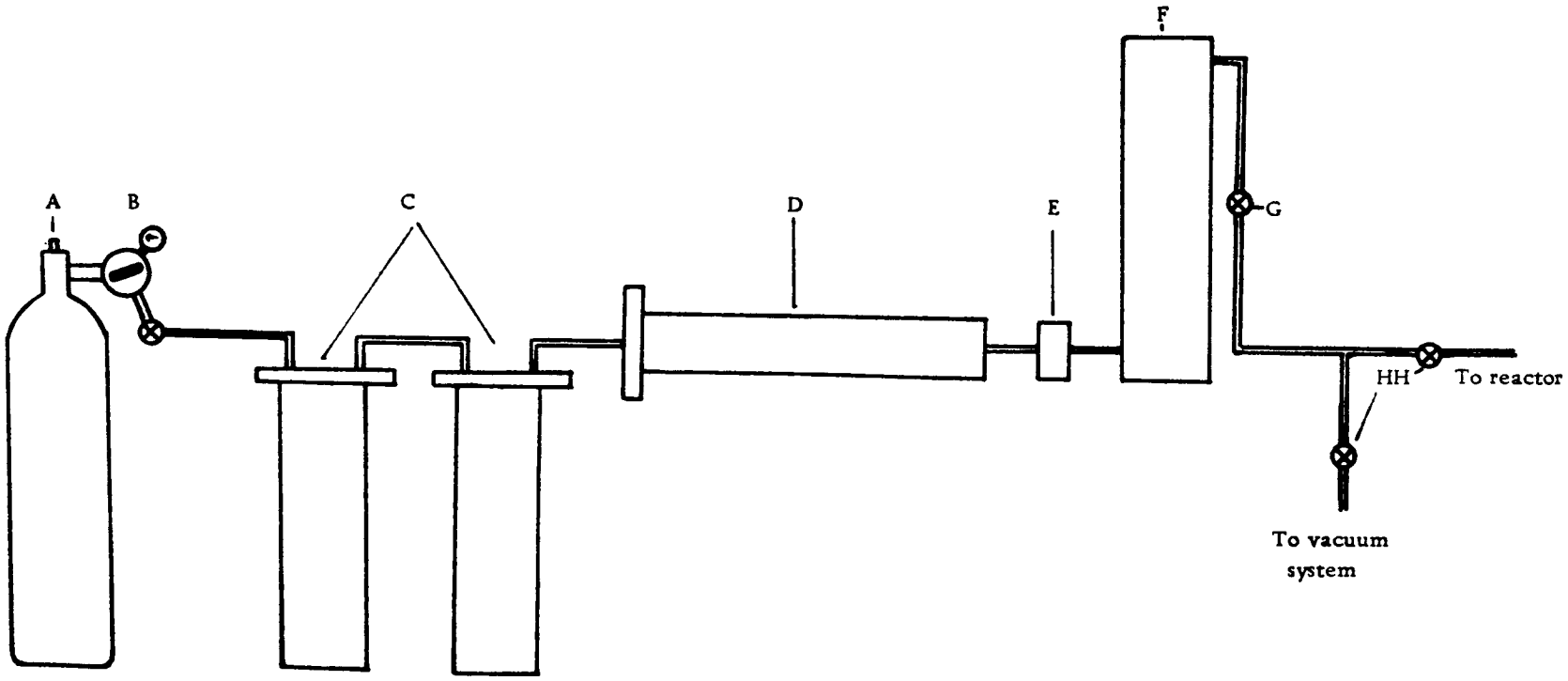

Figure 4. 1. Hydrogen sulfide purification and metering system. A) H_2S cylinder; B) Regulator; C) Cryogenic traps; D) SiO_2 dehydrator; E) Millipore filter; F) Rotameter flow meter; G) Metering valve; H) Toggle valve.

drying hydrogen sulfide in the gas phase.

The Millipore filter, using a filter disc with a pore size of 0.22 μc, was placed in the line after the traps and the desiccant tube and before the flow meter. It was to remove any solid particles being carried by the gas. After each use the filter disc was coated with a yellow, finely divided powder that evaporated upon standing in the open air. Prior to each use of the filling system, the filter disc was changed. This prevented the resistance due to a partially clogged filter from changing the flow due to the increased pressure drop across the filter. During the course of the calibration runs, a filter could be safely used for a continuous period of two hours. If this time period was exceeded, a decrease in the flow was noted.

The quantitative measurement of the amount of hydrogen sulfide condensed in the reactor was accomplished by using a Brooks Instrument Company, model 1110, size two, full-view Rotameter. This instrument is equipped with a stainless steel ball float which gives it a measuring range of 83.2 to 832 cubic centimeters per minute of dry air when under standard conditions of temperature and pressure.

The flow meter was calibrated for mass-flow of hydrogen sulfide by flowing the gas through all of the cold traps and filters that are used when the large reactors are filled. The length of time for each calibration point was measured at a constant flow rate and at a constant gauge pressure on the hydrogen sulfide tank within an

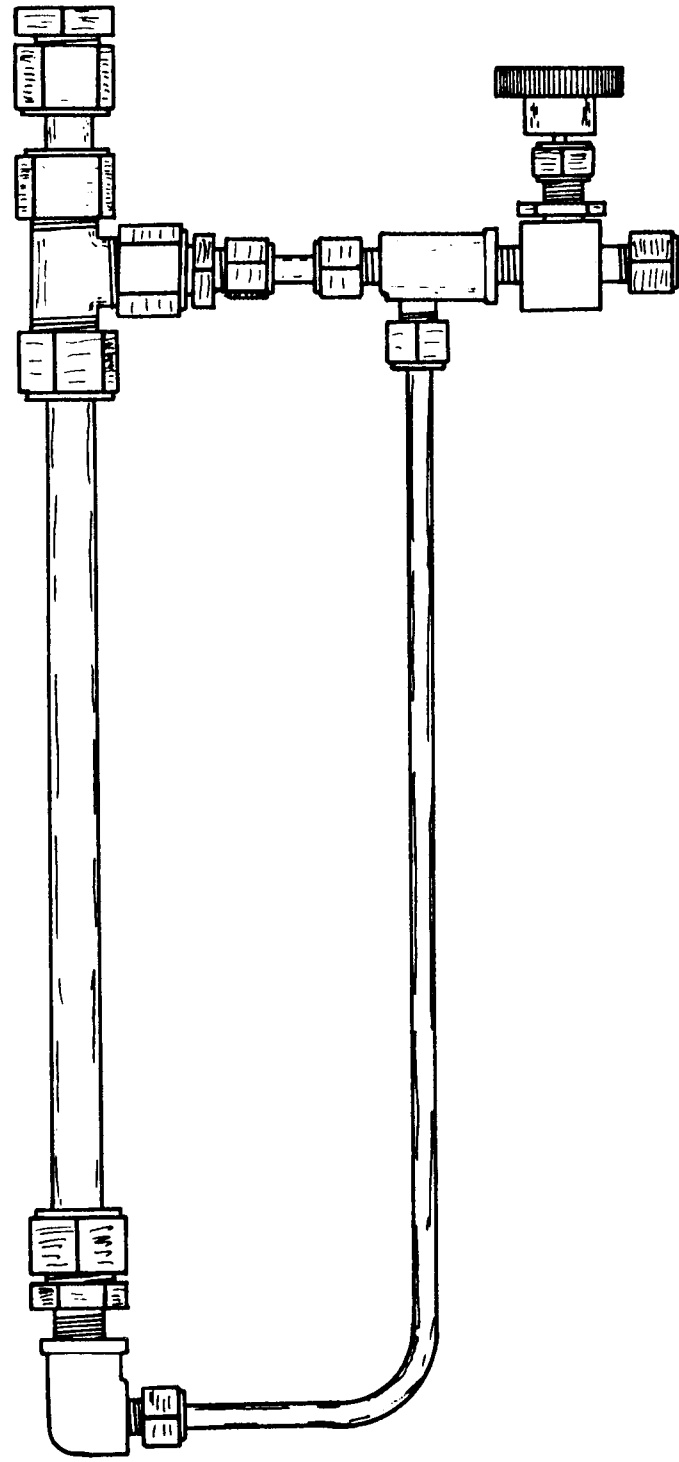

Figure 4. 2 Stainless steel calibration vessel.

accuracy of one second.

A small vessel prepared from stainless steel tubing and Swagelok tube fittings was used to condense the hydrogen sulfide. This vessel is shown in Figure 4. 2. During condensation this calibration vessel was immersed in a 1900 ml Dewar flask filled with Dry Ice and acetone. With this calibration vessel the maximum quantity of hydrogen sulfide which can be deposited is approximately nine grams. The amount of surface that is immersed in the Dry Ice-acetone bath limits the amount of hydrogen sulfide that can be deposited. When this surface decreases below a minimum value, due to the volume of condensed hydrogen sulfide, the flow rate decreases.

A modification to the flow meter was made by gluing a small mirror to the back window to eliminate parallax during the reading of the flow meter.

Calibration runs were of two types. The first and most extensive groups of runs were made at three different flow rates for varying time periods, while the second group was made at a series of different flow rates for a constant time period. All of the calibration runs were made at a constant gauge pressure at the regulator with the needle valve on the regulator fully open and the metering valve open exactly one turn.

The calibration runs were made in the following manner. The vessel, which was immersed in the Dry Ice-acetone cold bath, and the

rest of the filling system up to the metering valve was pumped out with a vacuum pump to a pressure of about 0. 1 mm of mercury.

During the pumping out process, the regulator on the hydrogen sulfide tank was adjusted so that the part of the system from the tank to the metering valve was under a pressure of approximately 16 psig and liquid nitrogen was added to the cold traps which contained chlorobenzene to form a slush. Then the valve on the vessel and the one to the vacuum pump were closed. The metering valve was opened exactly one full turn and the flow meter float allowed to come back to rest at zero percent flow. Simultaneously, the timer was started and the valve on the vessel opened and adjusted to give the desired flow rate at a gauge pressure of 15 psi while the gas was flowing.

At the end of a predetermined time period, the vessel valve was closed, the toggle valve, which is between the system and the vessel and had been open during this entire process, was closed, and the metering valve was closed. The calibration vessel was then removed from the filling system by means of a Swagelok connection between the toggle valve and the vessel valve.

The vessel was warmed by immersing the bottom half in water at room temperature, followed by a very careful drying. The vessel is weighed on a rider balance to a hundredth of a gram. After releasing the gas slowly, to prevent condensation of water on the outside of the vessel, the vessel was weighed again.

The first series of calibration experiments were run at 60% flow, 70% flow, and 80% flow for time periods varying from 3.00 minutes to 8.00 minutes with a phosphorus pentoxide desiccant. The data obtained for this series of runs is shown in Figure 4.3.

A check on the linearity of the flow meter was made by a second series of experiments with a phosphorus pentoxide desiccant. These experiments were run in the same manner as the first series except that all were run for exactly 5.00 minutes. Figure 4.4 shows the results from these experiments.

A third series of experiments were run identically to those in the first series except that the desiccant tube was packed full of silica gel in place of the boat of phosphorus pentoxide and only the 80% flow rate was used. The greater resistance offered by the packed desiccant tube over the boat of phosphorus pentoxide in the desiccant tube had the effect of decreasing the flow. The results of this series of experiments are shown in Figure 4.5.

The method of least squares was used to find an equation of the form

$$W = a + bt \tag{4.1}$$

that best fit the data. In equation 4.1 W is the weight of hydrogen sulfide, t is the time required in minutes, and a and b are constants obtained statistically from the data according to the equations

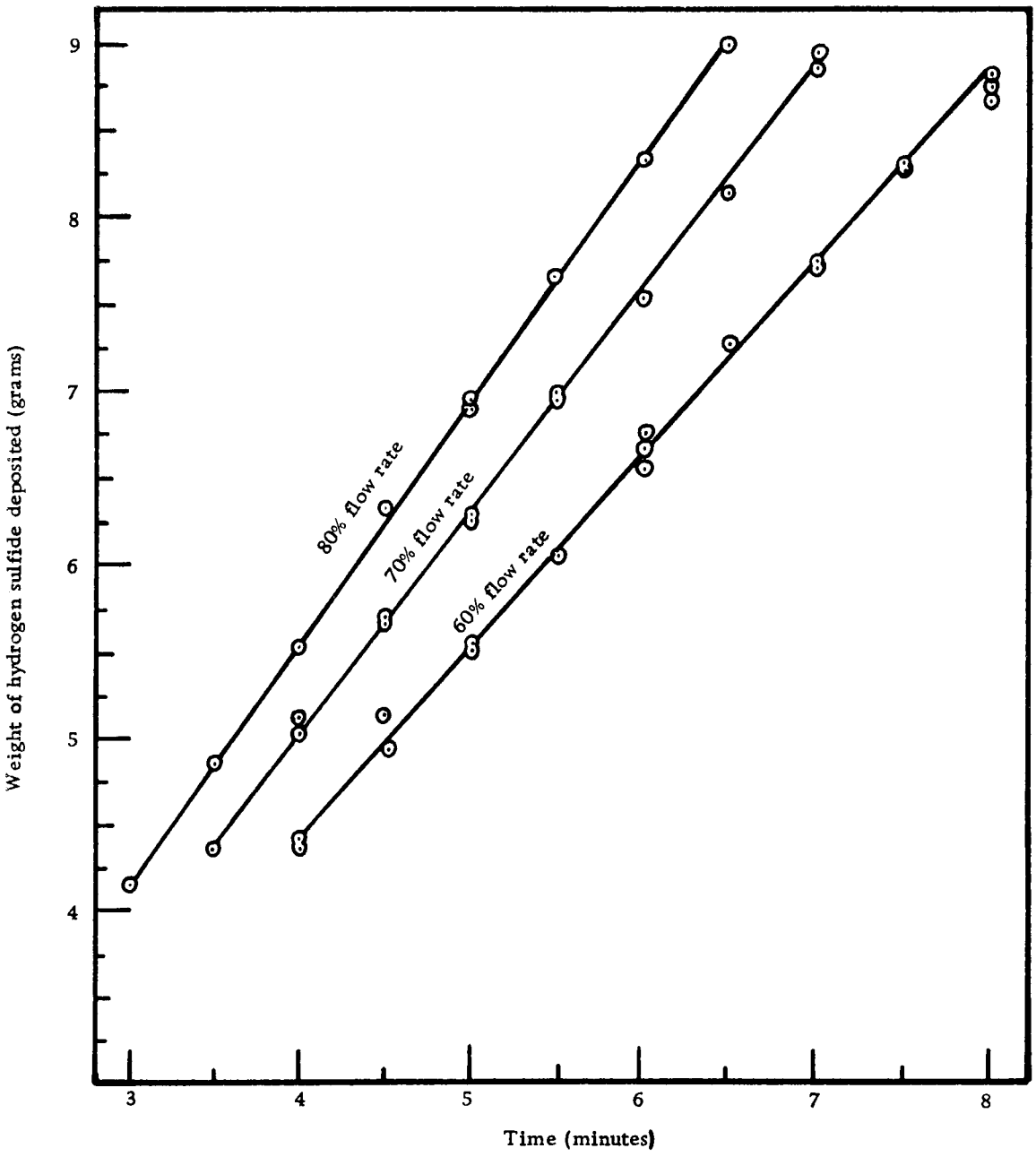

Figure 4. 3. Calibration curves of the flow meter using phosphorus pentoxide in the desiccant tube.

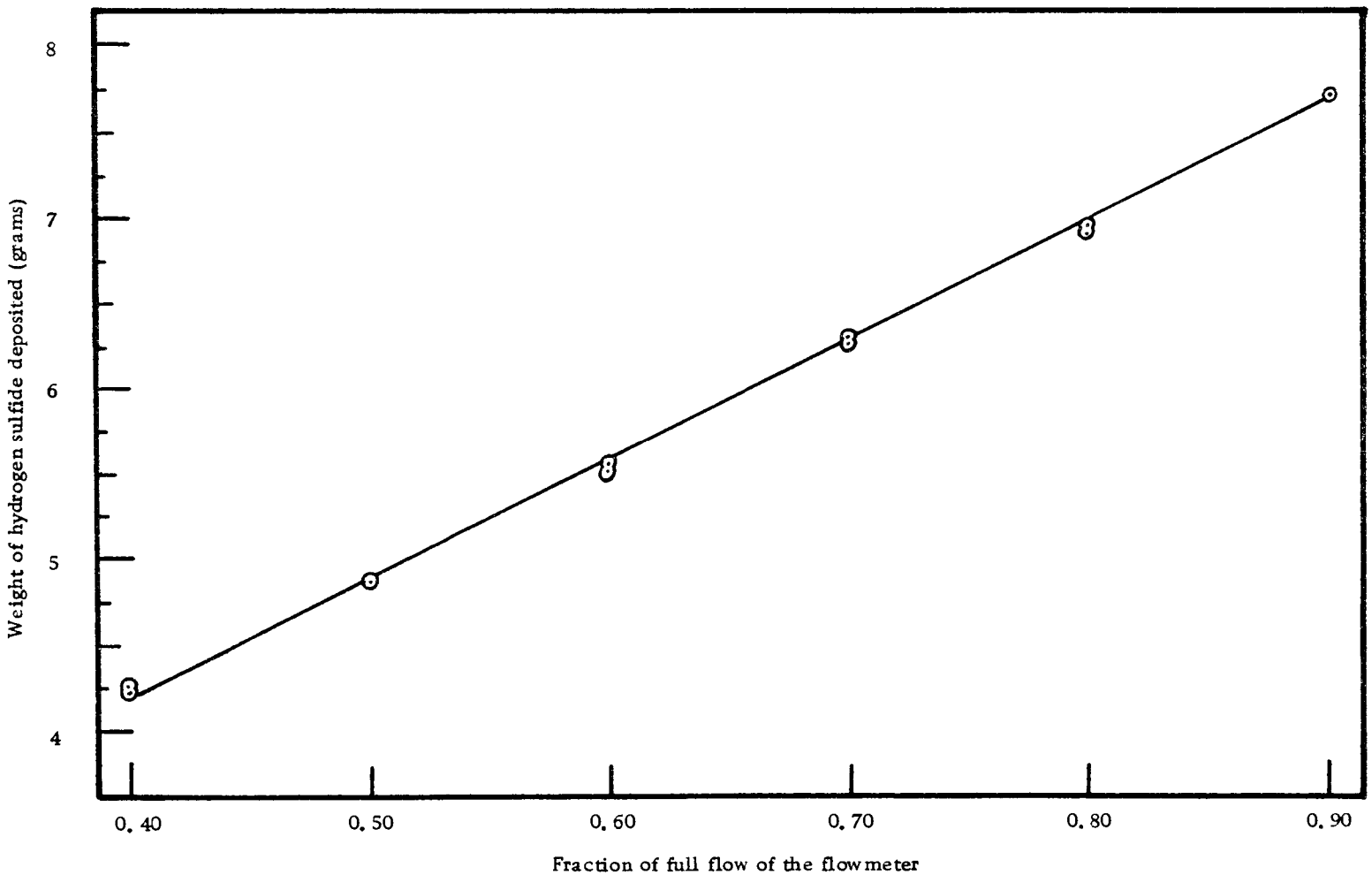

Figure 4. 4. Effect of flow rate at constant time on the quantity of hydrogen sulfide deposited.

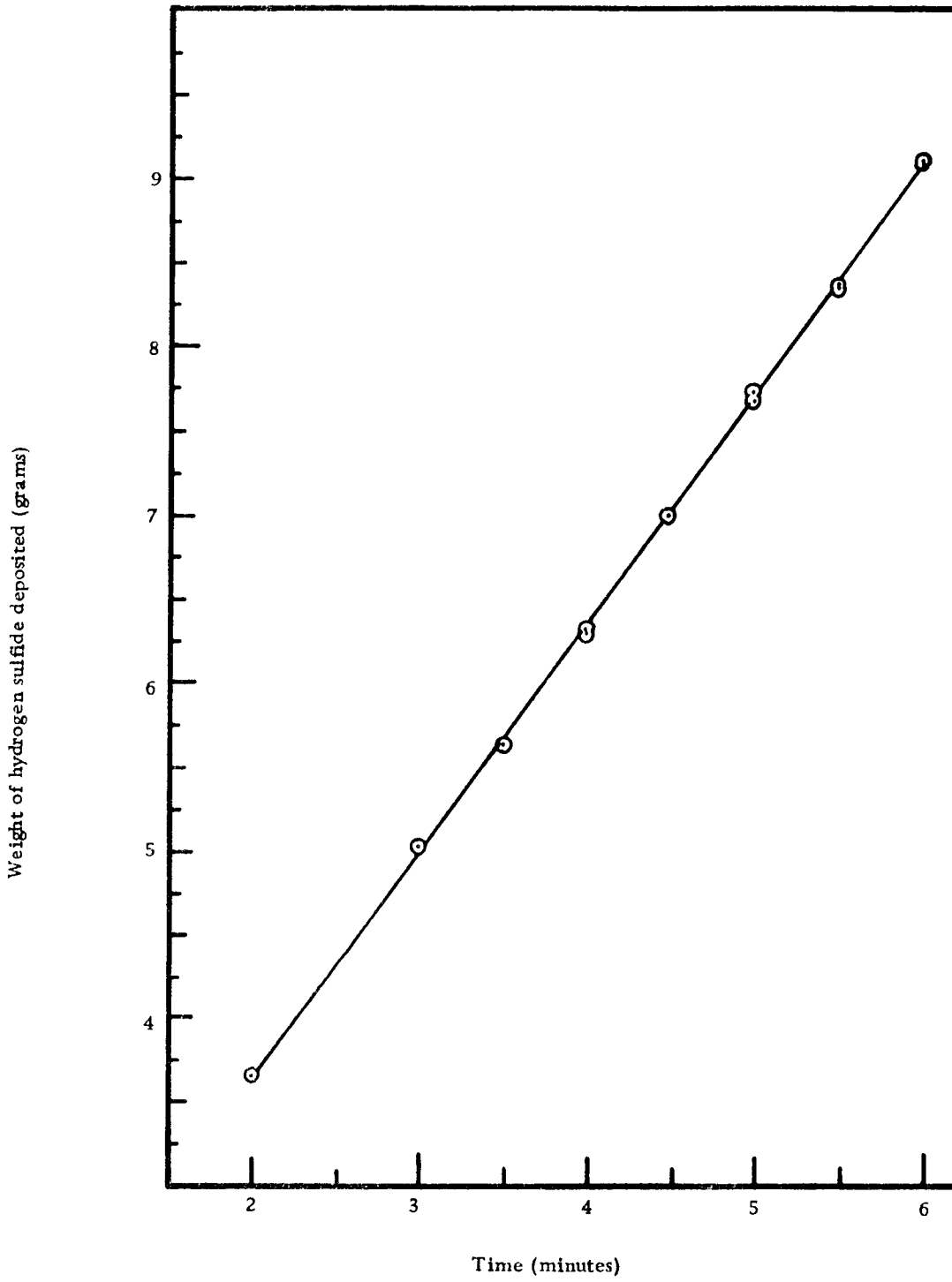

Figure 4. 5. Flowmeter calibration curve at 80% flow rate with a silica gel desiccant trap.

$$a = \frac{\Sigma w \Sigma t^2 - \Sigma t \Sigma tw}{n\Sigma t^2 - (\Sigma t)^2} \tag{4.2}$$

and

$$b = \frac{n\Sigma tw - \Sigma t \Sigma w}{n\Sigma t^2 - (\Sigma t)^2} \tag{4.3}$$

In these equations, n is the number of sample points and t and w are the measured times and weights respectively. The flow constant is b.

The standard deviation, σ, from the regression line obtained by the least squares analysis was then calculated from the expression

$$\sigma = \sqrt{\frac{1}{n} \Sigma (w - \overline{w})^2}, \tag{4.4}$$

where $\overline{w}$ is the value calculated from the regression formulas.

If the times involved are long, then the errors introduced at the beginning of the run, while the flow meter was being set to deliver a given flow, will be small enough that the deviations should follow a normal probability distribution curve. In that case, over 99% of the values will lie within three standard deviations of the regression line.

The regression formulas obtained for the first series of calibration experiments using a boat of phosphorus pentoxide in the desiccant tube, the traps held at -45° C, the dynamic gas pressure measured at the regulator set to 15 psig, and the valves set as described

earlier are

$$W_{60\%} = 0.03 + 1.093t \tag{4.5}$$

$$W_{70\%} = 0.07 + 1.275t \tag{4.6}$$

$$W_{80\%} = 0.02 + 1.386t \tag{4.7}$$

having standard deviations of

$$\sigma_{60\%} = \pm 0.28 \text{ g}$$

$$\sigma_{70\%} = \pm 0.05 \text{ g}$$

$$\sigma_{80\%} = \pm 0.04 \text{ g}.$$

The dependence of mass flow per minute on the fractional rate of full flow is given by the regression formula

$$W = 1.380 R + 0.285 \tag{4.8}$$

with a standard deviation of

$$\sigma = \pm 0.01 \text{ grams/minute}.$$

Silica gel was used in the third series of calibration experiments because of the apparent reaction taking place between the hydrogen sulfide and phosphorus pentoxide. Only the 80% flow rate was calibrated for mass flow because the increased flow times at the lower flow rates did not increase the accuracy enough to warrant the calibrations. The regression formula, under the conditions of 15 psig

while the gas is flowing, traps held at -45°C by chlorobenzene slush bath, a silica gel filled desiccant tube, the regulator needle valve open full, and metering valve open exactly one turn, is

$$W = 0.01 + 1.334t. \qquad (4.9)$$

The standard deviation from this expression is

$$\sigma = \pm 0.07 \text{ g.}$$

This expression for mass flow was used for all but the first six crystal growth experiments. Agreement between the hydrogen sulfide actually present in one of the high pressure vessels as determined by weighing it out in the calibration vessel and the amount metered in under the conditions governing equation 4.9 indicates that the calibration is accurate to 0.5%.

V. PRESSURE-VOLUME-TEMPERATURE BEHAVIOR OF HYDROGEN SULFIDE

Introduction

The pressure-temperature behavior of a high-density fluid in a constant volume is surprisingly uncomplicated. A plot of pressure against temperature is divided into two portions by the vapor pressure curve. The vapor pressure curve denotes the presence of two phases coexisting in a closed system and gives the pressure of the vapor in equilibrium with the liquid. On this curve the critical point is the maximum value attainable.

Below the vapor pressure curve is the region where a single gaseous phase exists. This region in the plot is reached when the density of the single gaseous phase is less than the critical density, that is, the density maximum of the vapor and the minimum of the liquid.

The region of interest in this particular investigation is the area above the vapor pressure curve. This area is reached when the density of the fluid is greater than the critical density. In this region of the pressure-temperature plot, for most substances, the pressure varies linearly with the temperature. Examples of this type of behavior can be seen from the data of Kennedy (50) for water, from the data of Reamer, Sage, and Lacey (80) for propane, and from the data of Beattie, Simard, and Su (8) for normal butane.

Several investigations have established the vapor pressure curve of hydrogen sulfide. Some significant studies are those of Klemenc and Bankowski (54), Giauque and Blue (35), Steele and Bagster (92), and Steele, McIntosh, and Archibald (93) who studied the gas at low pressures and low temperatures. Beyond the boiling point of hydrogen sulfide, Cardoso (24) studied the vapor pressure of the coexisting phases up to the critical point.

Reamer, Sage, and Lacey (81) studied the single phase properties of hydrogen sulfide between the temperatures of 5°C and 171°C and at pressures up to 10,000 psi. At 171°C they noted thermal decomposition taking place, probably as the result of the hydrogen sulfide coming in contact with mercury that was present in their system as a volume changing element.

Because no work had been done on the pressure-volume-temperature properties of hydrogen sulfide at the high densities and high temperatures of interest in this investigation, it became necessary to extend the data of Reamer, Sage, and Lacey (81) into this region.

Experimental

The apparatus used during these measurements consisted of the simplest possible system for containing the hydrogen sulfide. This apparatus is shown in Figure 5.1. The vessel, which had been designed for crystal growth experiments, was manufactured by

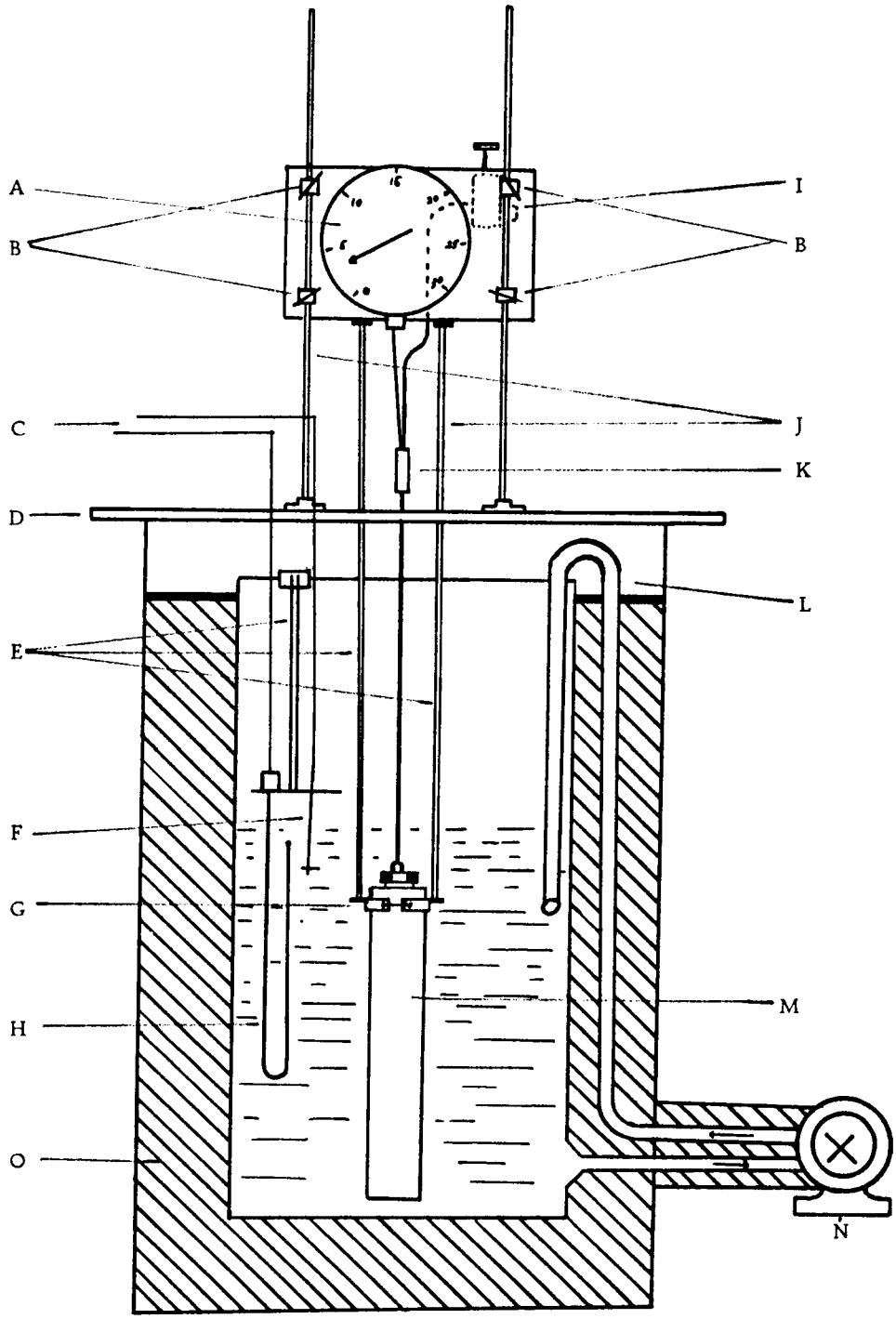

Figure 5.1. Cut-away view of the oil bath showing the apparatus used in making the PVT measurements. A) Bourdon tube gauge; B) Screw clamps; C) Control leads; D) Base plate; E) Aluminum support rods; F) Thermistor probe; G) Reactor support clamp; H) Heater; I) High pressure valve; J) Support rods for variation of the gauge height above the base plate; K) Tee; L) Discharge tube; M) High pressure vessel; N) Circulating pump; O) Vermiculite insulation.

Pressure Products Industries from a bar of number 410 stainless steel 13 1/2 inches in length and 2 1/2 inches in diameter. The inside dimensions of the vessel were one inch by ten inches. The vessel was designed for a working pressure of 30, 000 psi at 250° C.

Pressure-tight closure of the vessel was made by a highly polished, close-tolerance plug which fit into a Teflon ring in the mouth of the vessel. The main nut forced the plug into a wedge ring, which caused the Teflon to extrude enough to make the initial seal. Thermal expansion of the Teflon is about ten times that of the stainless steel. During the heating of the vessel, the greater expansion of the Teflon made the ultimate high pressure seal.

Tubing connections are made through the plug of the vessel to a Bourdon tube gauge, manufactured by the Astragauge Corporation, and to the valve required for filling the vessel.

The gauge and valve are mounted vertically on adjustable aluminum rods allowing some variation of the height of the vessel below the base plate.

An oil bath, employing Aero Shell S. A. E. #120 airplane oil, is used for the constant temperature bath. Circulation of the oil in the oil bath is by a gear pump equipped with high temperature seals. Flexible metal hoses connect the pump to the bath reservoir. The intake port is at the bottom of the bath and the discharge port is at the top of the bath just below the surface of the oil.

Thermal control of the oil bath was by a Yellow Springs Instrument Company thermistor controller which controlled one 1500 watt heater. The other 1500 watt heater was controlled by a Variac. Thermal variation of the oil bath with depth was less than 1°C at 200°C.

The fluid friction of the oil through the circulating pump was high enough to maintain a temperature of 50°C. Placing a cooling coil in the bath would depress the temperature, but it also decreased the circulation of the oil due to the increased viscosity. For this reason the lowest working temperature was approximately 50°C while the upper limit was arbitrarily set at 225°C so as to be well below the manufacturer's specification of a 250°C working temperature on the vessel and because above 225°C thermal decomposition of the oil was rapid.

An accurate determination of the volume of the vessel, gauge, and associated tubing is necessary to establish the densities of the hydrogen sulfide used during these experiments. The volume measurement was made by quantitatively measuring the volume of alcohol required to displace the air in each part of the system. This volume was found to be 138.06 cm^3.

The vessel was pumped out with a vacuum pump for 24 hours and then filled with hydrogen sulfide under the standard conditions of 80% flow at 15 psig with both cryogenic traps filled with

chlorobenzene slush while the vessel was immersed in a Dry Ice-acetone cold bath. On the first run, hydrogen sulfide was metered into the vessel until the condensation rate was less than the 80% flow rate. This occurred after 112.14 g of hydrogen sulfide had been condensed.

The vessel was immersed completely in the oil bath and temperature-pressure readings taken as soon as equilibrium had definitely been established. Between four and five readings per day were made on the system.

When a run at one density had been completed, with pressure-temperature points being taken as the temperature was increased and then decreased, the vessel was hoisted from the oil bath and the pressure allowed to drop to 300 psi. It was then connected to the evacuated calibration vessel through the filling system and a small quantity of hydrogen sulfide removed by condensing it into the calibration vessel with a Dry Ice-acetone cold bath. The calibration vessel was warmed up to room temperature and weighed to an accuracy of 0.01 g. Then the gas was released and the vessel was evacuated rapidly with an aspirator and reweighed. Most of the weights of the evacuated vessel were within $\pm$ 0.02 g of each other and were 0.03 g less than the weight of the empty unevacuated vessel.

Discussion

The range of densities used was from 10. 20 moles per liter to 22. 95 moles per liter uncorrected. According to Bierlein and Kay (12) the critical density of hydrogen sulfide is 10. 24 moles per liter. Thus, both the region above the vapor pressure curve and a very small region below the vapor pressure curve are represented by the data.

Figure 5. 2 shows the uncorrected pressure-temperature data just as it was taken. In analyzing the data obtained from this experiment, two sources of error had to be considered.

The first source of error, and the more insignificant of the two is the effect of thermal expansion of the vessel on the volume. A value for the mean linear coefficient of thermal expansion, $\frac{1}{L}\frac{dL}{dT}$, for number 410 stainless steel of

$$\frac{1}{L}\frac{dL}{dT} = 6.4 \times 10^{-6} \text{ in/in/°F} \qquad (5.1)$$

over the temperature range from 68° to 1300° F is given in the Allegheny Ludlum Steel Corporation's Stainless Steel Handbook (2). For a homogenous medium, the linear coefficient of expansion can be shown to be equal to one-third the coefficient of volume expansion, $\frac{1}{V}\frac{dV}{dT}$, by the following relationship:

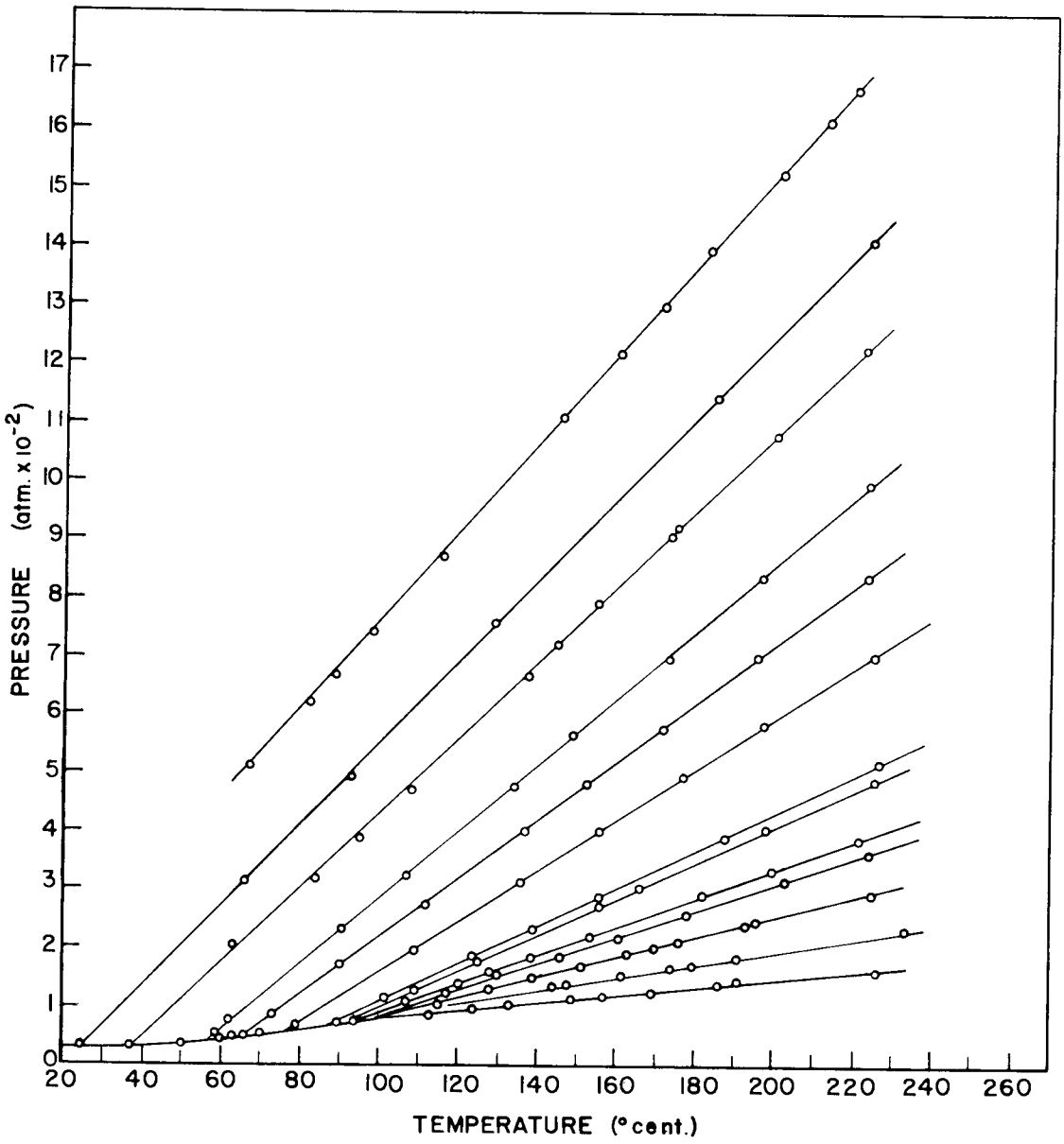

FIG. 5.2. P-T DATA FOR HYDROGEN SULFIDE ABOVE CRITICAL POINT. EACH LINE CONNECTS POINTS OF EQUAL DENSITY.

$$\frac{1}{V}\frac{dV}{dT} = \frac{1}{L^3}\frac{d(L^3)}{dT} = \frac{3L^2}{L^3}\frac{dL}{dT} = \frac{3}{L}\frac{dL}{dT}. \qquad (5.2)$$

The maximum change in the volume of the vessel will be less than the volume of a bar of steel having the same outside dimensions as the high pressure vessel. This volume change for a 360° F thermal change in a vessel having the dimensions L = 13.5 inches and r = 1.25 inches is

$$\Delta V = V \cdot \frac{1}{V}\frac{dV}{dT}\Delta T = 3V\frac{1}{L}\frac{dL}{dT}\Delta T = 4.58 \times 10^{-1} \text{ cubic inches} \qquad (5.3)$$

The fractional change, $\frac{\Delta V}{V}$, under these conditions is 0.00691, a change in volume of less than 0.7%. This will introduce a maximum error in the value of the pressure of 0.7%, calculated from the virial expressions obtained from this data.

The second source of error is the more serious of the two. This error arises because the gauge and the tubing leading to it and to the valve could not be immersed in the oil bath. Consequently, this volume, which comprises nearly 4% of the total volume of the system, was at a different temperature from the rest of the system.

A density correction was therefore needed to make the pressure a function of the amount of hydrogen sulfide actually undergoing thermal expansion. This was accomplished using the data of Reamer, Sage, and Lacey (81) as a standard.

Figure 5. 3 compares the data of Reamer, Sage, and Lacey (81) and the results from this investigation as a plot of pressure against density at constant temperature.

From Figure 5. 3 the density difference as a function of pressure at constant temperature was read and plotted in Figure 5. 4, which in turn was used to obtain Figure 5. 5--a graph showing density difference as a function of temperature at constant pressure. These corrected densities and the observed pressures and temperatures were then used to obtain the virial expressions.

At low densities there is a significant variation in the density difference, becoming larger as the temperature is increased, signifying that the low density fluid is relatively compressible. At high densities, the density difference is almost independent of temperature, reflecting the relative incompressibility of the high density fluid. At low densities the error between the corrected data as observed in this investigation and that of Reamer, Sage, and Lacey (81) is slightly less than two percent at the lower temperatures. At the higher temperatures at all densities and at the lower temperatures at the higher densities, the error of this correction is less than 0. 5%. These errors are due to the difficulty of reading accurately the pressure gauge at low pressures. At the higher pressures this error, which remains constant over the range of the gauge, becomes insignificant with respect to the total pressure.

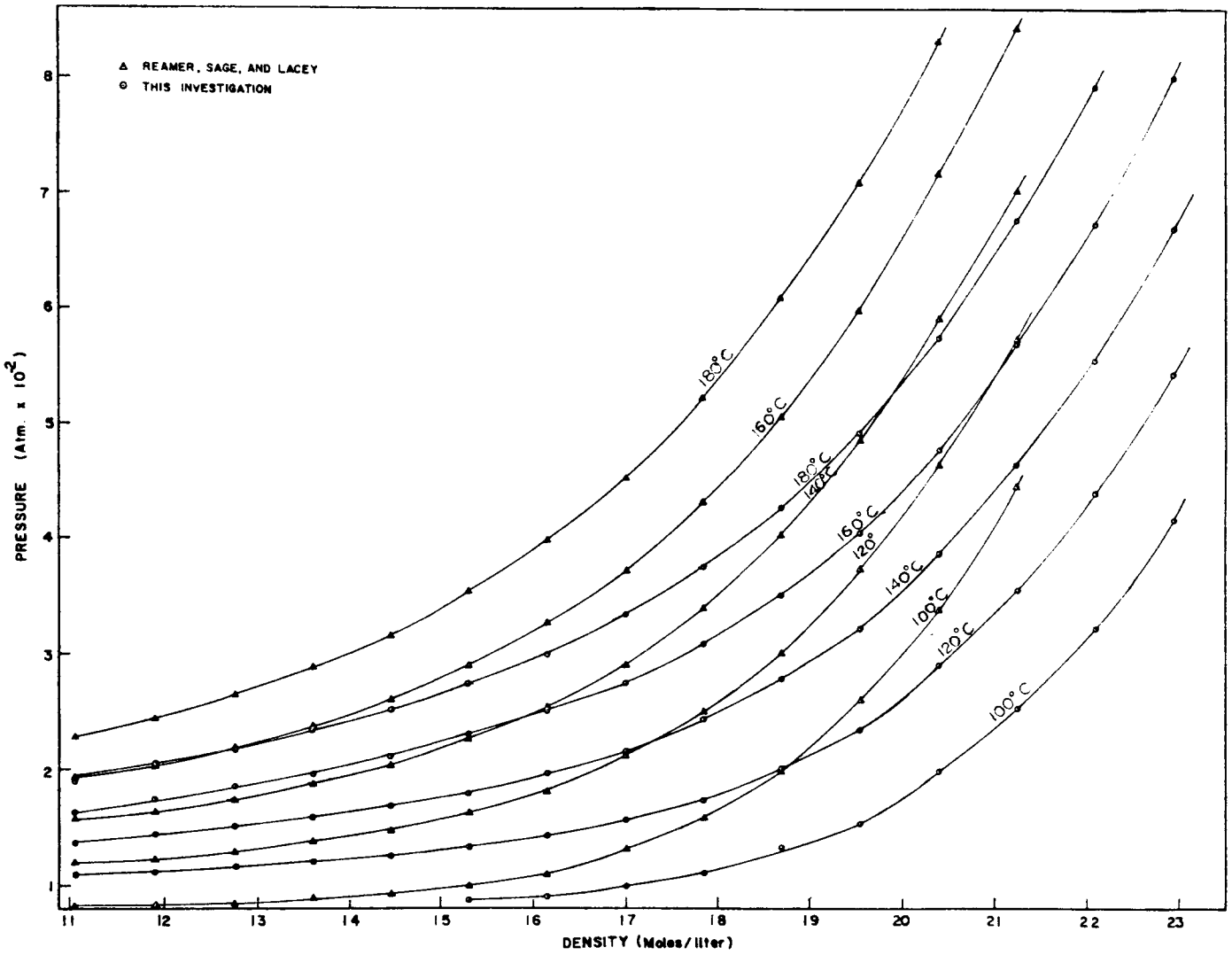

FIGURE 5.3. COMPARISON OF THE UNCORRECTED DATA FROM THIS INVESTIGATION AND THAT FROM AN EARLIER INVESTIGATION.

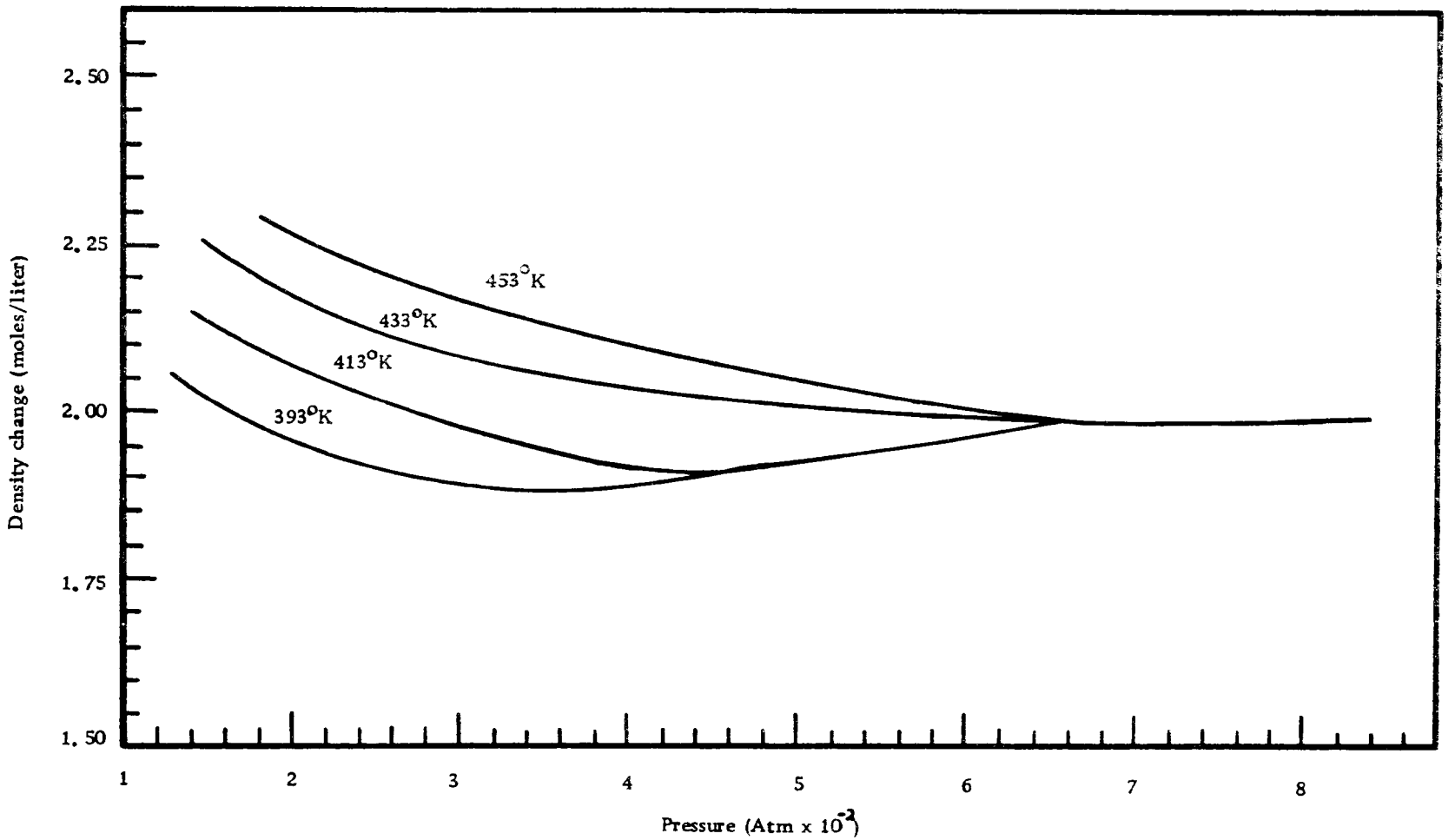

Figure 5.4. Isotherms showing density change with pressure.

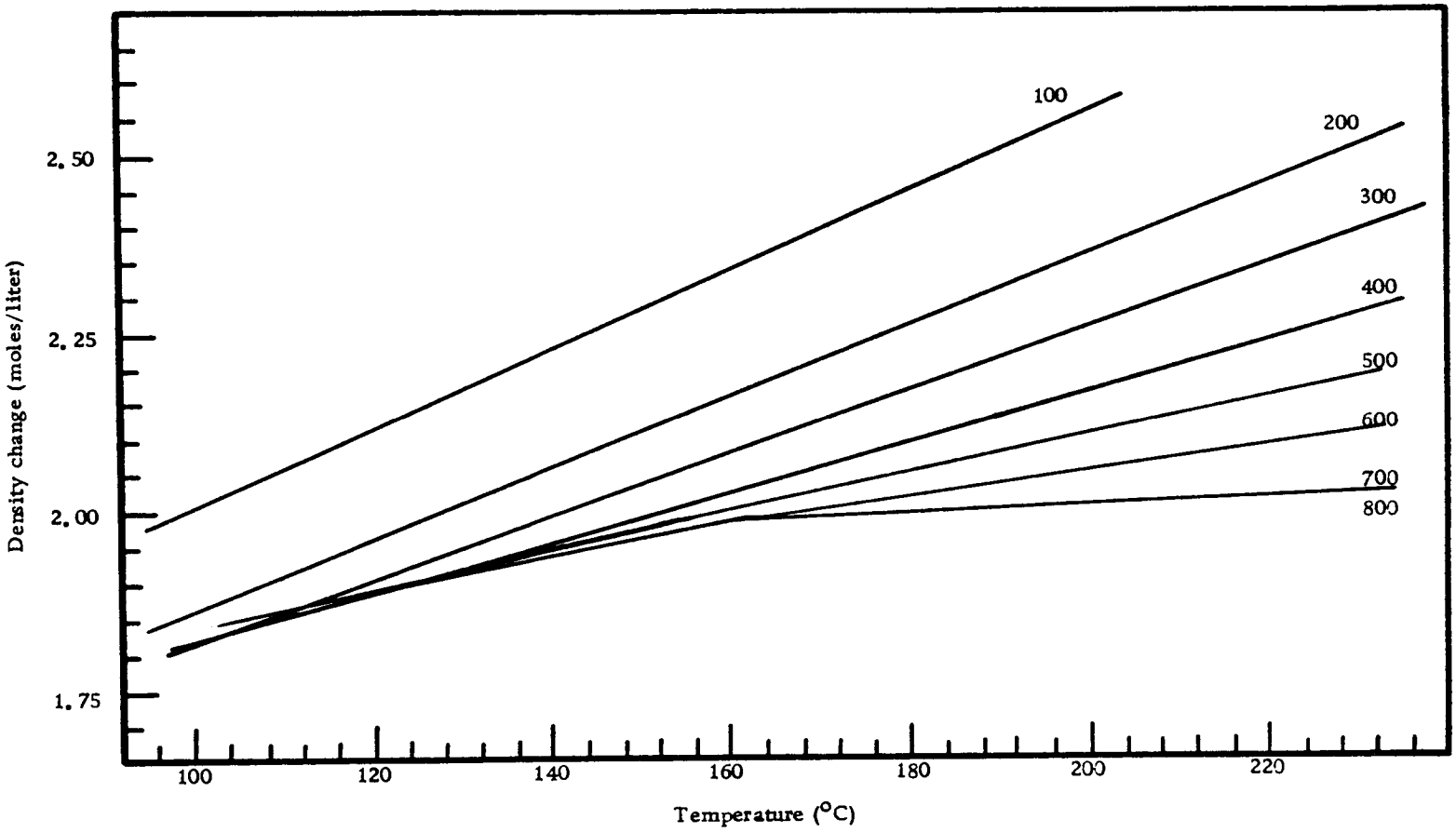

Figure 5.5. Isobars showing density change with temperature. Pressures are given in atmospheres.

The compressiblity factor, Z, is defined by the equation

$$Z = \frac{PV}{nRT}, \tag{5.4}$$

where P is the pressure, V is the volume, n is the number of moles of gas, R is the gas constant, and T is the absolute temperature. If the gas behaves ideally, a plot of Z against P is a horizontal line with Z equal to unity. For real gases the plot of Z begins at Z = 1 for low pressures and high temperatures, drops below one as the temperature is increased, and begins a fairly linear climb through the perfect gas value to the values of Z greater than unity. At sufficiently high temperatures the volume will always be greater than the perfect gas volume--that is, the compressibility factor will always be greater than unity.

The virial coefficients were obtained by subjecting the data to a stepwise linear regression analysis on the computer. An equation of the form

$$\frac{Z - 1}{d} = A + Bd + Cd^2 + Dd^3 + Ed^4, \tag{5.5}$$

in which A, B, C, D, and E are empirical coefficients, d is the density, and Z is the compressibility factor, was fit to the data by the computer. The coefficients, as a function of temperature, are tabulated in Table 5.1

Table 5. 1. Coefficients of the virial expressions for single phase hydrogen sulfide.

T°K	A	B	C	D	E
373	-6.966×10^{-2}	---	---	3.74×10^{-6}	0.9×10^{-7}
393	-1.354×10^{-1}	1.026×10^{-2}	-3.647×10^{-4}	---	3.6×10^{-7}
413	-1.040×10^{-1}	6.048×10^{-3}	-1.667×10^{-4}	---	2.4×10^{-7}
433	-9.002×10^{-2}	4.912×10^{-3}	-1.165×10^{-4}	---	2.1×10^{-7}
453	-7.206×10^{-2}	2.886×10^{-3}	-2.156×10^{-5}	---	1.6×10^{-7}
473	-6.399×10^{-2}	2.412×10^{-3}	$+1.20 \times 10^{-6}$	---	1.4×10^{-7}
493	-5.256×10^{-2}	1.524×10^{-3}	$+3.836 \times 10^{-5}$	---	1.2×10^{-7}

Table 5. 2 compares the observed values of the pressure and compressibility factor as functions of the temperature and the density with the calculated pressure and compressibility factor.

Figure 5. 6 shows the agreement between the points calculated for the compressibility factor, the compressibility factors observed in this investigation, and the compressibility factors from the data published by Reamer, Sage, and Lacey (81).

Even though the amount of data that could be taken at the lowest temperature, 373°K, was limited and of poorer quality than the higher pressure and temperature data, virial coefficients were calculated for this temperature. They should be used with caution because of these limitations. This is evident from the pattern of coefficients of the 373°K isotherms which do not conform to the pattern of coefficients for the isotherms at higher temperatures.

The virial development is particularly useful for indicating interactions between the molecules in a gas. The virial expression represents the deviation from ideal behavior as the terms having the coefficients A, B, C, . . . are added to the zero-order coefficient. Thus, the second virial coefficient indicates the interaction between pairs of molecules. Higher order coefficients indicate the interactions between larger numbers of molecules.

The second virial coefficient, A, behaves as it should for all of the isotherms except the 373°K isotherm. Pair formation occurs

Table 5. 2 Observed and calculated values for the pressure and compressibility factor as functions of temperature and density.

P_{obs} is the observed pressure in atmospheres.

Z_{obs} is the compressibility factor calculated from the observed values of the pressure at the given temperature and density.

P_{calc} is the pressure calculated from the virial expressions for the given density and temperature.

Z_{calc} is the compressibility factor calculated from the virial expressions at the given temperature and density.

Density in moles per liter.

	T = 373° K				T = 393° K				T = 413° K			
Density	P_{obs}	Z_{obs}	P_{calc}	Z_{calc}	P_{obs}	Z_{obs}	P_{calc}	Z_{calc}	P_{obs}	Z_{obs}	P_{calc}	Z_{calc}
8.00	---	---	---	---	103	0.399	103	0.399	130	0.480	130	0.478
9.00	---	---	---	---	106	0.365	107	0.368	135	0.443	136	0.447
10.00	---	---	---	---	111	0.344	111	0.344	144	0.424	143	0.423
11.00	---	---	---	---	116	0.330	115	0.325	152	0.408	151	0.406
12.00	---	---	---	---	121	0.313	121	0.313	161	0.395	161	0.396
13.00	---	---	---	---	130	0.310	129	0.307	173	0.393	174	0.395
14.00	90	0.210	93	0.216	140	0.310	140	0.309	192	0.405	192	0.404
15.00	99	0.216	97	0.211	153	0.316	156	0.322	217	0.427	216	0.424
16.00	110	0.225	109	0.223	178	0.345	179	0.346	249	0.459	248	0.458
17.00	133	0.256	132	0.253	208	0.379	211	0.385	290	0.503	293	0.508
18.00	167	0.303	168	0.305	256	0.441	257	0.443	350	0.574	353	0.578
19.00	223	0.383	222	0.381	324	0.528	322	0.525	434	0.674	431	0.670
20.00	297	0.485	297	0.486	413	0.640	410	0.635	535	0.789	534	0.788
21.00	398	0.619	400	0.623	533	0.787	528	0.780	669	0.940	668	0.938
22.00	533	0.792	536	0.795	682	0.961	685	0.966	838	1.124	839	1.125
23.00	715	1.016	711	1.010	890	1.200	892	1.202	1054	1.352	1055	1.353

Table 5. 2. Continued.

	T = 433° K				T = 453° K				T = 473° K				T = 493° K			
Density	P_{obs}	Z_{obs}	P_{calc}	Z_{calc}	P_{obs}	Z_{obs}	P_{calc}	Z_{calc}	P_{obs}	Z_{obs}	P_{calc}	Z_{calc}	P_{obs}	Z_{obs}	P_{calc}	Z_{calc}
8.00	154	0.542	154	0.542	178	0.599	179	0.602	201	0.647	201	0.648	226	0.698	227	0.701
9.00	164	0.513	165	0.515	196	0.586	194	0.579	218	0.624	220	0.629	249	0.684	249	0.685
10.00	177	0.498	176	0.496	209	0.562	209	0.562	240	0.618	239	0.616	274	0.677	274	0.677
11.00	189	0.484	189	0.484	227	0.555	226	0.553	264	0.618	261	0.612	304	0.683	301	0.676
12.00	205	0.480	204	0.479	246	0.552	246	0.552	289	0.621	287	0.616	335	0.690	332	0.684
13.00	227	0.491	224	0.484	272	0.563	271	0.561	320	0.634	318	0.630	368	0.700	369	0.702
14.00	252	0.507	248	0.498	301	0.578	302	0.581	353	0.650	356	0.655	413	0.729	414	0.731
15.00	277	0.520	280	0.525	341	0.612	342	0.614	397	0.682	403	0.693	467	0.770	468	0.772
16.00	316	0.556	321	0.565	390	0.656	393	0.660	462	0.744	463	0.745	533	0.824	536	0.828
17.00	373	0.618	376	0.622	456	0.722	457	0.723	537	0.814	536	0.813	613	0.891	608	0.884
18.00	443	0.693	446	0.698	537	0.803	539	0.806	628	0.899	629	0.901	714	0.981	722	0.992
19.00	538	0.797	538	0.796	644	0.913	642	0.909	742	1.006	732	0.992	852	1.108	848	1.103
20.00	657	0.925	654	0.920	778	1.046	771	1.037	889	1.145	886	1.141	1018	1.258	1002	1.238
21.00	810	1.086	801	1.074	934	1.197	931	1.193	1071	1.314	1060	1.301	1202	1.415	1188	1.399
22.00	989	1.265	987	1.263	1123	1.373	1129	1.381	1273	1.491	1273	1.491	1402	1.575	1415	1.590
23.00	1213	1.484	1220	1.493	1372	1.605	1372	1.605	1525	1.708	1532	1.716	1684	1.810	1688	1.814

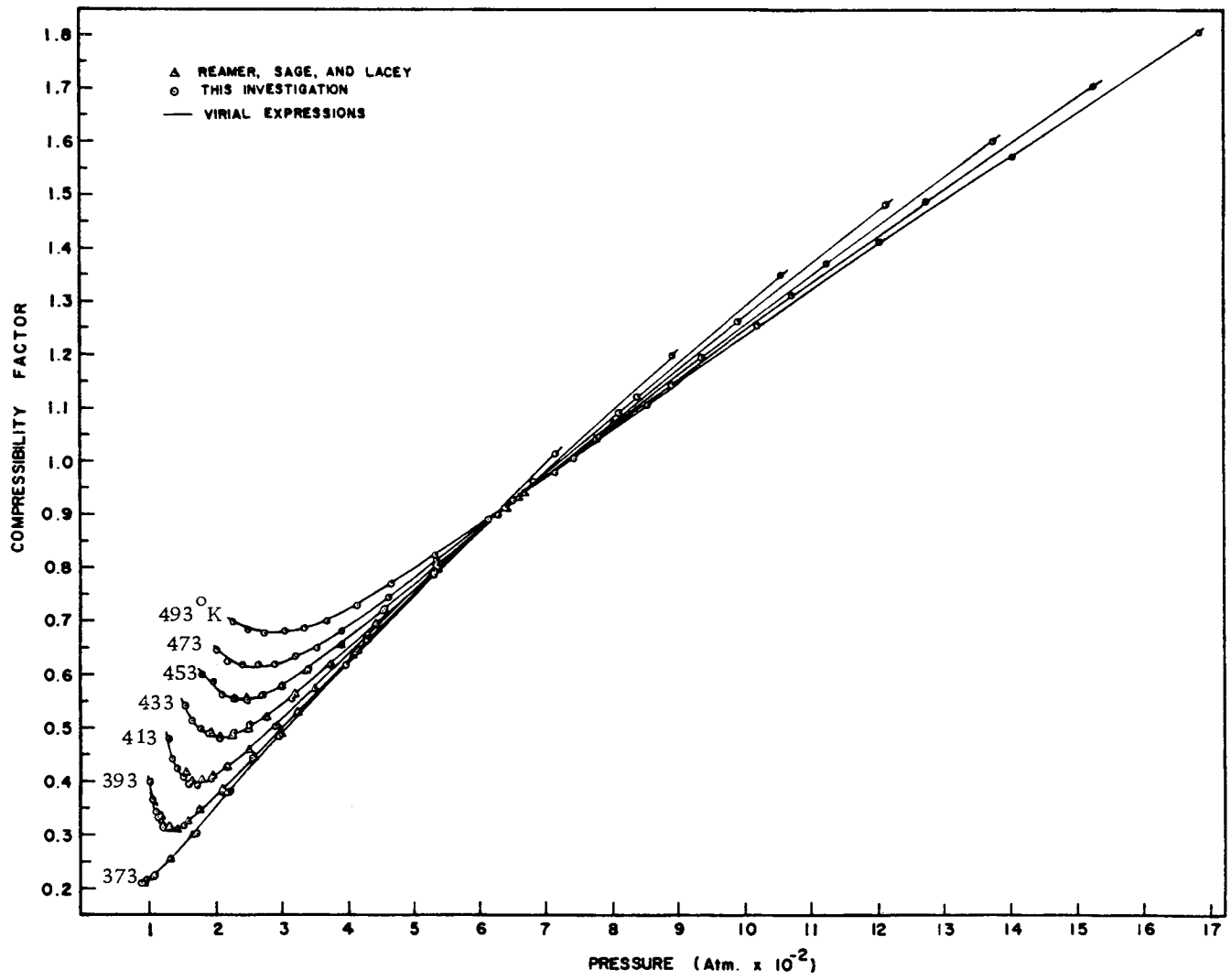

FIGURE 5.6. VIRIAL EXPRESSIONS COMPARED TO EXPERIMENTAL DATA.

predominantly at low temperatures. As the temperature increases the number of pairs decreases. This is reflected in the observed decrease in the coefficient A with increasing temperature. The fraction of molecules that are paired is significant, but this fraction is not large.

A comparison of the compressibility factor plotted against pressure at 413°K for some of the common equations of state proposed for hydrogen sulfide is shown in Figure 5.7. The simplest of these equations is the ideal gas equation of state,

$$PV = nRT, \tag{5.6}$$

or in terms of the compressibility factor, Z,

$$Z = 1. \tag{5.7}$$

This equation of state produces a horizontal line on the compressibility factor against pressure plot, which is a good approximation only at very low pressures and moderate temperatures. Thus, it comes as no surprise that at high pressures the behavior of hydrogen sulfide deviates extensively from the ideal gas equation.

The equation of state that is next in terms of complexity is the Van der Waals equation of state

$$\left(P + \frac{n^2 a}{V^2}\right)(V - nb) = nRT \tag{5.8}$$

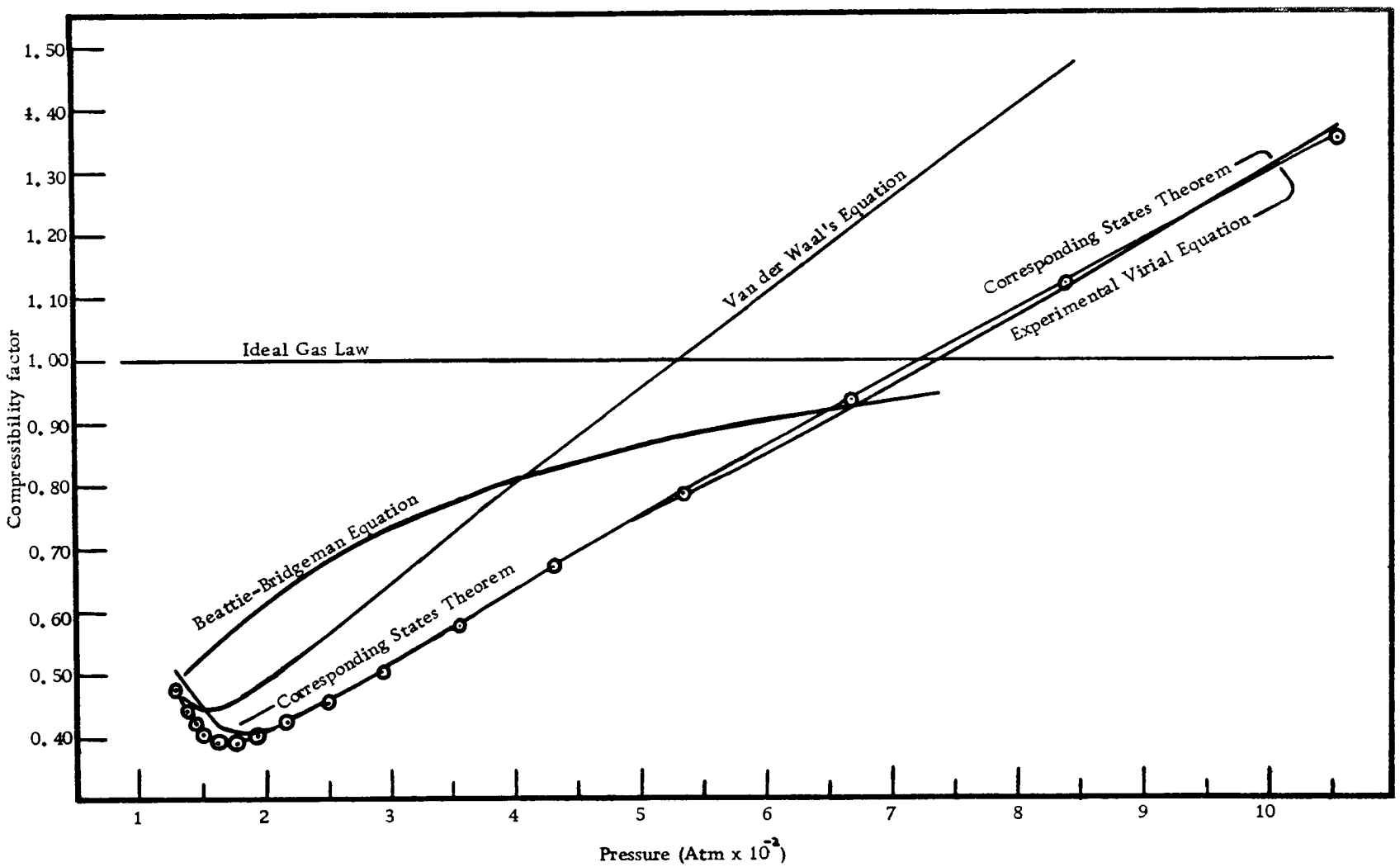

Figure 5.7. Comparison of the observed PVT data with some common equations of state for the 413° K isotherm. Points indicate experimental data.

in which there are two additional parameters, a and b. The parameter a is an attempt to correct for the attractive forces between the molecules in a real gas while the parameter b corrects for the volume of the molecules of the real gas. These constants, which are specific for each gas, are calculated from the values for the critical temperature and critical pressure by the equations

$$a = \frac{27\, R^2\, T_c^{\,2}}{64\, P_c} \tag{5.9}$$

and

$$b = \frac{R\, T_c}{8\, P_c} \,. \tag{5.10}$$

For hydrogen sulfide, using commonly accepted critical state values of $T_c = 373.5°K$ and $P_c = 88.9$ atm, as determined by Bierlein and Kay (12), the constants are

$$a = 4.431 \frac{\text{liters}^2\ \text{atmosphere}}{\text{mole}^2}$$

and

$$b = 0.04287 \frac{\text{liters}}{\text{mole}} \,. \tag{5.11}$$

This equation predicts the observed behavior better than the ideal gas law. However, the pressures calculated by this equation exceed the observed pressures in the pressure range above the critical temperature. The most useful range for the Van der Waals equation is below

the critical point.

The Van der Waal's constants may be directly compared to the second virial coefficient, A, in equation 5. 5. Van der Waal's equation (equation 5. 8) can be put into the form

$$PV = nRT\left[1 + \left(b - \frac{a}{RT}\right)\frac{n}{V} + \ldots\right] \tag{5.12}$$

where

$$\frac{n}{V} = \rho. \tag{5.13}$$

Therefore

$$\frac{PV}{nRT} = Z = 1 + \left(b - \frac{a}{RT}\right)\rho + \ldots. \tag{5.14}$$

Equating the like coefficients from equations 5. 5 and 5. 14

$$A = b - \frac{a}{RT}. \tag{5.15}$$

Table 5. 3 compares the experimentally determined second virial coefficient with those calculated from equation 5. 15. The coefficients are of the same sign and of approximately the same order of magnitude. The temperature dependence of the experimentally determined coefficients, in which the coefficient decreases with increasing temperature, agrees with equation 5. 15 for all temperatures but the lowest. The differences in the values of the experimentally determined coefficients and those related to Van der Waal's equation is due partially to the temperature dependence of the Van der Waal's coefficients and partially to the high densities used. Van der Waal's

equation is most effective for reduced temperatures, $\frac{T}{T_c}$, less than one. This investigation was carried out in the reduced temperature range from 1.0 to 1.3.

Table 5.3. Experimentally determined second virial coefficients compared to the function $(b - \frac{a}{RT})$.

Temperature	A	$b - \frac{a}{RT}$
373°K	-6.966×10^{-2}	-1.019×10^{-1}
393°K	-1.354×10^{-1}	-9.453×10^{-2}
413°K	-1.040×10^{-1}	-8.788×10^{-2}
433°K	-9.002×10^{-2}	-8.184×10^{-2}
453°K	-7.206×10^{-2}	-7.634×10^{-2}
473°K	-6.399×10^{-2}	-7.130×10^{-2}
493°K	-5.256×10^{-2}	-6.665×10^{-2}

As the number of empirical constants in an equation of state is increased, the accuracy with which the equation of state reproduces the experimentally determined behavior increases. This is true as long as the conditions under which the constants were determined are not exceeded. Such an equation of state is the Beattie-Bridgeman equation (7)

$$P = \frac{RT(1 - \epsilon)(V + B)}{V^2} - \frac{A}{V^2}, \qquad (5.16)$$

where

$$\epsilon = \frac{C}{VT^3}$$

$$A = A_0(1 - \frac{a}{V}) \qquad (5.17)$$

$$B = B_0(1 - \frac{b}{V})$$

in which A_0, B_0, a, b, and C are empirical constants specific for each gas.

West (101) evaluated the Beattie-Bridgeman constants for hydrogen sulfide using the method of Maron and Turnbull (65). This equation has the form

$$P = (1 - \frac{1.79 \times 10^6}{VT^3})(\frac{RTn}{V^2})[V + 0.0514(1 + \frac{0.0289}{V})]$$

$$- \frac{4.1497}{V^2}(1 - \frac{0.02086}{V}). \qquad (5.18)$$

No limits on the pressure or temperature range were put on the equation by West (101). It can be seen from Figure 5.7 that the conditions for which the constants were evaluated have been exceeded. West (101) did not extend his data, calculated from this equation of state, even to the critical point. The range in which the Beattie-Bridgeman equation is useful is 100 - 200 atm and for densities below the critical density. However, the equation does not correspond to the observed data very well, even in the supposedly useful range.

A technique that does produce good agreement over the range of interest is the use of the theorem of corresponding states. A statement of the theorem as given by Comings (26, p. 252) is:

> All gases, when each is compared at a temperature and pressure that is the same fraction of its critical temperature and critical pressure, have nearly the same compressibility factor, and all deviate from perfect-gas behavior to the same degree. They may thus be considered as in corresponding states.

Charts of compressibility factor plotted against the reduced pressure, P/Pc, at various values of reduced temperature, T/Tc, have been prepared. The charts of Nelson and Obert (71) based on a survey of 30 gases, of which one was hydrogen sulfide, are the most complete. These charts, while not published in the article by Nelson and Obert (71), are reproduced in Comings (26, p. 255-257). Agreement between the observed data and the values calculated by this theorem is quite good over the entire range of interest in this investigation, as can be seen from Figure 5. 7.

Pressures calculated from the virial equation of state obtained in this investigation are accurate to one percent for all pressures greater than 200 atm. At pressures below 200 atm the errors due to reading the gauge become significant and errors as large as three percent are observed for the lowest densities used. The inaccuracy over the entire pressure range arises from two sources.

The first source of error is the uncertainty in the volume due to thermal expansion. This will be a maximum at the highest temperatures attained but is less than 0. 7%. At lower temperatures this error is less than for the higher temperatures. Since the volume

increases, this will decrease the pressure reading from the true value.

The second source of error is that arising through the dead-space correction that had to be made. Two sources contributed to the error in this correction. The first source of error in the correction was that connected with the pressure gauge. It could be read accurately to three atmospheres. At low pressures this error was significant, while at high pressures it was insignificant. The inaccuracy due to the calibration of the gauge was small. It was calibrated at the factory with standards traceable to the National Bureau of Standards to 1/4% accuracy of full scale at a minimum of five points. Since the limiting accuracy of the Bourdon tube gauge is at the high pressure end (26, p. 85) and since most of the measurements in this investigation were made below the 3/4 of full scale recommended range, most of the pressures read will be more accurate than the 1/4% claimed for the gauge. Bourdon tube gauges read high at the high pressures.

The final source of error is that due to the density measurements. Errors arise from two sources in determining the density of the hydrogen sulfide. These are errors in determining the volume of the vessel and in removing and weighing the hydrogen sulfide in the vessel. Since a low surface tension liquid, such as ethyl alcohol, was used as a displacement fluid, the possibility of bubbles of air

trapped in the vessel is small. Rapid displacement of the air in the vessel would reduce the possibility of loss due to evaporation. The loss is estimated to be less than 0. 2 ml resulting in an error of less than 0. 2%. A negligible source of error is that due to the transfer of hydrogen sulfide from the high pressure vessel to the calibration vessel. Hydrogen sulfide was condensed into a partially evacuated vessel. It could be removed almost completely, from the tubing connecting the calibration vessel to the filling system manifold, by the cryogenic pumping action of the Dry Ice-acetone cold bath. Since evacuation of the calibration vessel was carried out rapidly and at room temperature, the possibility of a detectable quantity of water being condensed in the calibration vessel is small. The error arising from the density measurements would result in a smaller density value and consequently a lower value for the pressure.

VI. ELECTRICAL MEASUREMENTS ON SUPERCRITICAL HYDROGEN SULFIDE

Introduction

The electrical properties of a solution provide some insight into the physical nature of that solution. Even solutions in supercritical fluids, while they are not liquids in the ordinary sense, lend themselves to analysis by this method.

Conductivity and dielectric constant measurements have been made on hydrogen sulfide, but they have been restricted to low temperatures with three exceptions. The earliest measurements were made by Eversheim (31) who also made one of the three sets of dielectric constant measurements in the supercritical state. He examined the dielectric constant of hydrogen sulfide in a specially designed cell. By simply inverting the cell he could measure either the vapor in equilibrium with the liquid or the liquid. The measurements were made with no account taken of the density of the hydrogen sulfide. His measurements were made up to a temperature of 160° C. The dielectric constant he measured had a value of about 2. 7 in the region above the critical temperature and was nearly independent of temperature in the supercritical region. The density in his cell could not have been more than 0. 5 g/cc because of the physical limitations imposed by the design of the cell.

Von Braunmühl (96) made a set of dielectric constant measurements at very low gas densities over the temperature range from room temperature to slightly above the critical temperature.

Zahn and Miles (105), in the third set of measurements above the critical temperature, studied the dielectric constant of gaseous hydrogen sulfide over the temperature range of -74 to +269°C and gas pressures up to atmospheric pressure. They found that the dielectric constant of hydrogen sulfide could be interpreted by the Debye equation

$$(\epsilon - 1)VT = AT + B, \qquad (6.1)$$

where ϵ is the dielectric constant, V is the molar volume, T is the absolute temperature, and A and B are arbitrary constants assigned the values 0.001223 and 0.722 respectively.

Kemp and Denison (49) and Smyth and Hitchcock (43, 90) studied the dielectric properties of the three phase modifications of solid hydrogen sulfide.

Bickford and Wilkinson (11) measured the dielectric constant of liquid hydrogen sulfide at -78.5°C. Their value was 8.27. Bickford (10) later measured it under the same conditions and found a value of 9.05.

Lineken and Wilkinson (64) report a value for the dielectric constant at -78.5°C as 9.05 in agreement with that found by

Bickford (10).

Havriliak, Swenson, and Cole (41) studied hydrogen sulfide from -210°C through the melting point and up to the boiling point at -61°C. They also observed the three solid phases and reported values of 8.04 for the dielectric constant at the boiling point and 8.99 at Dry Ice-acetone temperature (-78.6).

The electrical conductivities have been measured a number of times. There is very little agreement in anything except the order of magnitude. The earliest measurement was made by Skilling (86) who reported that there was no galvonometer deflection even when a 40 volt battery was placed in the circuit. The electrodes were a platinum wire in one end of the tube that he used to condense the hydrogen sulfide and a pool of mercury at the other end.

Walker, McIntosh, and Archibald (100) qualitatively measured conductivities of a number of organic compounds dissolved in liquid hydrogen sulfide at -80°C. They concluded that the best conductors were the solutions containing one of the organic bases.

The first quantitative estimate of the specific conductance was made by Antony and Magri (4) who reported for 81°C an upper limit of 0.1×10^{-6} $ohm^{-1} cm^{-1}$.

The same result was obtained by Steele, McIntosh, and Archibald (93) who made quantitative measurements on the systems examined by Walker, McIntosh, and Archibald (100).

Quam and Wilkinson (75, 76) reported an upper limit to the conductivity of 1×10^{-11} ohm^{-1} cm^{-1} for pure liquid hydrogen sulfide at -78.5°C. They used a direct current Wheatstone bridge for the measurements. All of the measurements were made in an open cell.

Chipman and McIntosh (25) concluded, on the basis of conductivity measurements, that amines, halogens, and some heavy metal halides are ionized in liquid hydrogen sulfide at -78.5°C.

Ralston and Wilkinson (77) reported a value of 1×10^{-11} $ohm^{-1}cm^{-1}$.

In a series of experiments specifically designed to dispel the controversy surrounding the value of the specific conductance of liquid hydrogen sulfide, Satwalekar, Butler, and Wilkinson (84) reported a value of 3.78×10^{-11} $ohm^{-1}cm^{-1}$ at -78.5°C. They were the first to note the effect of small quantities of water on the conductance of liquid hydrogen sulfide. The measurements were made by a direct current method.

Bickford and Wilkinson (11), using an alternating current impedance bridge, reported a value of 1.17×10^{-9} $ohm^{-1}cm^{-1}$. Bickford (10) later reported a value for the same temperature, -78.5°C, of 3.1×10^{-10} $ohm^{-1}cm^{-1}$.

The average value for the conductance of 23 samples at -78.5°C was found to be 3.08×10^{-10} $ohm^{-1}cm^{-1}$. Lineken and Wilkinson (64) reported this result in connection with some work on the

conductances of solutions of a number of the organosubstituted ammonium chlorides in liquid hydrogen sulfide.

Lineken (63) later used hydrogen sulfide having conductance values from 5.5×10^{-10} to 8.8×10^{-10} $ohm^{-1} cm^{-1}$ in experiments to show the effect of the concentration of iodine in liquid hydrogen sulfide on the conductivity.

Experimental

An electrical impedance is a vector quantity that, when reduced to its simplest equivalent circuit, has two components that must be compensated independently to obtain a true null. In the particular application of concern to this investigation, a resistive component and a capacitative component must be accurately determined. As the result, information on two aspects of the solution under study will be provided.

The impedance bridge used in this investigation was based on a design by McGregor et al. (67). It is essentially a direct capacitance comparison bridge with a resistance compensating network to balance the shunt resistance around the unknown capacitance. Stray capacitances were eliminated through the use of a three-terminal network. The entire assembly is shown schematically in Figure 6.1A.

An Electro Scientific Industries CA 719 standard decade transformer was used to provide the accurate voltage division necessary

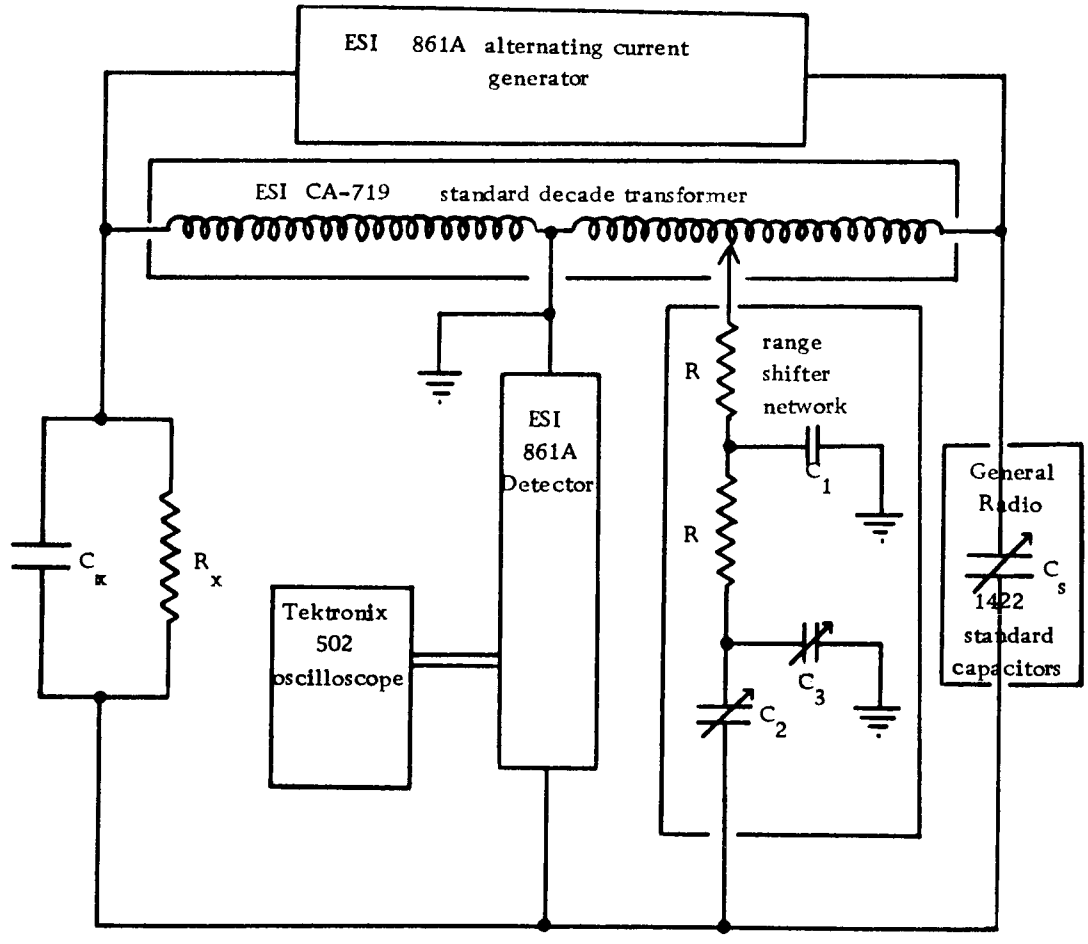

Figure 6. 1. A) Bridge network with the transformer arms in a one to one ratio to each other.

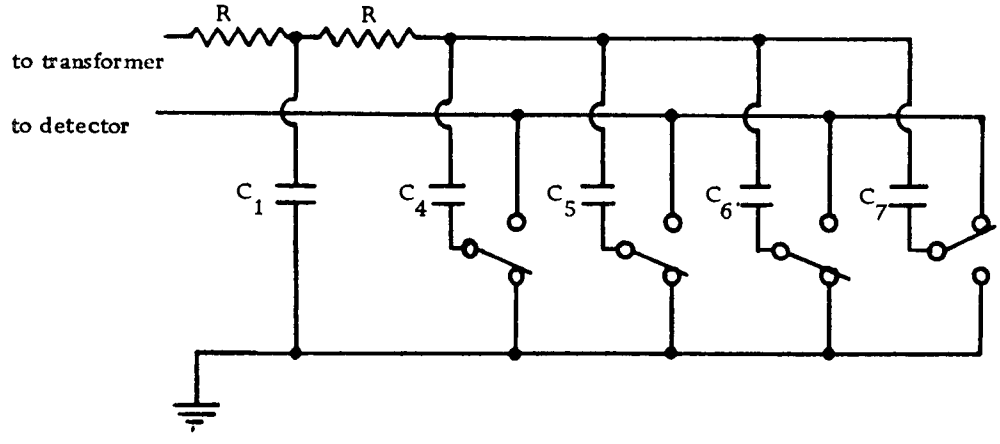

Figure 6. 1. B) Range shifter network showing the arrangement of the capacitors used to change the conductivity range.

for this type of bridge. Range multiplication factors of 1:1, 1.2:1, 10:1, and 12:1 were possible due to the arrangement of taps on the transformer.

General Radio series 1422 variable standard capacitors with worm gear corrections were the capacitance standards to which the unknown capacitances were compared. Direct capacitance measurements were possible over the range of 0.05000-11.000 pf with the 1422 CD capacitor and over the range of 50.0-1100.0 pf with the 1422 CB capacitor. By changing the output connections on the transformer, the range of 11.000-50.0 pf could be obtained and the upper end could be extended to 12,300 pf.

The transformer and the standard capacitors were calibrated by Electro Scientific Industries and by General Radio, respectively, against standards traceable to the National Bureau of Standards. A certificate showing the corrections to be made was furnished with each component.

The resistance compensating network is shown schematically in Figure 6.1B. All capacitors used in this circuit were selected by comparing them to the standard capacitors. The resistances were measured on the Electro Scientific Industries PVB-300 standard bridge. All component values were chosen to conform to those given for a frequency of 1000 hz by McGregor et al. (67).

The alternating current generator and detector was an Electro

Scientific Industries model 861A. Calibration of the generator at 1000 hz was carried out with a Hewlett-Packard 5232A electronic counter. A Tektronix model 502 oscilloscope was used as a phase detector by observing the Lissajous pattern produced by the different phase properties of the generator output and the detector output. The detector had a sensitivity of 1 μV full scale on the most sensitive range.

A derivation of the balance conditions

$$\frac{1}{R_u} = \frac{S\omega^2 C_1 R[2(C_1 + C_2) + C_T]}{[1 - R^2\omega^2 C_T(C_1 + C_2)]^2 + R^2\omega^2[2(C_1 + C_2) + C_T]^2} \quad (6.2)$$

and

$$C_u = C_s - \frac{SC_1[1 - R^2\omega^2 C_T(C_1 + C_2)]}{[1 - R^2\omega^2 C_T(C_1 + C_2)]^2 + R^2\omega^2[2(C_1 + C_2) + C_T]^2} \quad (6.3)$$

for the bridge, using the 1:1 multiplication range, is given in the Appendix. Using the values for the fixed parameters for this particular bridge, the balance conditions may be simplified to

$$R_u = \frac{1.124 \times 10^{10}}{SC_1} \quad (6.4)$$

and

$$C_u = C_s - 2.440 \times 10^{-5} SC_1, \quad (6.5)$$

where R_u and C_u are the unknown resistance and capacitance in

ohms and picofarads respectively, C_s is the value of the standard capacitor in picofarads, S is the reading on the transformer and C_1 is the value of the range shifting capacitor in picofarads.

The bridge was calibrated on the capacitance ranges by the intercomparison of 3 three-terminal capacitors. All of the ranges examined showed complete agreement between the capacitances after the calibration correction was applied. The resistance measuring portion of the bridge was calibrated by measuring a series of shielded, Victoreen carbon film, high value resistors. The resistance calibration is shown in Figure 6. 2. Calibration was carried out over the resistance range from 10^5 - 10^{10} ohms. The resistance and capacitance balance independently in all cases except on range 5 when the resistance is low (S is large). In that case a slight correction must be made. At 10^{10} ohms the plot of actual resistance against transformer reading becomes non-linear. This is due to the leakage through the insulation to the shielding. It effectively puts another resistance in parallel with the actual resistance. This limits the bridge effectiveness to a range of 10^5-10^{10} ohms.

A cell for making the measurements was designed and built from four concentric cylinders of tantalum. Teflon end pieces were used for spacing and insulating the cylinders. To compensate for the large difference in the coefficients of expansion of the Teflon and the tantalum, the ends of the tantalum tubes were slit to form

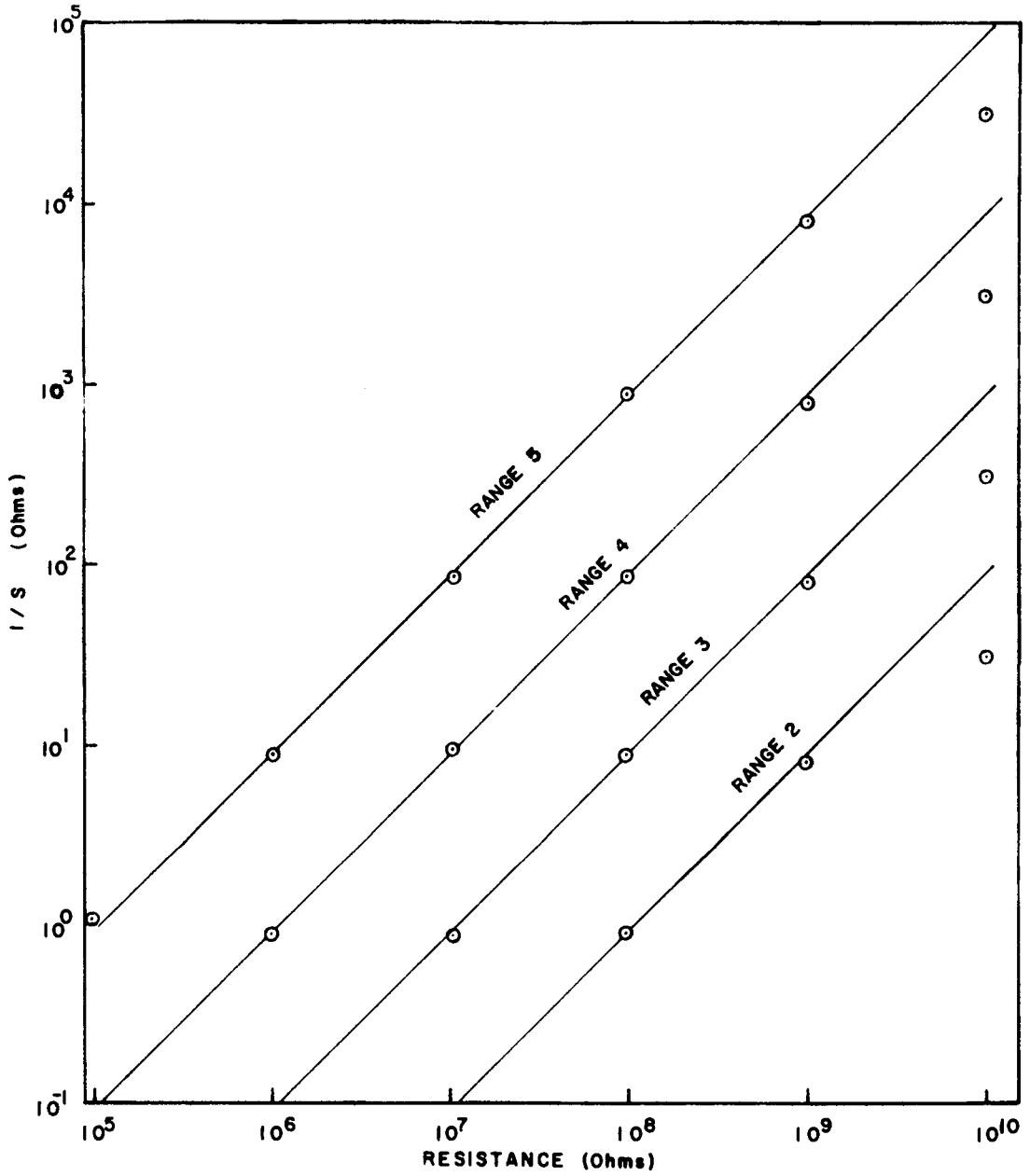

FIGURE 6.2. CALIBRATION OF THE RESISTANCE MEASURING PORTION OF THE IMPEDANCE BRIDGE.

"springs". These "springs" kept each of the tantalum cylinders from moving independently of the other cylinders and, as the result, mechanically changing the value of the capacitance and of the cell constant. The construction of the cell is shown in Figure 6. 3A.

Each cylinder had a small diameter wire spot-welded to it. These wires passed through holes in the Teflon end plates and were used to connect alternate cylinders together on top of the Teflon end plate. The connections to the lead-ins on the reactor cover were made to these wires.

Bridgman (18) reported a polymorphic phase transition that occurs with Teflon at 5000 atm and room temperature. The 2. 3% change in volume is not much greater than the change in volume due to thermal expansion and in the opposite direction. Thus, if the temperature coefficient of the phase transition could occur at the extremes of temperature and pressure (220°C and 2000 atm) any sudden change should be compensated for by the "springs" cut into the ends of the cylinders.

Calculation of the capacitance can be made from the formula for the capacitance of two long concentric cylinders as given in Hirst (42, p. 370),

$$C = \frac{2\pi \epsilon_r \epsilon_o L}{\log_e \frac{R}{r}} \quad , \tag{6. 6}$$

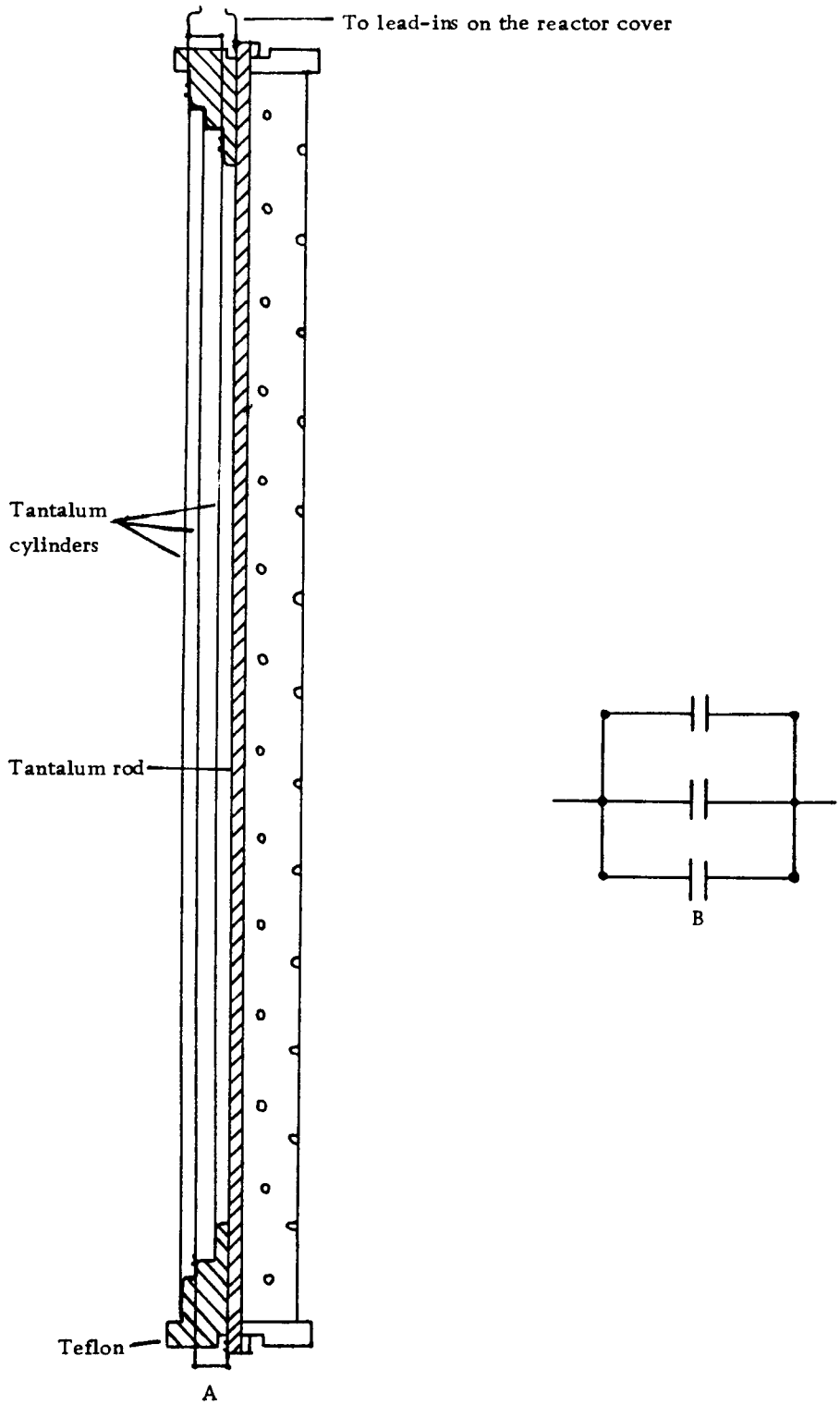

Figure 6. 3. A) A cut-away view of the conductivity cell. B) The network of capacitances making up the cell.

where C is given in farads if ϵ_r is the dielectric constant of the medium, ϵ_o is the permittivity of free space (8.85×10^{-12} farads/meter), L is the cylinder length in meters, R is the radius of the larger cylinder, and r is the radius of the smaller cylinder. The cell can be considered to be three capacitors in parallel as shown in Figure 6.3B. Thus, the calculated capacitance is composed of the sum of three terms like that in equation 6.6. A vacuum capacitance value of 76.7 pf was calculated for the cell. The measured value is 76.6 pf.

The cell constant, which is the geometrical factor

$$K = \frac{L}{A} \tag{6.7}$$

where L is the inter-cylinder difference and A is the area of the cylinder, is equal to 0.0025 cm^{-1}.

A possible pressure effect on the electrode was checked for by measuring the capacitance of a non-polar dielectric. Argon was chosen as the dielectric and the capacitance measurements were made as a function of pressure. There was a linear variation of the capacitance with the pressure indicating that there was no pressure effect on the electrode.

The vacuum capacitance was found to be independent of temperature over the temperature range used in this investigation.

An oil bath, described in the section on the pressure-

temperature properties of hydrogen sulfide, was used to provide a constant temperature environment.

The high pressure system consisted of a reactor constructed from #316 stainless steel which was designed for use to 250°C and 30,000 psi, a 0-30,000 psi Bourdon tube gauge, a high pressure valve, a gauge isolator, and the high pressure tubing required to make the connections to the various components. The high pressure system is shown in Figure 6.4. To keep the volume to a minimum in this system, a gauge isolator was used. National Research Corporation DC 704 silicone diffusion pump fluid was used as the pressure transmitting fluid between the gauge isolator and the gauge. Water was passed through a cooling coil mounted on the gauge isolator to prevent thermal deterioration of the quad-ring used as a seal on the gauge isolator piston.

The entire assembly was mounted rigidly on an aluminum stand. This stand was securely fastened to a steel plate that formed the base. Heaters and thermal sensing devices were mounted on an aluminum plate that was attached to the stand. The entire assembly rested on the bottom of the oil bath.

A standardized filling procedure was adopted. After assembling the vessel, it was connected to the bridge and a "zero point" measurement was made to check for a short circuit or an open circuit. If values of 76.9 pf and 10^{10} ohms were not obtained with air

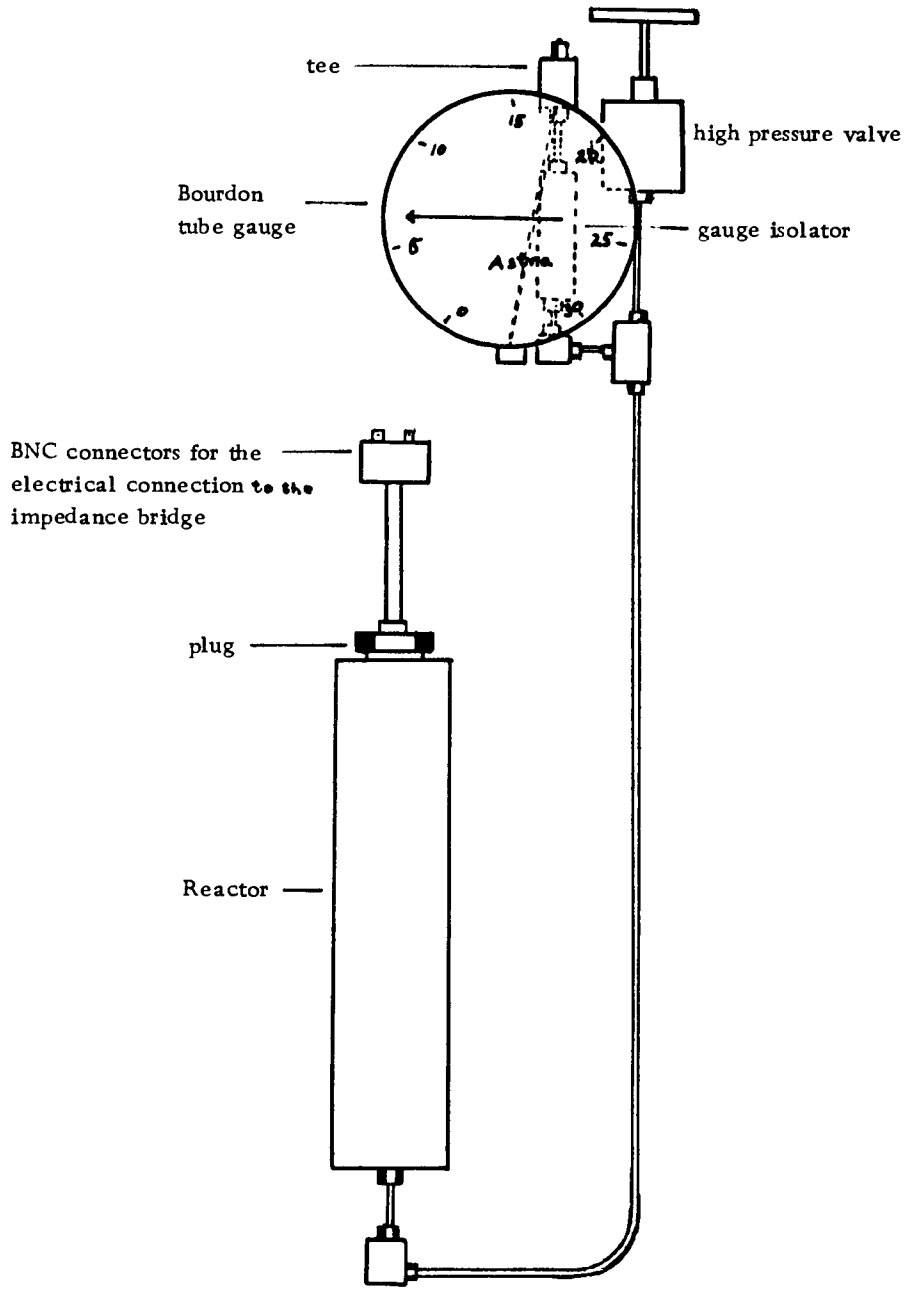

Figure 6. 4. Stainless steel high pressure system used for the electrical measurements.

as the dielectric, the vessel was disassembled and the difficulty corrected. The vessel was evacuated for a period of at least two hours. During this time period the Millipore filter disc was changed. At the end of the evacuation time the large cold bath was prepared, the chlorobenzene slush in the cold traps was prepared, and the valves were set in the manner under which the calibration of the flow meter took place. Metering of the hydrogen sulfide into the vessel could then be carried out using a stop watch, the pressure gauge, and the flow meter to determine the quantity deposited.

Four series of experiments were conducted in which the conductivity and the dielectric constant of pure supercritical hydrogen sulfide or solutions of salts in supercritical hydrogen sulfide were measured. The first and most extensive experiment in this series was conducted on pure hydrogen sulfide over approximately the same density-temperature range investigated during the pressure-volume-temperature experiments. The second and third series of experiments were performed on solutions of lead sulfide and stannic sulfide over a narrow density range in the high density region. The final experiment was a study of a solution of triethylammonium chloride over a narrow density range at the low density end of the experimentally feasible density region. All of these experiments were conducted over the temperature range of 373-493° K.

A sampling technique was used to vary the density in the vessel.

After the set of measurements were made on the initial quantity present, the vessel was connected to the calibration vessel through another high pressure valve. Increments of hydrogen sulfide were removed that were equal to the quantity of liquid that could be held in the tubing between the two high pressure valves. The exact quantity was determined by weighing on the rider balance.

Measurements on the system were made at intervals long enough for the system to come to thermal equilibrium.

A leak, due to a defective Mycalex insulator, was present throughout the set of measurements. The insulators were defective as the result of the manufacturing process. Thus, a constant density system was virtually impossible to achieve.

Since the leak problem could not be circumvented by replacing the insulator with an equally defective insulator, a number of materials were examined in an attempt to stop the leak by filling the cracks. The only material that worked at all satisfactorily was water glass, a soluble sodium silicate. By putting a drop of this material around the lead on the high pressure side of the insulator, filling the vessel with nitrogen directly out of a commercial cylinder, and then heating it to 220°C in the oil bath, the leak could be slowed to the point where measurements could be made over a time period of several days.

The knowledge of the quantity of hydrogen sulfide actually

present in the vessel could not be used to determine the density because of the decrease caused by the continual slow leak. An alternate method is the use of a pressure-density plot at constant temperature using the virial expressions that were obtained during another portion of this investigation. Interpolation at constant pressure allows this graph to be used to determine the density for temperatures between two of the plotted isotherms.

There are several sources of error in this method. The least serious is the assumption that the variation of the density with temperature in a constant volume and constant pressure system is linear over a 20° C temperature range. The more serious error arises as the result of the gauge circuit. Any pressure drop across the gauge isolator piston due to friction would cause an error in the pressure reading with a resultant error in the density. A slight error in the pressure reading would cause a sizeable error in the density, particularly at low pressures. The process of graphically inverting virial series is good at high densities where the pressure-density curve is steep. At low densities where the slope of the curve is more gentle, the inversion process is not as accurate. The advantage to this method is that no dead-space correction, such as the corrections that were necessary for the pressure-volume-temperature data, would have to be made.

Discussion

The imposition of an electric field between two parallel plates is effected by the presence of a gas. The extent of these effects for a polar molecule will be derived below following a treatment due to Mayer and Mayer (66, p. 327-340).

If the electric field across the plates is $\overline{E}$, one of the definitions of the dielectric constant is

$$\epsilon - 1 = \frac{4\pi \overline{P}}{\overline{E}} \tag{6.8}$$

where $\overline{P}$ is the vector sum of the dipole moments per unit volume

$$\overline{P} = \frac{N}{V} \overline{\mu}, \tag{6.9}$$

where $\overline{\mu}$ is the average oriented dipole moment and $\frac{N}{V}$ is the number of molecules per unit volume. Both the polarization, $\overline{P}$, and the electric field, $\overline{E}$, are vector quantities. The relationship between the permanent dipole moment, μ_o, and the oriented average dipole moment, $\overline{\mu}$, is found by a consideration of the probability that the dipoles will be oriented in space by the field $\overline{E}$ and is found to be for all practical electrical fields

$$\overline{\mu} = \frac{1}{3} \frac{\mu_o^2}{kT} \overline{E}, \tag{6.10}$$

where k is Boltzmann's constant and T is the absolute temperature. In addition to the polarization due to the orientation of the dipoles, there is superimposed on the permanent dipole moment the effect of an induced dipole moment due to the effect of the field acting on the positively and negatively charged parts of the molecule. The average induced dipole moment is proportional to the field and is in the direction of the field

$$\overline{\mu}_i = \alpha \overline{E}, \tag{6.11}$$

where α is the proportionality constant and is called the polarizability. Thus, the average projection of the dipole moment in the direction of the field is

$$\overline{\mu} + \overline{\mu}_i = (\alpha + \frac{1}{3}\frac{\mu_o^2}{kT})\,\overline{E}. \tag{6.12}$$

The field within any material having a dielectric constant greater than one ($\epsilon > 1$) is different than the value of the field outside the material. This local field, $\overline{E}_{loc}$, which must be calculated from the average polarization density in the material, is given by the Clausius-Mosotti formula

$$\overline{E}_{loc} = \overline{E} + \frac{4\pi \overline{P}}{3} \tag{6.13}$$

for which a derivation is given in Debye (29, p. 9-11). The polarization from equations 6.9 and 6.12 is given by the expression

$$\overline{P} = \frac{N}{V}\left(a + \frac{1}{3}\frac{\mu_o^2}{kT}\right)\overline{E}\,. \qquad (6.14)$$

Substituting the field actually experienced by the molecule from equation 6.13 into equation 6.14 yields

$$\overline{P} = \frac{N}{V}\left(a + \frac{1}{3}\frac{\mu_o^2}{kT}\right)\left(\overline{E} + \frac{4\pi\overline{P}}{3}\right) \qquad (6.15)$$

and then using the definition of the dielectric constant given in equation 6.8, the result is

$$\left(\frac{\epsilon - 1}{\epsilon + 2}\right)\frac{V}{N} = \frac{4\pi}{3}\left(a + \frac{1}{3}\frac{\mu_o^2}{kT}\right). \qquad (6.16)$$

Equation 6.16 is called the Debye equation.

According to Mayer and Mayer (66, p. 340) the quantity on the left hand side of equation 6.16 is nearly independent of density up to very high pressures for most gases at a constant temperature.

The electrical measurements on this system were made at random temperatures due to the lack of a precision setting device on the thermoregulator. This necessitated an interpolation process to obtain the values of the dielectric constant as a function of density for a series of isotherms. The errors introduced by this technique were small because the variation of the dielectric constant with temperature was small. Large scales were used throughout to maintain the original accuracy. A plot of the variation of the

dielectric constant with density is shown in Figure 6. 5. The Clausius-Mosotti function,

$$CM = \frac{N}{V}\left(\frac{\epsilon - 1}{\epsilon + 2}\right), \tag{6.17}$$

is commonly used to present dielectric constant data as it is a relatively invariant function. Even though hydrogen sulfide is a polar molecule the variation of the Clausius- Mosotti function as a function of density is less than ten percent for all temperatures investigated. This is in agreement with the conclusion drawn by Mayer and Mayer (66, p. 340) regarding the density dependence of the dielectric constant and indicates that the fraction of hydrogen sulfide involved in pair interactions and higher order interactions is small.

Buckingham and Pople (21) suggest the use of a virial expression of the type

$$\left(\frac{\epsilon - 1}{\epsilon + 2}\right)\frac{V}{N} = A + B\left(\frac{N}{V}\right) + C\left(\frac{N}{V}\right)^2 + \ldots \tag{6.18}$$

for the analysis of data of this type. A least squares analysis was used to determine the virial coefficients A, B, and C by setting up the expressions

$$nA + \sum_{i=1}^{n} \rho_i B + \sum_{i=1}^{n} (\rho_i)^2 C = \sum_{i=1}^{n} \left(\frac{\epsilon_i - 1}{\epsilon_i + 2}\right)\frac{1}{\rho_i} \tag{6.19}$$

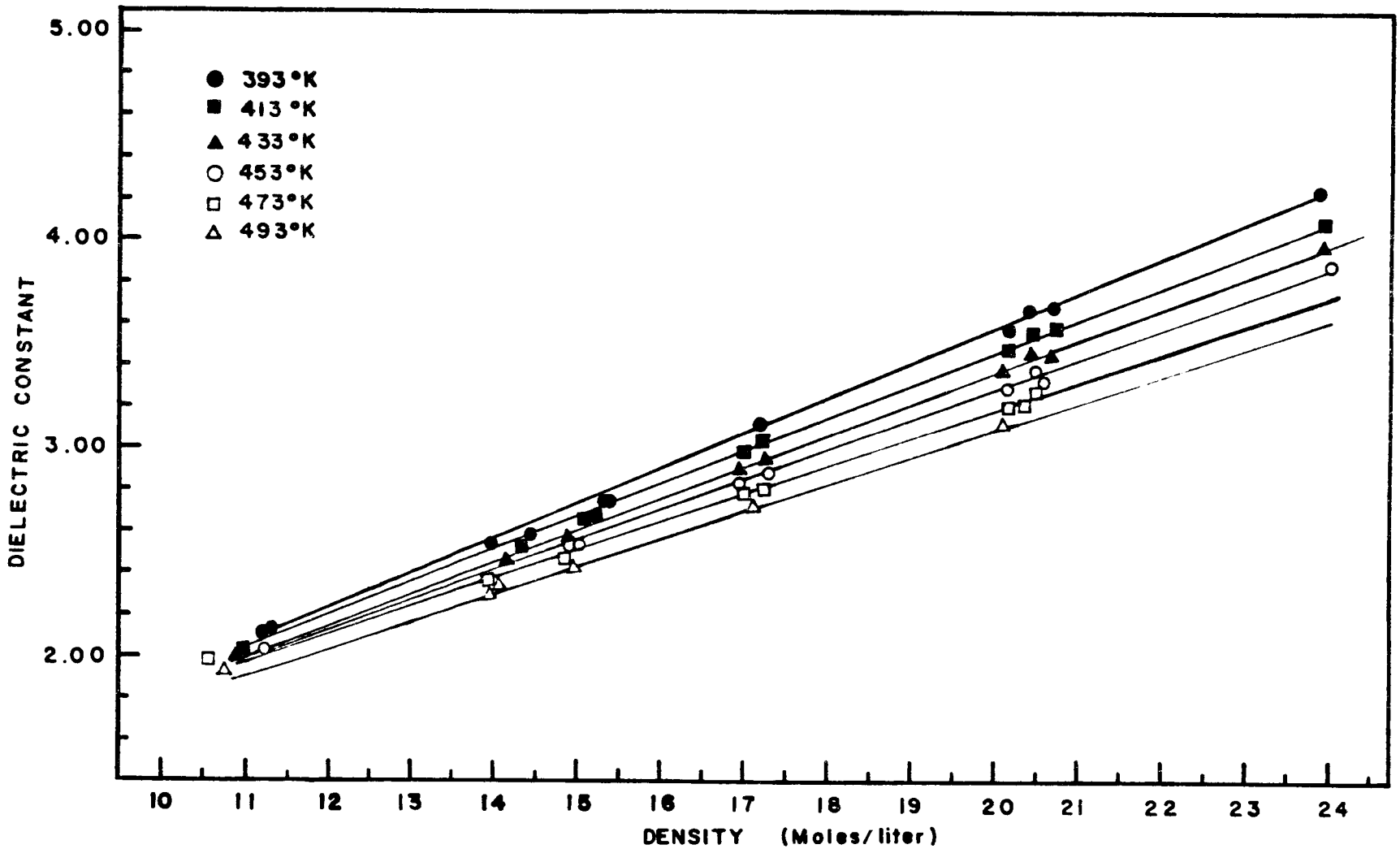

FIGURE 6.5. VARIATION OF THE DIELECTRIC CONSTANT WITH DENSITY.

$$\sum_{i=1}^{n} \rho_i A + \sum_{i=1}^{n} (\rho_i)^2 B + \sum_{i=1}^{n} (\rho_i)^3 C = \sum_{i=1}^{n} \left(\frac{\epsilon_i - 1}{\epsilon_i + 2}\right) \tag{6.20}$$

$$\sum_{i=1}^{n} (\rho_i)^2 A + \sum_{i=1}^{n} (\rho_i)^3 B + \sum_{i=1}^{n} (\rho_i)^4 C = \sum_{i=1}^{n} \left(\frac{\epsilon_i - 1}{\epsilon_i + 2}\right)\rho_i \tag{6.21}$$

and then solving this set of equations for A, B, and C. In equations 6.19, 6.20, and 6.21, n is the number of sample points, ρ_i and ϵ_i are the density and dielectric constant, respectively, of the i^{th} point.

Dielectric virial coefficients were determined for the supercritical fluid phase of hydrogen sulfide for 20° K intervals beginning with a temperature of 393° K. The maximum temperature was 493° K. The dielectric constant data obtained during this investigation is given in Table 6.1. Table 6.2 gives the values obtained for A, B, and C from the solution of equations 6.19, 6.20, and 6.21. A comparison between the curves obtained by use of the coefficients in Table 6.2 and the experimental points are shown in Figure 6.6.

Unfortunately the small differences between large numbers that had to be used in solving equations 6.19, 6.20, and 6.21 for A, B, and C did not yield a completely consistent set of coefficients. Some observations regarding these coefficients are possible. The coefficient A is related to the term on the right side of equation

Table 6. 1. Dielectric constants and Clausius Mosotti function for pure, supercritical hydrogen sulfide.

Density, ρ, in moles per liter.
Clausius-Mossotti function, $(\frac{\epsilon - 1}{\epsilon + 2})\frac{1}{\rho}$, in liters per mole.

ρ	ϵ	$(\frac{\epsilon - 1}{\epsilon + 2})\frac{1}{\rho}$	ρ	ϵ	$(\frac{\epsilon - 1}{\epsilon + 2})\frac{1}{\rho}$
	T = 393° K			T = 413° K	
23. 97	4. 31	0. 0219	23. 85	4. 15	0. 0215
20. 73	3. 69	0. 0228	20. 74	3. 58	0. 0223
20. 42	3. 67	0. 0231	20. 46	3. 56	0. 0225
20. 17	3. 57	0. 0229	20. 14	3. 47	0. 0224
17. 20	3. 12	0. 0241	17. 21	3. 04	0. 0235
15. 34	2. 74	0. 0239	17. 04	2. 99	0. 0234
15. 33	2. 74	0. 0239	15. 23	2. 66	0. 0234
14. 95	2. 62	0. 0235	15. 08	2. 65	0. 0234
14. 46	2. 58	0. 0239	14. 88	2. 55	0. 0229
13. 99	2. 52	0. 0240	14. 32	2. 52	0. 0235
11. 31	2. 12	0. 0240	13. 95	2. 46	0. 0234
11. 22	2. 11	0. 0241	11. 29	2. 08	0. 0235
			11. 25	2. 08	0. 0236
	T = 433° K			T = 453° K	
23. 83	4. 01	0. 0210	23. 80	3. 91	0. 0207
20. 68	3. 45	0. 0218	20. 56	3. 32	0. 0212
20. 45	3. 47	0. 0221	20. 49	3. 38	0. 0215
20. 11	3. 38	0. 0220	20. 13	3. 29	0. 0215
17. 24	2. 95	0. 0229	17. 30	2. 88	0. 0223
16. 97	2. 90	0. 0229	16. 96	2. 83	0. 0223
14. 95	2. 59	0. 0231	15. 01	2. 53	0. 0225
14. 89	2. 57	0. 0231	14. 92	2. 52	0. 0225
14. 72	2. 48	0. 0224	14. 28	2. 43	0. 0226
14. 22	2. 47	0. 0231	14. 08	2. 41	0. 0227
13. 95	2. 40	0. 0228	11. 10	2. 01	0. 0227
11. 36	2. 05	0. 0228			
11. 23	2. 04	0. 0229			
	T = 473° K			T = 493° K	
20. 50	3. 29	0. 0211	20. 51	3. 21	0. 0208
20. 38	3. 22	0. 0209	20. 22	3. 13	0. 0205
20. 21	3. 21	0. 0210	17. 08	2. 72	0. 0213
17. 24	2. 80	0. 0218	14. 90	2. 43	0. 0217
17. 03	2. 78	0. 0218	13. 87	2. 31	0. 0219
14. 96	2. 47	0. 0220	10. 82	1. 94	0. 0221
14. 91	2. 47	0. 0221			
14. 01	2. 37	0. 0224			
13. 98	2. 36	0. 0223			

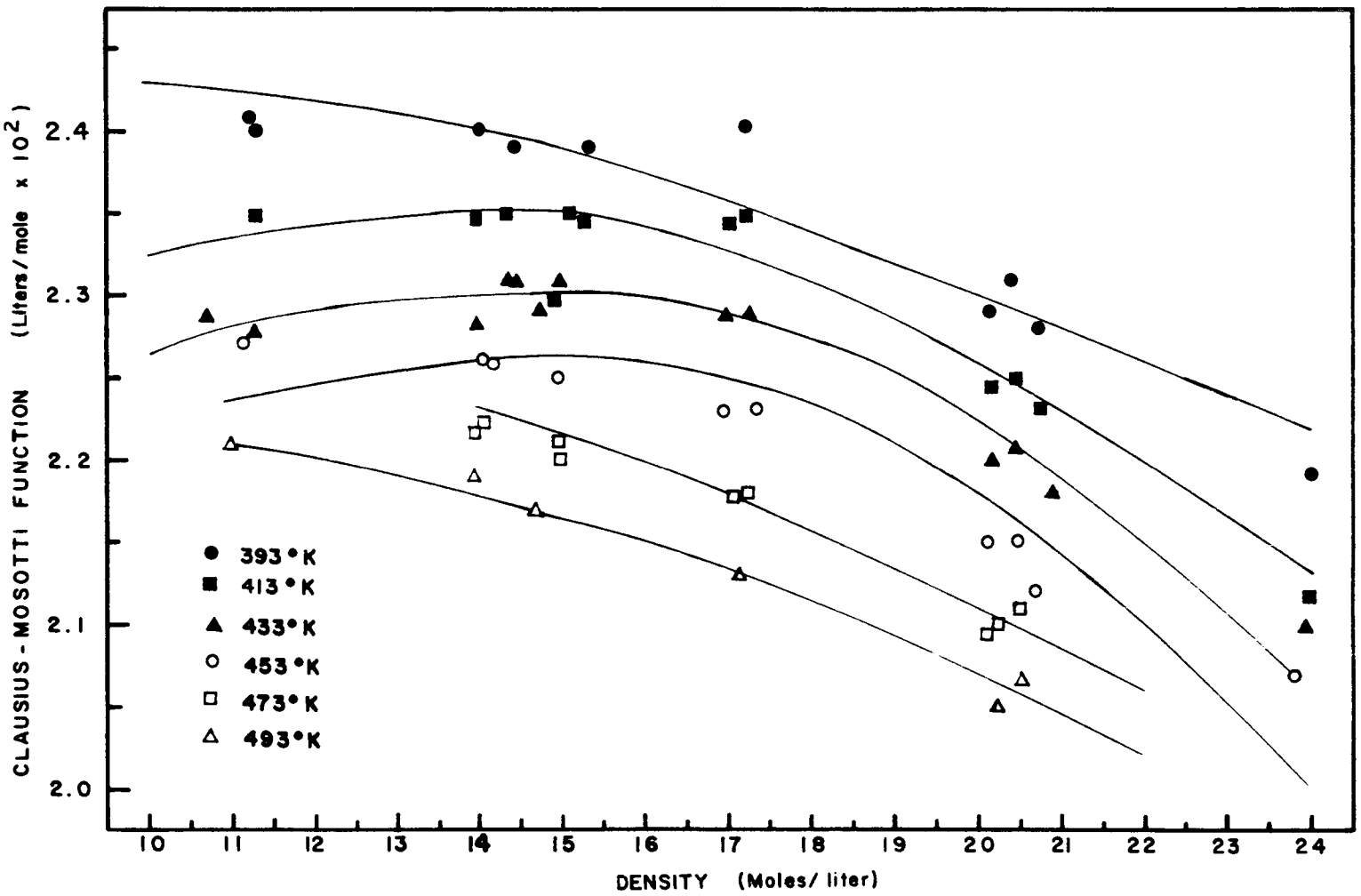

FIGURE 6.6. DIELECTRIC VIRIAL EQUATIONS. SOLID LINES ARE THE DIELECTRIC VIRIAL EXPRESSIONS. POINTS ARE EXPERIMENTAL DATA.

6. 16. It is an inverse function of the temperature and as the result should decrease with increasing temperature. This was observed for the first four temperatures examined with anomalous behavior noted for the last two temperatures.

Table 6. 2. Dielectric virial coefficients.

T	A	B	C
393°K	2.441×10^{-2}	5×10^{-5}	-6×10^{-6}
413°K	1.984×10^{-2}	5.4×10^{-4}	-2×10^{-5}
433°K	1.626×10^{-2}	9.0×10^{-4}	-3×10^{-5}
453°K	1.616×10^{-2}	8.8×10^{-4}	-3×10^{-5}
473°K	2.328×10^{-2}	0.3×10^{-4}	-7×10^{-6}
493°K	2.154×10^{-2}	1.6×10^{-4}	-1×10^{-5}

The coefficient B arises through the interactions due to pairing of molecules. A positive coefficient indicates that the dipoles are enhancing one another such that the resultant dipole is greater than that of the dipole due to the single molecule. A pair complex such as

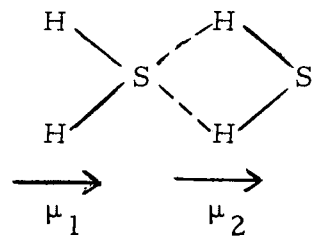

in which the dipoles are aligned and the dipole moment of the pair complex is the vector sum of the two dipoles, is the geometrical configuration of the complex. An unsymetrical pair complex, in which one of the weak S-H bond distances (shown by dotted lines) is longer than the other weak S-H bond distance, would also lead to an increased dipole moment. A complex such as shown would be expected to be a low temperature form. As the result the number of these complexes would decrease with increasing temperature. This would be reflected in a decrease in the magnitude of B. This appears to be true for three of the four high temperature coefficients. Comparison between the first order virial coefficients for the volumetric properties and the first order virial coefficients for the dielectric properties indicates that pair interaction is significant but that the fraction of molecules involved in pairing is not large. Both sets of coefficients differ from the preceding zero order coefficients by a factor of approximately 10^{-2}. This indicates that both methods of measurement are consistent with respect to the extent of pairing of molecules in the high temperature, supercritical fluid phase of pure hydrogen sulfide.

The third coefficient, C, is dependent upon third and higher order molecular interactions and consequently arises partially from dipole moment contributions of neighboring molecules in addition to the triplet complex. Whether there is any significant thermal

variation is difficult to say due to the scatter of the coefficients.

The dielectric constants observed for the solutions did not differ significantly from those observed for the pure solvent.

A distinct disadvantage of the use of water glass to seal the leak is its solubility in hydrogen sulfide. Because it is basic, ionization of the hydrogen sulfide takes place with a consequent increase in conductivity. The baked-on water glass was extremely hard and presented such a small surface to the action of the hydrogen sulfide that dissolution was a slow process. A hysteresis-like effect was observed in which the conductivity increased with increasing temperature, while with decreaseing temperature the conductivity decrease was much less for the corresponding increasing temperature. An example of this type of behavior is shown in Figure 6.7B.

The conductivity data measured during these experiments is not capable of yielding anything better than an upper limit due to the dissolution of the basic components in the water glass. In order to obtain a set of consistent data, only the points taken immediately after the vessel was filled and as the temperature was increased were considered. Because the thermal controller could be set only approximately to the temperature desired, no attempt was made to make the measurements at the six 20°C intervals considered for the virial expressions. Instead an interpolation process was used to obtain the conductivity values at the temperatures of interest.

A plot of the logarithm of specific conductivity against density is shown in Figure 6.7. It appears to be non-linear with density over the density range from 10 moles per liter to 24 moles per liter. Table 6.3 gives the conductivity data for pure hydrogen sulfide.

Table 6.3. Specific conductivity of pure, supercritical hydrogen sulfide.

Density, ρ, in moles per liter.
Specific conductivity, k, in ohm^{-1} cm^{-1}.

ρ	k	ρ	k	ρ	k
T = 393°K		T = 413°K		T = 433°K	
23.80	4.00×10^{-9}	23.84	4.25×10^{-9}	23.82	6.20×10^{-9}
20.70	2.05×10^{-11}	20.66	3.23×10^{-11}	20.69	5.11×10^{-11}
14.91	6.50×10^{-13}	14.90	9.78×10^{-13}	14.70	1.21×10^{-12}
T = 453°K		T = 473°K		T = 493°K	
23.79	1.04×10^{-8}	--	--	--	--
20.65	8.11×10^{-11}	20.70	1.46×10^{-10}	20.66	2.03×10^{-10}
14.15	1.18×10^{-12}	13.96	1.25×10^{-12}	13.88	1.39×10^{-12}

Slight increases in the specific conductivity were noted for solutions of stannic sulfide and silver sulfide in supercritical hydrogen sulfide. The specific conductivity of the solution of stannic sulfide was greater than that of silver sulfide. This agrees with the results of the solubility studies in which stannic sulfide was found

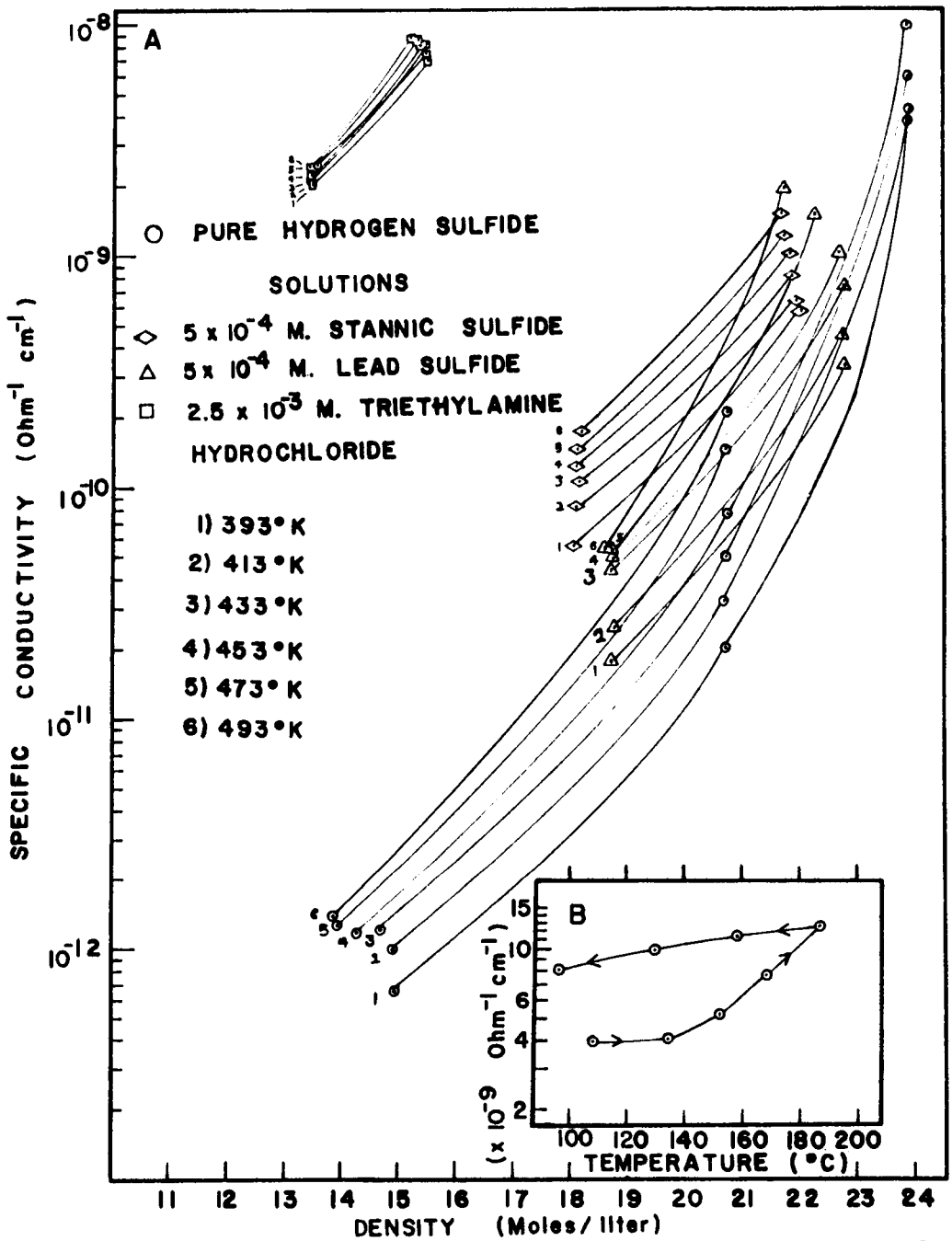

FIGURE 6.7. A) VARIATION OF THE SPECIFIC CONDUCTIVITY WITH DENSITY. B) TEMPERATURE EFFECT ON THE CONDUCTIVITY DUE TO DISSOLUTION OF THE LEAD-IN SEALANT.

to be more soluble than the silver sulfide. Maximum solution concentration in both cases was 5×10^{-4} molal. At the end of the experiment, salt was found distributed throughout the vessel, the electrode, and the tubing, although with stannic sulfide there was a very faint line of salt down the side of the vessel where it had been poured into the vessel. The conductivities of lead sulfide and stannic sulfide in solution with hydrogen sulfide are shown in Figure 6.7. Table 6.4 and 6.5 give the conductivity data for stannic sulfide and silver sulfide in supercritical, high density hydrogen sulfide.

Table 6.4. Specific conductivity of a 5×10^{-4} molal solution of stannic sulfide in hydrogen sulfide.

Density, ρ, in moles per liter.
Specific conductivity, k, in $ohm^{-1}\ cm^{-1}$.

ρ	k	ρ	k	ρ	k
T = 393° K		T = 413° K		T = 433° K	
22.04	5.80×10^{-10}	21.92	6.40×10^{-10}	21.83	8.38×10^{-10}
18.08	5.62×10^{-11}	18.10	8.42×10^{-11}	18.17	1.06×10^{-10}
T = 453° K		T = 473° K		T = 493° K	
21.81	1.08×10^{-9}	20.72	1.26×10^{-9}	20.65	1.56×10^{-9}
18.09	1.27×10^{-10}	18.12	1.50×10^{-10}	18.21	1.74×10^{-10}

Table 6.5. Specific conductivity of a 5×10^{-4} molal solution of lead sulfide in hydrogen sulfide.

Density, ρ, in moles per liter.
Specific conductivity, k, in $ohm^{-1} cm^{-1}$.

ρ	k	ρ	k	ρ	k
T = 393°K		T = 413°K		T = 433°K	
22.76	3.41×10^{-10}	22.68	4.52×10^{-10}	22.64	7.28×10^{-10}
18.67	1.75×10^{-11}	18.70	2.43×10^{-11}	18.70	4.81×10^{-11}
T = 453°K		T = 473°K		T = 493°K	
22.62	1.05×10^{-9}	22.20	1.55×10^{-9}	21.70	2.06×10^{-9}
18.72	5.08×10^{-11}	18.77	5.38×10^{-11}	18.71	5.74×10^{-11}

Anhydrous triethylamine hydrochloride was prepared by bubbling hydrogen chloride through vacuum-distilled triethylamine. The resultant fluffy, white solid was placed in a 150°C oven to remove any water or unreacted triethylamine. This material was used to prepare two 2.5×10^{-3} molal solutions at different solvent densities. The resultant solutions had conductivities that were over a thousand times that of the pure solvent. This agrees with the work of Quam and Wilkinson (75, 76) who found a thousandfold increase in the conductivity of 0.01 molal triethylammonium chloride at Dry Ice-acetone temperatures. The results of this experiment are also plotted in Figure 6.7 for comparison to the pure solvent and the other solutions. Table 6.6 gives the conductivity of

triethylammonium chloride in supercritical hydrogen sulfide.

Table 6.6. Specific conductivity of a 2.5×10^{-3} molal solution of triethylammonium chloride in hydrogen sulfide.

Density, ρ, in moles per liter.
Specific conductivity, k, in $ohm^{-1} cm^{-1}$.

ρ	k	ρ	k	ρ	k
T = 393° K		T = 413° K		T = 433° K	
15.48	8.36×10^{-9}	15.32	8.64×10^{-9}	15.20	8.82×10^{-9}
13.47	2.07×10^{-9}	13.48	2.16×10^{-9}	13.45	2.27×10^{-9}
T = 453° K		T = 473° K		T = 493° K	
15.39	8.38×10^{-9}	15.42	7.80×10^{-9}	15.47	7.34×10^{-9}
13.43	2.44×10^{-9}	13.51	2.48×10^{-9}	13.55	2.51×10^{-9}

Hydrogen sulfide as a solvent is apparently only slightly dissociated even at temperatures in excess of the critical temperature. The conductivity is affected very little by the presence of any material such as the heavy metal sulfides that interact only slightly with the solvent. Conductivity changes, such as were seen with triethylammonium chloride, are due to the formation of ionic species. With triethylammonium chloride the bisulfide ion and the triethylammonium ion are formed according to the reaction

$$(C_2H_5)_3N \cdot HCl + H_2S \longrightarrow (C_2H_5)_3NH^+ + HS^- + HCl. \qquad (6.22)$$

The hydrogen chloride molecule also dissociates into ions and contributes to the conductivity.

VII. CRYSTAL GROWTH EXPERIMENT

Introduction

The growth of crystals of difficultly soluble materials from supercritical solutions is one of the oldest processes occurring in nature. Hydrothermal deposits of quartz and other pegmatite minerals are found scattered throughout the world. These deposits were formed under conditions of high temperature and high pressure that are readily attainable under proper geological conditions.

Because quartz is geologically so important in the structure of the earth and because of its importance to the electronics industry, more effort has been expended in the elucidation of the conditions under which crystalline quartz is formed hydrothermally than for any other material. Thus, much of the technology currently in use for the study of supercritical systems was developed during the study of the silicon dioxide-water system. The commercial success of quartz crystal growth provided a great impetus to experimentation on crystal growth processes from hydrothermal solutions. The extensive work done on quartz crystal growth provides guide lines for designing experiments dealing with crystal growth from non-aqueous supercritical solvents.

Historical

In the years between the 1840's and 1943, there were at least 30 investigators who attempted to grow quartz crystals by one method or another. The investigators met with varying degrees of success, reporting crystal growth from the formation of microscopic crystals to the addition of 14 mm onto a seed crystal. The duration of the experiments ranged from three hours to eight years and the temperatures ranged from room temperature to 870° C. A survey of all of the recorded experiments conducted on the growth of quartz crystals, up to 1943, was made by Kerr and Armstrong (51). The significant experiments conducted in sealed metal containers above atmospheric pressures are briefly reviewed here.

The first recorded attempt to grow quartz crystals in a sealed tube was made by von Schafhäutl (97) who claimed to have produced microscopic crystals from an aqueous solution of freshly precipitated silica in a vessel that was probably not heated above 120° C and whose pressure did not exceed two atmospheres.

The most significant of the early attempts to duplicate, in the laboratory, the conditions under which these hydrothermal deposits are formed was made by Spezia (91) who noted that quartz crystals could be grown on seeds from alkaline supercritical water solutions over a six-month period. The small amount of growth occurring over

such a long period of time seemed to discourage all other attempts to grow quartz crystals until the needs of the military during World War II revived the interest in synthetic quartz crystals. During 1943 the German mineralogist, Nacken, was commissioned to devise a process to produce quartz oscillator plates in quantity for the German Army. A pilot plant was in operation toward the end of the war but the work apparently did not yield a commercially feasible process. The work of Nacken, taken in part from captured German documents, is reviewed in some detail by Van Praagh (94).

About the same time the Woosters (103) in England worked on the growth of quartz crystals and achieved some growth.

In 1946, at a symposium on the synthesis of single crystals held during the Boston meeting of the American Association for the Advancement of Science, the U. S. Army Signal Corps announced that some grants were available to study the problem of hydrothermal synthesis of crystals. A number of grants were awarded from which commercially feasible success was met by the Brush Development Company under the direction of Hale (38) and by the Bell Telephone Laboratories under the direction of Walker and Buehler (99). Brown et al. (19) in England also met with success at the same time.

This success in the growth of quartz under supercritical conditions led to the investigation of other materials. Walker (98) reported an attempt to grow zinc oxide crystals from an aqueous solution

in which crystals as large as 1/16 of an inch in cross section were produced. Kolb and Laudise (55, 56) report the growth of zinc oxide from solutions containing either ammonium ions or lithium ions.

Attempts to grow sulfide crystals under hydrothermal conditions have been reported by Laudise and Ballman (58) in which zinc sulfide crystals were produced from sodium sulfide-zinc sulfide mixtures and from sodium hydroxide-zinc sulfide mixtures.

Smith (87) reported the preparation of microscopic crystals of lead sulfide and zinc sulfide from sodium polysulfide and sodium hydrogen sulfide solutions during experiments concerned with determining the order of precipitation of the salts upon cooling the hydrothermal solution. He found that zinc sulfide precipitated at a higher temperature than lead sulfide. This agrees with the order of deposition of lead sulfide and zinc sulfide in nature.

Kremheller and Levine (57) reported the accidental growth of zinc sulfide crystals from hydrothermal solutions. They were attempting to coprecipitate copper salts with zinc sulfide for luminescent studies and found that the particle size had increased by crystal growth over 200 times the original particle size.

Allen, Cremshaw, and Merwin (3) studied zinc sulfide, cadmium sulfide, and mercuric sulfide in an attempt to explain the geological formation of these minerals. They were able to prepare microscopic crystals of zinc sulfide beginning with zinc sulfate in a dilute sulfuric

acid solution.

Experiments on the growth of lead sulfide crystals and cadmium sulfide crystals, from freshly prepared aqueous ammonium polysulfide solutions, were reported by Laudise and Nielsen (61).

Bryatov and Kuz'mina (20) reported the crystallization of lead sulfide and zinc sulfide from aqueous solutions containing lithium chloride and sodium chloride. Crystals up to two millimeters in size were produced.

Badikov and Godovikov (5) produced lead sulfide crystals up to 0.08 mm from a very dilute aqueous solution of ammonium chloride. Plate-like, columnar, and isometric crystals were present.

A series of experiments departing radically from the usual hydrothermal solution experiments were those reported by Rau and Rabenau (79) who used strong hydrogen halide acid solutions as hydrothermal solvents for cupric sulfide, cadmium sulfide, mercuric sulfide, lead sulfide, and several other more complex salts. Lead sulfide isometric crystals 5 mm on a side were prepared in 12 molar hydrochloric acid over an 11 day period in a 450-400°C temperature gradient.

The only attempt to grow crystals from pure liquid hydrogen sulfide was made by Fredericks, Rosztoezy, and Hatchett (34) who reported unsuccessful experiments concerned with the growth of cadmium sulfide and zinc sulfide.

It is well known that solids are soluble in high density supercritical fluids. Ingerson (44) points out that all gases above their critical temperature can carry non-volatile solids in solution even when the pressure is less than the critical pressure. A number of systems made with the "inorganic gases", such as carbon dioxide, sulfur dioxide,and ammonia, as supercritical solvents were studied around the turn of the century. These systems, as well as some systems with organic solvents above their critical temperatures, were reviewed by Booth and Bidwell (14) and by Rowlinson and Richardson (82). Hydrogen sulfide has demonstrated, during another portion of this investigation, its ability to dissolve small amounts of many of the inorganic sulfides at room temperature. The temperature-enhanced solubility increase should permit large enough saturation concentrations that, under the proper conditions, crystal growth from solution could occur at reasonable rates.

Experimental

Crystal growth experiments were undertaken in this laboratory using basically the same type of apparatus that was used by Walker and Buelher (99) for the growth of quartz crystals. The apparatus consists of a high pressure vessel connected to a valve and gauge. The pressure vessel was machined by Pressure Product Industries, Hatboro, Pennsylvania from a bar of number 410 stainless steel

2 1/2 inches in diameter and 13 1/2 inches in length. Inside dimensions of the vessel are one inch in diameter by ten inches in length. It is designed to operate in the temperature range up to 250° C and at pressures up to 30, 000 psi.

The vessel closure device consists of a plug driven by a nut into a Teflon ring that is held in the vessel by a pair of wedge rings. Extrusion of the Teflon ring in any direction other than toward the center of the vessel is prevented by the wedge rings. The nut is tightened down with a torque wrench to a torque of 45 ft-lb. This makes a seal that is very effective to 30, 000 psi.

A tubing connection is made through the plug. Tubing runs were kept as short as possible and, wherever possible, the tubing was bent around a 2 1/2 inch radius. By bending the tubing at least one fitting per bend is eliminated. This eliminates two potentially leaky connections for each fitting that would have had to be used in place of the bend.

A short length of tubing comes directly out of the reactor plug and into a tee. One arm of the tee goes vertically to the valve used for filling the vessel and the second arm makes a direct connection to the gauge by a U-shaped tube.

A base plate of shallow aluminum channel is used to hold the vessel. The gauge is mounted on a plate which is connected to two one-half inch aluminum rods by four screw clamps. These aluminum

rods are connected to the base by two Flexaframe feet. This provides for the adjustment of the height of the vessel below the level of the base plate. In addition, there are two aluminum rods connected to the gauge plate and to a brass ring that is clamped around the top of the vessel.

Placing the base plate on top of the furnace suspends the vessel into the furnace. An asbestos paper maché covering is used to enclose the upper parts of the vessel, preventing heat loss through conduction and convection.

The furnace is built from two tube furnaces stacked one on top of the other. The two elements of each tube furnace are connected in series. This reduces the maximum temperature attainable and produces a more slowly varying volt-temperature curve which allows easier control. A Fenwal safety switch is installed between the two tube furnaces and is set to shut the bottom furnace off if the temperature exceeds 250°C. To prevent the voltages to the furnaces from being accidentally set too high, the Variacs are fused with a 1 1/2 amp slow-blow fuse. The furnace liner is made out of a piece of Pyrex glass tubing three inches in diameter. The entire furnace assembly was mounted on a fire brick in a five gallon solvent can. Vermiculite was packed around the furnaces and sealed in with asbestos paper maché.

The temperature of each tube furnace is independently controlled by a Variac. The line voltage fluctuated over such a wide

range that a constant temperature is impossible to achieve. For this reason, the Variacs are plugged into a Sola type CVN constant voltage transformer. The only other effect on the temperature of the furnaces was the room temperature which fluctuated 3°C. A room temperature fluctuation of this magnitude had little effect on the temperature of the vessel after it was sealed up by the asbestos covering.

Temperatures of the vessel are measured by four chromel-alumel thermocouples strapped to the vessel at 1 3/4 inches, 4 3/4 inches, 6 3/4 inches, and 9 1/2 inches from the bottom of the vessel.

Figure 7.1 shows the construction of the entire apparatus.

Three crystal growth frames made of tantalum were used to hold the seeds and the nutrient salt in the vessel. The first frame consisted of a pan to hold the nutrient, a baffle to slow the convective flow of solution from the warmer nutrient region to the cooler growth region, and two baskets woven of fine tantalum wire to hold the seeds. The baffle, with ten percent of its total area open, was mounted on the frame 3 7/8 inches above the nutrient pan. The two baskets were suspended 3 1/16 inches and 4 1/16 inches above the baffle. The second frame consisted of a nutrient pan and three baskets. The baskets were hung 2 inches, 4 3/4 inches, and 7 1/2 inches above the nutrient pan. There was no baffle on this frame. The third crystal growth frame was a modification of the second frame. A second spun tantalum pan was mounted 3 1/2 inches above the first pan and a

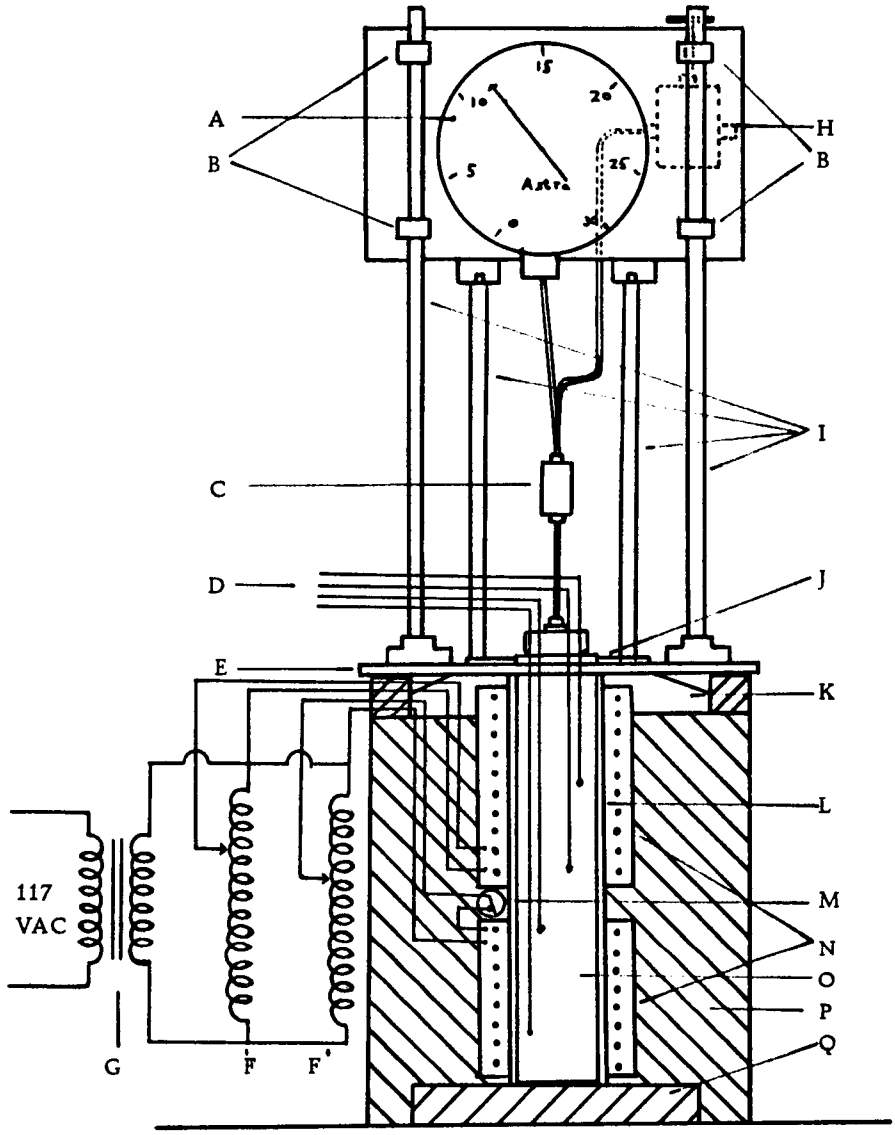

Figure 7.1. Cut-away view of the apparatus used in the crystal growth experiments. A) Bourdon tube gauge; B) Screw clamps; C) Tee; D) Thermocouple leads; E) Base plate; F) Variac autotransformer; G) Constant voltage transformer; H) High pressure valve; I) Aluminum support rods; J) Reactor support clamp; K) Asbestos insulation; L) Pyrex furnace liner; M) Fenwal safety switch; N) Furnace elements; O) High pressure vessel; P) Vermiculite insulation; Q) Fire brick base.

baffle, open ten percent of the area, was mounted one-half inch above the upper pan. Seed crystals were hung 1/2 inch, 2 1/4 inches, and 4 1/2 inches above the baffle. The frames are shown in Figure 7. 2.

Seed crystals, whenever they were available, were placed in baskets or drilled and hung from wires. If none were available, polycrystalline material was used to provide nucleation sites.

When the seed crystals were too small to remain in the basket, small glass dishes, made by cutting half dram shells down to a height of 1/8 inch, were used. These dishes were placed in the baskets and the seeds placed on them.

Seed crystals were obtained in various ways. Crystals of cadmium sulfide, zinc sulfide, and stannic sulfide were grown by the chemical transport method as described by Nitsche (72, 73). The method involved sealing the polycrystalline solid and a small quantity of iodine into a Vycor ampoule. Placing the ampoule in a thermal gradient, with the polycrystalline solid at the hot end, allows the iodine to react with the metallic sulfide forming free sulfur and a metallic iodide, both of which diffuse to the cold end where they react again to form the metallic sulfide and free iodine. The metallic sulfide was deposited slowly enough so that small, well-formed, single crystals were able to grow.

Silver sulfide crystals were grown accidentally in one of the Pyrex capillary "test-tubes" containing hydrogen sulfide,

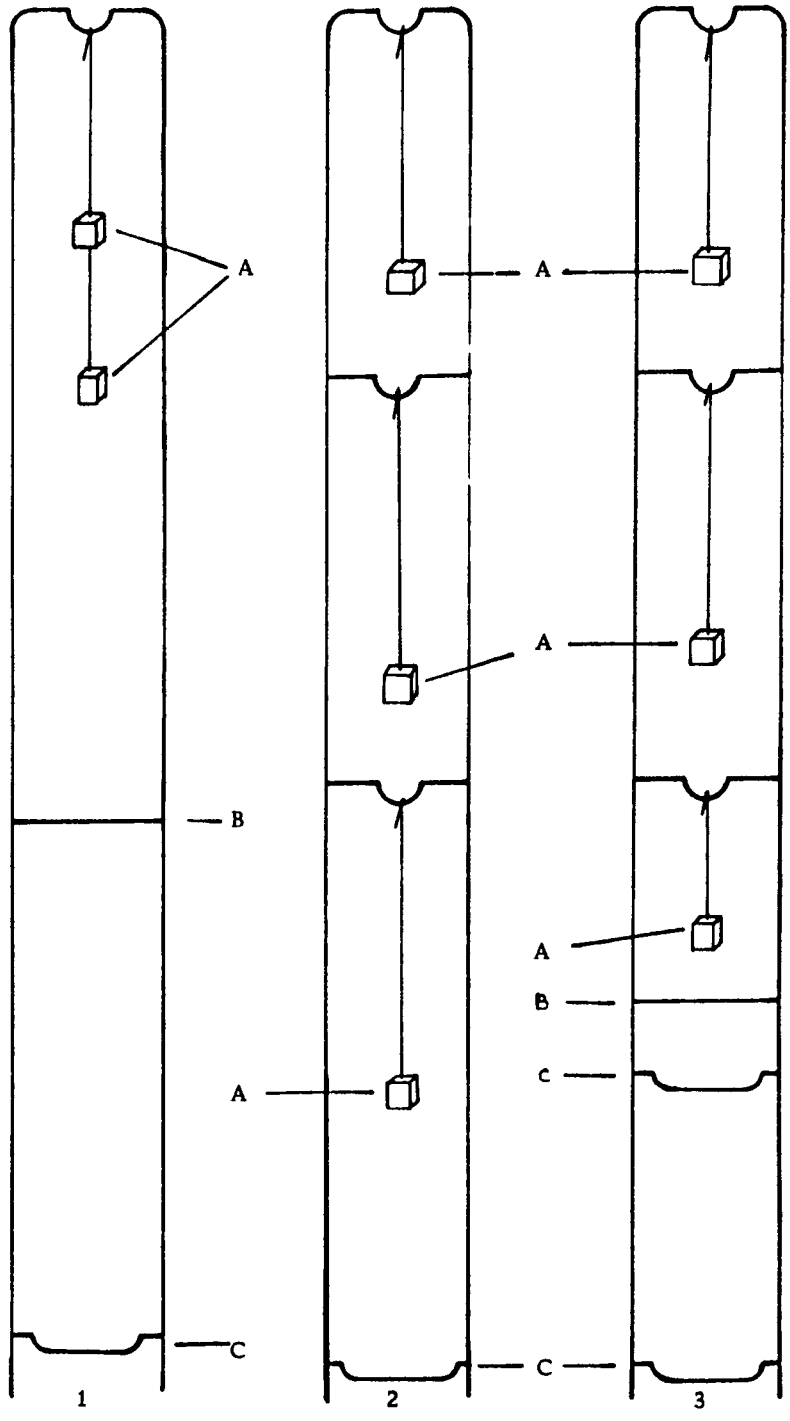

Figure 7. 2. Crystal growth frames. A) Seed crystal; B) Baffle; C) Nutrient pan.

triethylamine, and silver sulfide. The crystals that were formed were very small clusters with well defined faces.

Lead sulfide seed crystals also came about by accident. In the first high pressure lead sulfide crystal growth experiment some small chunks of polycrystalline lead sulfide were placed in the baskets since there were no lead sulfide seed crystals available. Crystal growth did not occur on the polycrystalline material in the baskets. Instead, small columnar crystallites were formed below the baffle and were found sticking to the frame and to the walls of the vessel. In addition, the space below the nutrient pan contained a sizeable deposit of this recrystallized salt.

A standardized procedure for filling the vessel was used. The vessel was first pumped out with a vacuum pump for 24 hours prior to the actual filling of the vessel. All conditions on the gas cleaning train duplicate the conditions under which the flow meter was calibrated. These conditions were a pressure of 15 psig while the gas was flowing, both cryogenic traps filled with chlorobenzene-liquid nitrogen slush, the desiccator tube filled with silica gel, the metering valve opened exactly one turn, the tank valve completely opened, the flow adjusted to 80% of full flow, and the vessel immersed in a Dry Ice-acetone cold bath. In addition, prior to each use of the flow system, the Millipore filter disc was changed.

The cold baths were prepared before flowing started. All valves

on the system were adjusted to their respective settings except the high pressure valve on the vessel which remained closed. As the high pressure valve was opened, a stop watch was started. The flow of gas was adjusted by the high pressure valve. After it had once been set, only minor adjustments of the high pressure valve and the tank pressure regulator needed to be made to maintain the desired conditions.

Discussion

At least two of the four salts for which the possibility of crystal growth from supercritical hydrogen sulfide solutions was examined have pressure induced phase transitions. Samara and Drickamer (83) report the first phase transition for cadmium sulfide occurs at a pressure of 20, 000 atm. Bridgman (18) reports a phase transition for lead sulfide at a pressure of 22, 300 atm. This transtion was examined crystallographically by Bassett, Takahashi, and Stook (6), who confirmed Bridgman's estimate of the pressure involved and who found that lead sulfide went from the cubic sodium chloride structure to the stannous sulfide structure. The stannous sulfide structure is a highly distorted sodium chloride structure. Stannic sulfide and silver sulfide undoubtedly have phase transitions but, as for cadmium sulfide and lead sulfide, the transitions are apparently far above the 2000 atm possible in this system. Thus, the possibility

of a phase transition preventing the crystal growth of a stable phase is very remote.

Although hydrogen sulfide is a polar molecule, it has a very low dielectric constant and it has little tendency to form solvation spheres around the solute molecules. In order to dissolve the essentially ionic sulfides, the dielectric constant should be as high as possible. As seen in the electrical measurements section, high dielectric constants are possible by going to high solvent densities. High temperatures were used in an effort to increase the solubility of the heavy metal sulfide in spite of the slight decrease in the dielectric constant that accompanies increased temperatures. In order to assure crystal perfection by preventing too rapid transfer of nutrient material, small temperature gradients were used. These were the guiding principles used in setting up the crystal growth experiments.

The first seven experiments were performed on the cadmium sulfide-hydrogen sulfide system. This system was chosen for three reasons: (1) seed crystals were readily obtained by the vapor transport method of growing crystals, (2) pure luminescent grade salt was available, and (3) cadmium sulfide crystals are interesting with respect to their optical and electrical properties.

From the standpoint of demonstrating the feasibility of crystal growth in this system, the choice of cadmium sulfide was poor.

Ferrous sulfide, as was demonstrated by the "H-tube" experiments, is more soluble in hydrogen sulfide than is cadmium sulfide. From the electrical measurements section for lead sulfide and stannic sulfide (both of which are more soluble than either cadmium sulfide or ferrous sulfide), it is apparent that the amount of ionization caused by the presence of the salt in the solution is small. Because of the slight ionization of the salt that does go into solution, there are the competing equilibria

$$FeS \rightleftharpoons Fe^{++} + S^{=} \tag{7.1}$$

$$CdS \rightleftharpoons Cd^{++} + S^{=}, \tag{7.2}$$

which are governed by the solubility product expressions

$$[Fe^{++}]\,[S^{=}] = K_1 \tag{7.3}$$

$$[Cd^{++}]\,[S^{=}] = K_2, \tag{7.4}$$

where

$$K_1 > K_2 . \tag{7.5}$$

The sulfide ion concentration from equation 7.1 will have the effect of depressing the cadmium ion concentration to a very low level preventing the cadmium sulfide from going into solution to any extent.

Slight darkening of the walls of the vessel occurred during the first experiment, but there was no build up of ferrous sulfide until

crystal growth experiment 5 at which point flakes of ferrous sulfide formed in large quantities. The first experiment was possibly too short for the build up of ferrous sulfide. Also, the presence of an "oily liquid", which was probably a polymeric phosphorus-sulfur compound, found in the first three experiments may have acted as a "mineralizer" in which the cadmium sulfide was more soluble than the ferrous sulfide. The "test-tube" experiments show that cadmium sulfide forms a complex with triethylamine and so it is plausible that it could form a complex with a phosphorus compound. The complex formation would certainly affect the equilibrium constant, K_2, possibly even to the extent that $K_2 > K_1$. If $K_2 > K_1$, then in crystal growth experiment 3, in which there was some gain in weight of the seed crystals, crystal growth may have taken place.

Due to the formation of large quantities of ferrous sulfide, crystal growth experiments 4 through 6 probably had a small probability that crystal growth would take place.

Crystal growth experiment 7 had a very small quantity of triethylamine added to the vessel in comparison to the quantity of hydrogen sulfide and cadmium sulfide present. The molar ratio of cadmium sulfide to triethylamine was 10:1 at the beginning of the experiment. The choice of that particular ratio was based on the formation of the highly unlikely four coordinate triethylamine-cadmium sulfide complex that had been indicated by the "test-tube" experiments. With

this ratio there would still be a quantity of solid, unreacted cadmium sulfide present to act as nutrient material in the event crystal growth was initiated. Two of the three cadmium sulfide seeds, as well as the nutrient cluster, showed a slight loss in weight. The weight loss was probably due to the formation of this cadmium sulfide-triethylamine complex. The fact that it did not involve a large fraction of the weight of the cadmium sulfide present was probably due to the loss of the triethylamine when the system was pumped out.

Crystal growth experiment 8 was conducted along the same lines that crystal growth experiment 7 followed with certain significant exceptions. Triethylamine was again used as a mineralizer but this time with silver sulfide instead of cadmium sulfide. The 1:4 ratio of triethylamine to silver sulfide was much higher than the 1:10 ratio of triethylamine to cadmium sulfide in crystal growth experiment 7.

The seeds used for crystal growth experiment 8 came from one of the "test-tube" experiments in which silver sulfide was sealed into a tube with triethylamine and hydrogen sulfide. After several days small crystals formed in clusters. They had well defined faces on them. A small cluster of these crystals was used as a seed. When the vessel was opened and the crystal cluster examined, the crystals in the cluster no longer had well defined faces and they appeared to be fused together. The sharp edges were rounded and the crystalline

luster was duller. It appeared, however, that recrystallization had taken place.

Crystal growth experiment 9 was the first of a series of experiments to explore the growth of lead sulfide crystals in liquid hydrogen sulfide. Polycrystalline powder clumps were used in the baskets to provide nucleation sites if crystal growth were to be initiated. Both the nutrient material and the nucleation powder clumps were C. P. grade lead sulfide with no preliminary treatment. This experiment lasted for 30 days at a pressure of 16, 000 psi in a thermal gradient of 218-204° C. The baffle opening was increased to 20% in an attempt to increase the convective flow due to the thermal gradient.

Upon opening the vessel, no apparent growth on the seed crystals was found. However, small crystals of sulfur, apparently extracted from the C. P. grade lead sulfide, were present. In addition, very small crystals of lead sulfide were found on the vessel walls up to, but not above the baffle, on the growth frame, and in the bottom of the vessel below the nutrient pan. An X-ray powder pattern that matched A. S. T. M. card number 5-0592 established that the crystals were lead sulfide. These crystals, which had a columnar habit, were less than 0. 01 mm in length.

Two possibilities exist to explain the location where the crystals were found. Either they grew below the nutrient pan or they were formed in a convection current much the same way hailstones

are formed in a storm cloud. The small crystals were carried in this current until they were heavy enough to drop under the influence of gravity to the bottom of the vessel where they ceased to grow. Over half of the nutrient material was found below the nutrient pan. The large quantity of material that was transported and the fact that no salt was found on top of the baffle rules out the possibility that the crystallites were formed when the hydrogen sulfide was released.

Since no recrystallization took place above the baffle in crystal growth experiment 9, a new growth frame without a baffle on it was constructed. Three tantalum baskets were hung on the frame as shown in Figure 7. 2. A few of the small crystals that were produced in crystal growth experiment 9 were used as seeds for crystal growth experiment 10. These seeds were placed in small glass dishes made from half dram shells.

The vessel was filled with 105. 6 g of hydrogen sulfide and placed in the furnace to warm up. As it warmed up, the main seal started to leak. A tight seal was made when the temperature got high enough. As a result of the leak there was uncertainty as to the quantity of hydrogen sulfide present. So the hydrogen sulfide was weighed out of the crystal growth vessel using the calibration vessel. There were 104. 68 g of hydrogen sulfide present at the end of the experiment. The experiment was conducted in a thermal gradient of 183-206°C at a pressure of 14, 000 psi for 35 days.

A large quantity of sulfur was found on the bottom basket, a much smaller quantity on the middle basket, and none on the top basket. The sulfur was deposited in the form of small needle-like crystals 3 mm long. A few of the crystals were ground up and mounted on the wedge for an X-ray powder diffraction pattern. The pattern conformed to A. S. T. M. card numbers 8-247 and 8-248 for orthorhombic sulfur.

In the bottom basket several small lumps of lead sulfide were found. They looked as though they had been pressed into their shape. Some of them appeared to have well defined faces as well as sharp corners between the faces. The lumps, which had apparently formed around the seeds, were very soft and crumbled to the touch.

Slightly larger crystals than were produced in crystal growth experiment 9 were found clinging to the walls of the vessel, on the frame, and below the nutrient pan. To get below the nutrient pan, the crystals either had to slide down the wall of the vessel or grow in that region. The nutrient pan is circular and nearly the same diameter as the vessel.

The presence of comparatively large quantities of sulfur found in crystal growth experiments 9 and 10, coupled with the anomalous results obtained during the solubility experiments that were being conducted simultaneously, lead to the conclusion that the C. P. grade lead sulfide was contaminated with elemental sulfur. Sulfur-free

lead sulfide was prepared by bubbling hydrogen sulfide through an aqueous solution of Baker and Adamson reagent grade lead nitrate. The resulting precipitate was filtered, washed with water and absolute alcohol, and then baked at 150°C for a week. This salt was used in all subsequent crystal growth experiments.

Crystal growth experiment 11 was a high density, high temperature, long term experiment conducted in a baffle-less vessel. There were no deposits of elemental sulfur present at the conclusion of the experiment. In addition, there was no formation of the small crystallites noted in experiments 9 and 10.

Experiment 15 was set up with crystal growth frame number three. Seed crystals from experiment 10 were placed in the three tantalum baskets. Nutrient material was placed in the upper pan. The furnaces were set to produce a thermal gradient varying from 137-130°C over the length of the vessel. Crystalline lead sulfide was found distributed throughout the vessel. All of the crystals formed were smaller than those formed in experiments 9 and 10.

In an attempt to produce more rapid saturation of the solvent, experiment 16 was set up with a 23°C thermal gradient across the vessel. The large thermal gradient prevented the lead sulfide from attaching to the walls of the vessel. Thus, very few and very small crystals were formed during this experiment.

The final lead sulfide experiment, 17, was set up with an

inverse thermal gradient in a high temperature, high density system. If a region of retrograde solubility (a region where the temperature coefficient of solubility is negative) were present in the phase diagram for the hydrogen sulfide-lead sulfide system, the presence of favorable growth conditions would show up as bands of crystals formed on the walls of the vessel. This, however, was not the case because crystal formation was distributed generally throughout the vessel with the majority of the crystals attached to the vessel wall in the bottom two inches (in the coldest part of the vessel). This experiment lends support to the "hailstone theory" for the deposition of crystals during experiments 9 and 10. Of the two cooler regions in those experiments, the top of the vessel was the colder. The convection currents would carry the saturated solution to the upper parts of the vessel where at least some of the crystals would have attached themselves to the plug body and to the upper wall of the vessel. Since this did not occur in either experiment, the "hailstone theory" seems the more plausible of the two.

A chemically more interesting system developed during the attempts to grow stannic sulfide crystals in supercritical hydrogen sulfide. All of the stannic sulfide used for these experiments was prepared by bubbling hydrogen sulfide through an aqueous solution of Baker and Adamson reagent grade stannic chloride. The stannic sulfide that was formed was centrifuged to collect it. Washing was

carried out by slurrying the salt with water and recentrifuging. Absolute ethyl alcohol was used to remove any traces of water present and the alcohol was removed by heating in an oven to 80°C under a vacuum.

Crystal growth experiment 12 was designed to examine the possibility of crystal growth at high temperatures. Three seeds obtained by vapor phase growth were drilled and hung from frame number three in place of the baskets. The vessel was placed in a thermal gradient that varied from 207-190°C for 29 days. A variety of products were formed during this experiment. At the end of the experiment the nutrient material was present as a yellow and a brown material that was caked in separate layers. A small quantity of sulfur was found in the bottom of the pan along with a volatile, odoriferous, oily liquid. The upper parts of the vessel and the plug were coated with a reddish-brown deposit of salt. In addition, the bottom seed crystal completely dissolved, the second crystal lost a significant amount of weight, and the top crystal lost less than one percent of its weight.

An X-ray powder diffraction pattern of the original material was compared to that found in the nutrient pan after the conclusion of the run. The material from the pan gave sharp lines out to large angles, while the pattern for the original material was fuzzy and faded out at a fairly small angle. Improvement of the pattern after

being subjected to the experimental conditions is due to improved crystallization.

X-ray analysis of the reddish-brown material found deposited on the top of the vessel proved to be a mixture of Sn_2S_3 and SnS_2. The mixed pattern conformed to A. S. T. M. card number 1-1010 for SnS_2 and card number 14-539 for Sn_2S_3. Volynsky and Sevryukov (95) report that Sn_2S_3 and SnS are formed successively in the thermal dissociation of SnS_2. Thus, in this system

$$2\ SnS_2 \rightarrow Sn_2S_3 + S \qquad (7.6)$$

is followed by the reaction

$$Sn_2S_3 \rightarrow 2SnS + S. \qquad (7.7)$$

The stannous sulfide immediately reacts with the hydrogen sulfide in the manner described earlier:

$$SnS + H_2S \rightarrow SnS_2 + H_2. \qquad (7.8)$$

This series of reactions explains the mixture of SnS_2 and Sn_2S_3 found deposited on the top of the vessel. Karakhanova, Pashinkin, and Novoselova (46) report that Sn_2S_3 can be formed by heating a tin-sulfur mixture for about 20 days at 500° C. This implies that reaction 7.6 is a slow process. The fact that Sn_2S_3 was present at the end of the experiment implies that reaction 7.7 is also slow.

The preliminary experiments demonstrated that reaction 7.8 is rapid at room temperature. Thus, a steady state probably existed between the SnS_2 and the Sn_2S_3 that was deposited in the cooler parts of the vessel.

The odoriferous, volatile, oily liquid is believed to be ethyl mercaptan formed by the reaction of ethyl alcohol and hydrogen sulfide at high temperatures and pressures in the same manner as was described by Cairns, Larchar, and McKusick (23). They note that methyl mercaptan can be formed from methyl alcohol in pure hydrogen sulfide at 8500 atm and 125°C, and that t-butyl and n-butyl alcohol undergo the same reaction. The presence of the ethyl alcohol in the vessel was probably due to adsorption of the solvent on the salt during the washing stage and was not removed by the gentle heating during the drying stage. It is estimated that less than 0.1 ml of the ethyl mercaptan was formed.

Experiment 13 was designed to decrease the thermal dissociation of stannic sulfide by lowering the temperature. While this helped, it did not completely eliminate the problem. A much smaller quantity was found deposited in the top of the vessel. The middle seed increased in weight by one percent, but the seeds above and below it both decreased in weight.

Crystal growth experiment 14 was run with a smaller thermal gradient, a higher density, and in the same temperature range as

experiment 13. Evidently these conditions were more conducive to crystal growth because the top two seeds gained weight. However, the bottom seed lost weight.

The experimental conditions for all of the crystal growth experiments are given in Table 7. 1. All weights are given in grams, temperatures are given in degrees centigrade, times are given in days, pressures are given in pounds per square inch, and densities are given in grams per cubic centimeter. The weights of the seed crystals are listed before and after completion of each experiment. The top seed is listed first, the middle seed, if present, is listed second, and the bottom seed is listed last.

The limited success obtained with all of the salts tried, except possibly cadmium sulfide, indicates that under the proper conditions heavy metal sulfide crystals can be grown from supercritical hydrogen sulfide. In order to be practically feasible, however, the growth rates must be increased.

The realistic approach to the problem of increasing the growth rate is the use of a mineralizer to increase the solubility or to change the compound that is transported from the region containing the nutrient to the growth region. Mineralizers are used extensively in hydrothermal crystal growth. Quartz is grown in basic solutions containing either hydroxyl ions or carbonate ions. Sulfides have been grown from aqueous solutions containing sodium sulfide or

Table 7. 1. Conditions before and after crystal growth experiments.

CG Expt.	Nutrient	H_2S g	Time Days	Pressure psi	Bottom to Top Temp. °C	Baffle open %	Seeds Weight Before Growth Top to Bottom g	Seeds Weight After Growth Top to Bottom g	Density g/cc
1	CdS	66	8 1/2	1,750	224- 92	10	0.0046 0.0097	0.0036 0.0095	0.48
2	CdS	79.2	17 1/2	5,250	211- 111	10	0.0036 0.0095	0.0036 0.0096	0.57
3	CdS	92.4	11 1/2	2,700	107 108 105 100	10	0.0205 0.0381	0.0212 0.0387	0.67
4	CdS	105.6	14 1/2	6,700	107 109 105 99	10	0.0212 0.0387	0.0204 0.0379	0.77
5	CdS	92.40	12 1/2	10,000	162 168 160 150	10	0.0164 0.0017 0.0215	0.0163 0.0017 0.0212	0.67
6	CdS	97.04	12 1/2	11,100	219 222 212 200	10	0.0163 0.0017 0.0212	0.0163 0.0018 0.0212	0.70
7	CdS- $(C_2H_5)_3N$ 10:1 mole ratio	74.40	13 1/2	5,250	212 219 214 203	10	0.0163 0.0017 0.0212	0.0163 0.0018 0.0212	0.54
8	Ag_2S- $(C_2H_5)_3N$ 4:1 ratio 0.654 g $(C_2H_5)_3N$	79.64	13 1/2	6,250	217 218 215 202	10	-- cluster 0.0014	-- 0.0012	0.58
9	PbS	105.30	30	16,000	215 220 218 204	20	polycrystalline		0.76

Table 7.1. Continued.

CG Expt.	Nutrient	H_2S g	Time Days	Pressure psi	Bottom to Top Temp. °C	Baffle open %	Seeds Weight Before Growth Top to Bottom g	Seeds Weight After Growth Top to Bottom g	Density g/cc
10	PbS	104.68	35	14,000	202 206 200 183	no baffle	several small crystals from expt. 9	--	0.76
11	PbS	106.20	60	15,700	207 216 213 208	no baffle	poly-crystalline	--	0.77
12	SnS_2	97.80	29	10,700	207 207 204 190	15	0.0230 0.0357 0.0094	0.0222 0.0310 dissolved	0.71
13	SnS_2	74.73	30	2,700	142 146 145 135	15	0.0393 0.0222 0.0310	0.0374 0.0224 0.0243	0.54
14	SnS_2	105.42	32	9,700	146 148 148 140	15	0.0224 0.0373 0.0245	0.0226 0.0375 0.0244	0.76
15	PbS	97.97	30	5,800	134 137 135 130	15	poly-crystalline	--	0.71
16	PbS	107.91	30	14,000	183 182 171 160	15	poly-crystalline	--	0.79
17	PbS	113.80	30	19,200	188 192 207 187	15	poly-crystalline	--	0.82

sodium hydroxide (58), from aqueous solutions containing the chlorides of sodium, lithium (20) or ammonium (5), from aqueous solutions containing ammonium polysulfide (61), from weak acid solutions (3), and from strong aqueous acid solutions (79). Laudise, Kolb, and DeNeufville (60) discuss how alkali metal-hydroxide mineralizers affect the growth of zinc sulfide crystals and speculate that the species that is carried by the solvent is the thiozincate ion ($ZnSOH^-$) and not a basic oxy-anionic species, the molecular species, or the simple ionic species. In neutral solutions they feel that the hydrated molecule is the transported species, and, in saturated ammonium chloride solutions, the transported species in a zinc amine complex.

In pure hydrogen sulfide the molecule in solution appears to be the predominant species. The addition of either lead sulfide or stannic sulfide appears to increase slightly the number of ions already present due to the auto-ionization of the solvent. Thus, it appears that such additives as water, triethylamine, hydrogen chloride gas, or any of the organosubstituted ammonium halides that cause a drastic change in the resistivity of hydrogen sulfide might act as a mineralizer in this system. The mechanism of transport in such a system would be the formation of an ionic complex.

VIII. CONCLUSION

The chemistry and physics of supercritical systems is in its infancy. Non-aqueous solvents in general and hydrogen sulfide in particular have not been investigated to any great extent. Only four investigations have been conducted in which hydrogen sulfide was heated above the critical temperature at densities above the critical density. They are the investigation of the reactions of hydrogen sulfide with organic compounds (23), a measurement of the dielectric constant at one apparently unknown density (31), an investigation of the pressure-volume-temperature relations (81), and the present investigation.

A number of significant contributions were made by this investigation regarding the chemistry and physics of hydrogen sulfide in both the subcritical state and the supercritical state. The adaptation of a method, based on Raoult's Law, permitted the measurement of the relative solubilities of sparingly soluble compounds in a solvent that is liquid at room temperature only under moderate pressures. Agreement of the observed solubilities with the calculated solubilities indicates that hydrogen sulfide is an ideal solvent on the basis of Raoult's Law.

Experiments to extend the range over which the volumetric properties of hydrogen sulfide are known were carried out. The data obtained from these experiments permitted the development of a set

of virial equations to describe the behavior of hydrogen sulfide. Good agreement was obtained between the pressures calculated from the virial equations obtained during this investigation and the pressures calculated from the charts of Nelson and Obert (71) based on the theorem of corresponding states. Good agreement with the more limited data published by Reamer, Sage, and Lacey (81) was also found.

The electrical measurements provided supporting evidence for some of the conclusions already mentioned. Dielectric constant measurements were represented as virial equations in density. The second virial coefficients from both the volumetric virial equations and the dielectric virial equations are related to the number of molecular pairs formed in the supercritical state. Both types of measurements are consistent in indicating that the number of pairs formed is small. Hydrogen sulfide is a low dielectric constant solvent even at high densities. This is consistent with the low solubilities observed for ionic compounds and the higher solubilities observed for covalent compounds.

Conductivity measurements indicate that auto-ionization in hydrogen sulfide occurs only slightly. Solutions of silver sulfide and stannic sulfide both showed a slightly larger conductivity than the pure solvent. The stannic sulfide had the larger conductivity of the two compounds. This observation was consistent with the results

from the solubility determinations.

Triethylammonium chloride exhibited an increase in the conductivity of over a thousand times that of the pure solvent. This occurred at low densities. This indicates that a compound such as triethylamine acts as a base in hydrogen sulfide by forming the bisulfide ion, HS^-. This ionization caused the large increase in the conductivity.

Crystal growth in pure hydrogen sulfide is possible, but not likely to be commercially practical under the conditions attainable with this system. To be practical, larger growth rates than were achieved with stannic sulfide and lead sulfide must be attained. A method that could increase the growth rate is the use of a mineralizer such as triethylamine that would change the molecular species that is transported from the nutrient region to the growth region.

BIBLIOGRAPHY

1. Achterhof, M., R. Conaway and C. Boord. The sulfur derivatives of the simple amines. I. Amine hydrosulfides. Journal of the American Chemical Society 53:2682-2688. 1931.

2. Allegheny Ludlum Steel Corporation. Stainless steel handbook, Pittsburgh, 1956. 120 p.

3. Allen, E. T., J. L. Cremshaw and H. E. Merwin. The sulfides of zinc, cadmium, and mercury; their crystalline form and genetic conditions. American Journal of Science 184:341-396. 1912.

4. Antony, U. and G. Magri. L'idrogeno solforato liquidato come solvente. Gazzetta Chimica Italiana 35:206-226. 1905.

5. Badikov, V. V. and A. A. Godovikov. Morphology of galena crystals produced under hydrothermal conditions. Zapiski Vsesoyuznogo Mineralicheskogo Obshchestva 95:526-536. 1966.

6. Bassett, W. A., T. Takahashi and P. W. Stook. X-ray diffraction and optical observations on crystalline solids up to 300 kilobars. Review of Scientific Instruments 38:37-42. 1967.

7. Beattie, J. A. and O. C. Bridgeman. A new equation of state for fluids. Proceedings of the American Academy of Arts and Sciences 63:229-308. 1929.

8. Beattie, J. A., G. Simard and G. J. Su. The compressibility of and an equation of state for gaseous normal butane. Journal of the American Chemical Society 61:26-27. 1939.

9. Beckmann, E. and P. Waentig. Kryoskopische Bestimmungen bei tiefen Temperaturen (-40 bis -117°). Zietschrift für Anorganische Chemie 67:17-61. 1910.

10. Bickford, W. G. The dielectric constant and the specific conductance of pure liquid hydrogen sulfide. Iowa State College Journal of Science 11:35-38. 1936.

11. Bickford, W. G. and J. A. Wilkinson. The dielectric constant and specific conductance of liquid hydrogen sulfide at 194. 5° K. Proceedings of the Iowa Academy of Science 40:89-91. 1933.

12. Bierlein, J. A. and W. B. Kay. Phase equilibrium properties of system carbon dioxide-hydrogen sulfide. Industrial and Engineering Chemistry 45:618-624. 1953.

13. Blitz, W. and E. Keunecke. Beiträge zur systematischen Verwandtschaftslehre. XXXI. Thiohydrate. Zeitschrift für Anorganische and Allgemeine Chemie 147:171-187. 1925.

14. Booth, H. S. and R. M. Bidwell. Solubility measurement in the critical region. Chemical Reviews 44:477-513. 1949.

15. Borgeson, R. W. and J. A. Wilkinson. Reactions in liquid hydrogen sulfide. VI. Reactions with organic compounds. Journal of the American Chemical Society 51:1453-1456. 1929.

16. Böttcher, C. J. F. Theory of electric polarization. Amsterdam, Elsevier, 1952. 492 p.

17. Bridgman, P. W. The compression of 46 substances to 50, 000 kg/cm^2. Proceedings of the American Academy of Arts and Sciences 74:21-51. 1940.

18. _____ Rough compressions of 177 substances to 40, 000 kg/cm^2. Proceedings of the American Academy of Arts and Sciences 76:71-87. 1947.

19. Brown, C. S. et al. Growth of large quartz crystals. Nature 167:940-941. 1951.

20. Bryatov, L. V. and I. P. Kuz'mina. Crystallization of the sulfides of lead and zinc from aqueous solutions of the chlorides. In: Growth of crystals, ed. by A. V. Shubnikov and N. N. Sheftal'. Vol. 3. New York, Consultants Bureau, 1959. p. 294-296. (Translated from Russian)

21. Buckingham, A. D. and J. A. Pople. Electromagnetic properties of compressed gases. Discussions of the Faraday Society 22:17-21. 1956.

22. Cady, H. P. and H. M. Elsey. A general conception of acids and bases. Science 56:27. 1922.

23. Cairns, T. L., A. W. Larchar and B. C. McKusick. Reactions of hydrogen sulfide with various organic compounds at high pressures. Journal of Organic Chemistry 18:748-752. 1953.

24. Cardoso, E. Sulle tensioni di vapore dell'idrogeno solforato. Gazzetta Chemica Italiana 51:153-164. 1921.

25. Chipman, H. R. and D. McIntosh. Liquid hydrogen sulfide as an ionizing medium. The Proceedings and Transactions of the Nova Scotian Institute of Science 16:189-195. 1926.

26. Comings, E. W. High pressure technology. New York, McGraw-Hill, 1956. 572 p.

27. Cotton, F. A. and G. Wilkinson. Advanced inorganic chemistry. New York, Interscience, 1962. 480 p.

28. Cotton, J. D. and T. C. Waddington. Liquid hydrogen sulfide as an ionizing medium. III. Reactions of compounds of Groups IV, V, and VI. Journal of the Chemical Society 1966A:793-797.

29. Debye, P. Polar molecules. New York, Dover, 1929. 172 p.

30. Ellis, A. J. and W. S. Fyfe. Hydrothermal chemistry. Reviews of Pure and Applied Chemistry 7:261-316. 1957.

31. Eversheim, P. Verhalten von Leitfähigkeit und Dielektrizitätskonstanten einiger substanzen vor und in dem kritischen Zustand. Annalen der Physik 13:492-511. 1904.

32. Farber, M. and D. M. Ehrenberg. High-temperature corrosion rates of several metals with hydrogen sulfide and sulfur dioxide. Journal of the Electrochemical Society 99:427-434. 1952.

33. Frank, E. Electrical measurement analysis. New York, McGraw-Hill, 1959. 443 p.

34. Fredericks, W. J., F. E. Rosztoczy and J. Hatchett. Investigation of crystal growth processes. Palo Alto, 1963. 24 numb. leaves. (Stanford Research Institute. SRI Project #PAU-3523. Final Report. Results presented at 1962 International Color Center Symposium, Stuttgart, Germany.)

35. Giauque, W. F. and R. W. Blue. Hydrogen sulfide. The heat capacity and vapor pressure of solid and liquid. The heat of vaporization. A comparison of thermodynamic and spectroscopic values of entropy. Journal of the American Chemical Society 58:831-837. 1936.

36. Guest, H. P. Reactions of inorganic compounds with liquid hydrogen sulfide. Iowa State College Journal of Science 8:197-198. 1933.

37. Hague, B. Alternating current bridge methods. 2d ed. London, Pitman, 1930. 391 p.

38. Hale, D. R. The laboratory growing of quartz. Science 107: 393-394. 1948.

39. Hamann, S. D. Physico-chemical effects of pressure. London, Butterworths, 1957. 246 p.

40. Hampel, C. A. Refractory metals. Tantalum, niobium, molybdenum, rhenium, and tungsten. Industrial and Engineering Chemistry 53:90-96. 1961.

41. Havriliak, S., R. W. Swenson and R. H. Cole. Dielectric constants of liquid and solid hydrogen sulfide. Journal of Chemical Physics 23:134-135. 1955.

42. Hirst, A. W. Electricity and magnetism. 3d ed. London, Blackie and Son, 1959. 438 p.

43. Hitchcock, C. S. and C. P. Smyth. The rotation of molecules or groups in crystalline solids. Journal of the American Chemical Society 55:1296-1297. 1933.

44. Ingerson, E. Relation of critical and supercritical phenomena of solutions to geologic processes. Economic Geology 29:454-470. 1934.

45. Jander, G. Die Chemie in Wasserahnlichen Losungsmitteln. Berlin, Springer-Verlag, 1949. 367 p.

46. Karakhanova, M. I., A. S. Pashinkin and A. V. Novoselova. Phase diagram of the tin-sulfur system. Izvestiya Akademii Nauk SSSR, Neorganicheskie Materialy 2:991-996. 1966.

47. Kelley, K. K. Contributions to the data on theoretical metallurgy. V. Heats of fusion of inorganic substances. Washington, D. C., 1936. 166 p. (U. S. Bureau of Mines. Bulletin 393)

48. _____ Contributions to the data on theoretical metallurgy. XIII. High-temperature heat-content, heat-capacity,

and entropy data for the elements and inorganic compounds. Washington, D. C., 1960. 232 p. (U. S. Bureau of Mines. Bulletin 504)

49. Kemp, J. D. and G. H. Denison. The dielectric constant of solid hydrogen sulfide. Journal of the American Chemical Society 55:251. 1933.

50. Kennedy, G. C. Pressure-volume-temperature relations in water at elevated temperatures and pressures. American Journal of Science 248:540-564. 1950.

51. Kerr, P. F. and E. Armstrong. Recorded experiments in the production of quartz. Bulletin of the Geological Society of America 54, sup. 1, 1943. 34 p.

52. Khodakovskii, I. L. The hydrosulfide form of the heavy metal transportation in hydrothermal solutions. Geokhimiya 1966: 960-971. (Abstracted in Chemical Abstracts 65:14502e. 1967 and Geochemistry International 1966:766.)

53. Kleinberg, J., W. Argersinger and E. Griswold. Inorganic chemistry. Boston, D. C. Heath, 1960. 614 p.

54. Klemenc, A. and O. Bankowski. Die Eigenschaften flüchtiger Hydride. II. Gewinnung von reinem Schwefelwasserstoff, Tensionen und Dichten. Zeitschrift für Anorganische und Allgemeine Chemie 208:348-366. 1932.

55. Kolb, E. D. and R. A. Laudise. Hydrothermally grown ZnO crystals of low and intermediate resistivity. Journal of the American Ceramic Society 49:302-305. 1966.

56. _____ Properties of lithium-doped hydrothermally grown single crystals of zinc oxide. Journal of the American Ceramic Society 48:342-345. 1965.

57. Kremheller, A. and A. K. Levine. Hydrothermal synthesis of electronically active solids. Sylvania Technologist 10:67-71. 1957.

58. Laudise, R. A. and A. A. Ballman. Hydrothermal synthesis of zinc oxide and zinc sulfide. Journal of Physical Chemistry 64:688-691. 1960.

59. Laudise, R. A., E. D. Kolb and A. J. Caporaso. Hydrothermal growth of large sound crystals of zinc oxide. Journal of the American Ceramic Society 47:9-12. 1964.

60. Laudise, R. A., E. D. Kolb and J. P. DeNeufville. Hydrothermal solubility and growth of sphalerite. The American Mineralogist 50:382-391. 1965.

61. Laudise, R. A. and J. W. Nielsen. Hydrothermal crystal growth. Solid State Physics 12:149-222. 1961.

62. LePage, W. R. Analysis of alternating current circuits. New York, McGraw-Hill, 1952. 444 p.

63. Lineken, E. E. The conductance of iodine in liquid hydrogen sulfide. Journal of the American Chemical Society 68:1966-1968. 1946.

64. Lineken, E. E. and J. A. Wilkinson. The conductance of organosubstituted ammonium chlorides in liquid hydrogen sulfide. Journal of the American Chemical Society 62:251-256. 1940.

65. Maron, S. H. and D. Turnbull. Calculating Beattie-Bridgeman constants from critical data. Industrial and Engineering Chemistry 33:408-410. 1941.

66. Mayer, J. E. and M. G. Mayer. Statistical mechanics. New York, Wiley, 1940. 495 p.

67. McGregor, M. C. et al. New apparatus at the National Bureau of Standards for absolute capacitance measurement. Institute of Radio Engineers Transactions on Instrumentation I-7:253-261. 1958.

68. Meints, R. E. and J. A. Wilkinson. Reactions in liquid hydrogen sulfide. V. Reaction with furfural. Journal of the American Chemical Society 51:803. 1929.

69. Mickelson, J. R. Isotopic exchange reactions in liquid hydrogen sulfide. Ph. D. thesis. Corvallis, Oregon State University, 1956. 141 numb. leaves.

70. Mickelson, J. R., T. H. Norris and R. C. Smith. Radiosulfur-exchange reactions in liquid hydrogen sulfide. I. Inorganic Chemistry 5:911-916. 1966.

71. Nelson, L. C. and E. F. Obert. Generalized PVT properties of gases. Transactions of the American Society of Mechanical Engineers 76:1057-1066. 1954.

72. Nitsche, R. The growth of single crystals of binary and ternary chalcogenides by chemical transport reactions. Physics and Chemistry of Solids 17:163-165. 1960.

73. Nitsche, R., H. U. Bölsterli and M. Lichtensteiger. Crystal growth by chemical transport reactions. I. Binary, ternary, and mixed crystal chalcogenides. Physics and Chemistry of Solids 21:199-205. 1961.

74. Quam, G. N. A study of reactions in liquid hydrogen sulfide. Journal of the American Chemical Society 47:103-108. 1925.

75. Quam, G. N. and J. A. Wilkinson. Conductance in liquid hydrogen sulfide solutions. Journal of the American Chemical Society 47:989-994. 1925.

76. _____ Conductance in liquid hydrogen sulfide solutions. Proceedings of the Iowa Academy of Science 32:324-325. 1925.

77. Ralston, A. W. and J. A. Wilkinson. Reactions in liquid hydrogen sulfide. III. Thiohydrolysis of chlorides. Journal of the American Chemical Society 50:258-264. 1928.

78. _____ Reactions in liquid hydrogen sulfide. IV. Thiohydrolysis of esters. Journal of the American Chemical Society 50:2160-2162. 1928.

79. Rau, H. and A. Rabenau. Crystal syntheses and growth in strong acid solutions under hydrothermal conditions. Solid State Communications 5:331-332. 1967.

80. Reamer, H. H., B. H. Sage and W. N. Lacey. Phase equilibria in hydrocarbon systems. Industrial and Engineering Chemistry 41:482-484. 1949.

81. _____ Volumetric behavior of hydrogen sulfide. Industrial and Engineering Chemistry 42:140-143. 1950.

82. Rowlinson, J. S. and M. J. Richardson. The solubility of solids in compressed gases. Advances in Chemical Physics 2:85-118. 1959.

83. Samara, G. A. and H. G. Drickamer. Pressure induced phase transitions in some II-VI compounds. Physics and Chemistry of Solids 23:457-461. 1962.

84. Satwalekar, S. D., L. W. Butler and J. A. Wilkinson. Reactions in liquid hydrogen sulfide. VIII. Specific conductance of liquid hydrogen sulfide. Journal of the American Chemical Society 52:3045-3047. 1930.

85. Sheffer, H. Physico-chemical measurements using isopiestic methods. Chemistry in Canada 2(10):40-42. 1950.

86. Skilling, W. T. The dissociating power of hydrogen sulfide. American Chemical Journal 26:383-384. 1901.

87. Smith, F. G. Solution and precipitation of lead and zinc sulfides in sodium sulfide solutions. Economic Geology 35:646-658. 1940.

88. Smith, R. C. Isotopic exchange in liquid hydrogen sulfide. Master's thesis. Corvallis, Oregon State University, 1952. 70 numb. leaves.

89. Smyth, C. P. Dielectric behavior and structure. New York, McGraw-Hill, 1955. 441 p.

90. Smyth, C. P. and C. S. Hitchcock. The dielectric constants and transitions of solid ammonia, hydrogen sulfide, and methyl alcohol. Journal of the American Chemical Society 56:1084-1087. 1934.

91. Spezia, G. On the growth of quartz crystals. Atti della Reale Accademia delle Scienze di Torino 44:1-15. 1908.

92. Steele, B. D. and L. S. Bagster. Binary mixtures of some liquified gases. Journal of the Chemical Society 97:2607-2620. 1910.

93. Steele, B. D., D. McIntosh and E. H. Archibald. The alogen hydrides as conducting solvents. I. The vapor pressures, densities, surface energies, and viscosities of the pure solvents. II. The conductivity and molecular weights of dissolved substances. III. The transport numbers of certain dissolved substances. IV. The abnormal variation of molecular conductivity, etc. Philosophical Transactions of the Royal Society of London, ser. A, 205:99-167. 1906.

94. Van Praagh, G. Synthetic quartz crystals. Geological Magazine 84:98-100. 1947.

95. Volynsky, I. S. and N. N. Sevryukov. Tin sulfides. Journal of General Chemistry of the USSR 25:2259-2265. 1955.

96. von Braunmühl, J. J. Über die Temperaturabhängigkeit der Dielektrizitätskonstante einiger Gase. Physikalische Zeitschrift 28:141-149. 1927.

97. von Schafhautl, K. F. E. Die neuesten geologischen Hypothesen und ihr Verhaltniss zur Naturwissenschaft uberhaupt. Gelehrte Anzeigen der Klasse der Bayerischen Akademie 20:557-595. 1845.

98. Walker, A. C. Hydrothermal synthesis of quartz crystals. Journal of the American Ceramic Society 36:250-256. 1953.

99. Walker, A. C. and E. Buehler. Growing large quartz crystals. Industrial and Engineering Chemistry 42:1369-1375. 1950.

100. Walker, J. W., D. McIntosh and E. Archibald. Ionization and chemical combination in the liquified halogen hydrides and hydrogen sulfide. Journal of the Chemical Society 85:1098-1105. 1904.

101. West, J. R. Thermodynamic properties of hydrogen sulfide. Chemical Engineering Progress 44:287-292. 1948.

102. Wilkinson, J. A. Liquid hydrogen sulfide as a reaction medium. Chemical Reviews 8:237-250. 1931.

103. Wooster, N. and W. A. Wooster. Preparation of synthetic quartz. Nature 157:297. 1946.

104. Wortley, J. P. A. The corrosion resistance of titanium, zirconium and tantalum. Corrosion Prevention and Control 10(4):21-26. 1963.

105. Zahn, C. T. and J. B. Miles, Jr. The dielectric constant and electric moment of CO, COS, CS_2, and H_2S. Physical Review 32:497-504. 1928.

106. Zelvenskii, Ya. D., V. A. Shalygin and A. N. Bantysh. Preparation of organic compounds, tagged with radioactive sulfur and chlorine isotopes, by means of isotopic exchange. Radiokhimiia 1:683-686. 1959.

APPENDIX

APPENDIX

THE BALANCE CONDITIONS FOR THE IMPEDANCE BRIDGE

One method that may be used to obtain the balance conditions for the bridge is the loop current method of alternating current analysis. Because the exact impedance of the transformer is unknown, the usual method for evaluating the balance conditions based upon the values for each impedance in the circuit cannot be used. However, it is possible, because of the voltage dividing properties of the transformer, to replace the unknown impedances of the transformer with the known fractions of the impressed voltage as potential sources in the various branches. Figure 1A shows a schematic diagram of the actual bridge, while Figure 1B shows the bridge with the transformer impedances replaced by potential sources. Although the transformer has other voltage-ratio potentialities, the balance conditions are obtained only for the case in which there is an equal impedance on either side of the center tap.

Loop currents are indicated in Figure 1B by the arrows. The actual direction of the loop current is immaterial provided that each current is consistent with all the rest of the current loops.

Equations may be written for each loop by applying Kirchhoff's potential law to each loop. These equations are

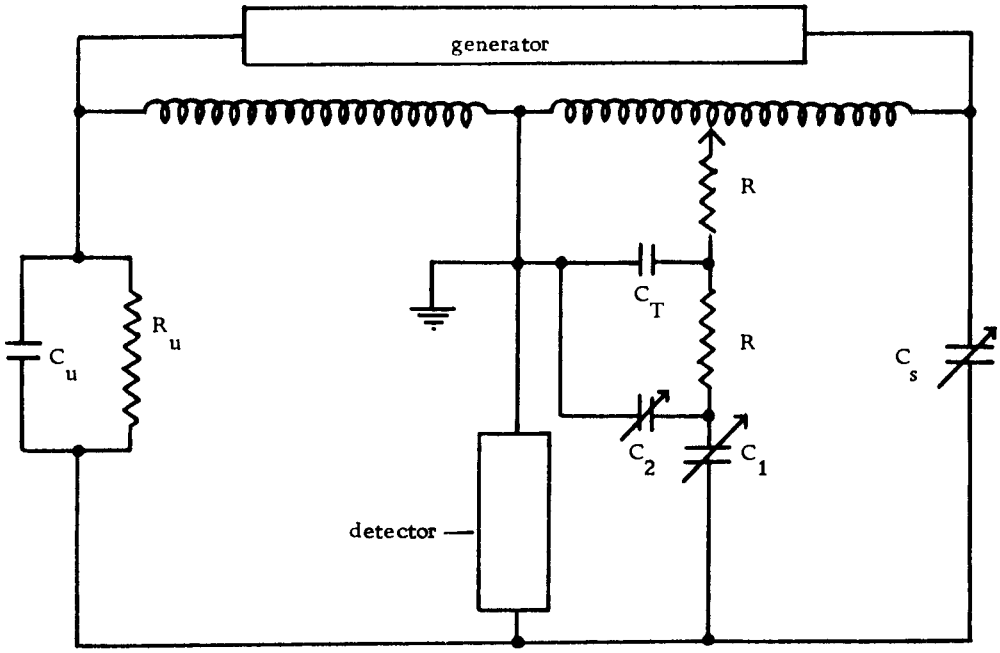

Figure 1A. Schematic diagram of the bridge.

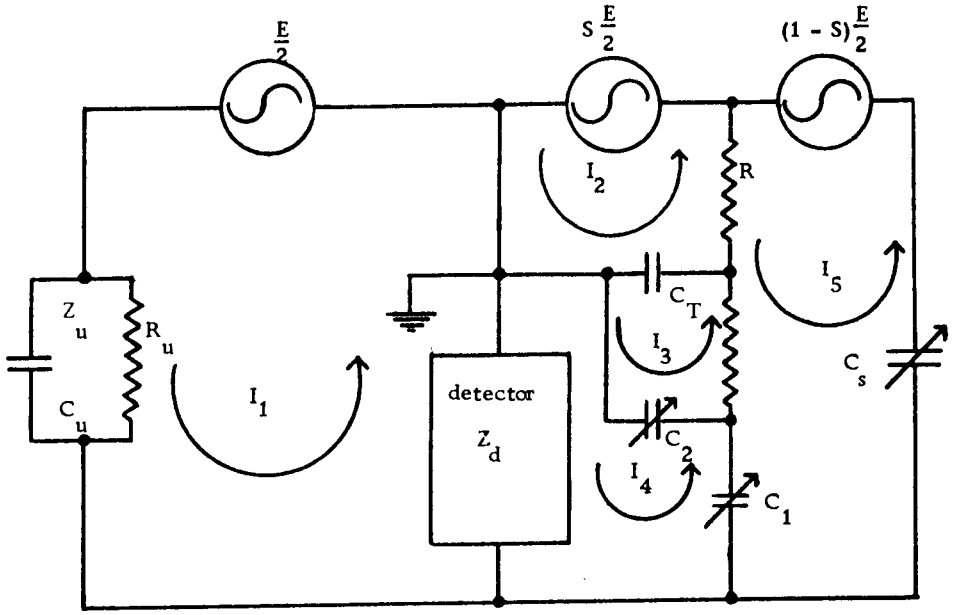

Figure 1B. Schematic diagram of the bridge showing the current loops used in the derivation of the balance conditions. Note that the unknown transformer impedances are replaced by known potential sources.

Loop 1: $Z_u I_1 + Z_D(I_1 - I_4) = \frac{E}{2}$ (1)

Loop 2: $\frac{-j}{\omega C_T}(I_2 - I_3) + R(I_2 - I_5) = S\frac{E}{2}$ (2)

Loop 3: $\frac{-j}{\omega C_T}(I_3 - I_2) + \frac{-j}{\omega C_2}(I_3 - I_4) + R(I_3 - I_5) = 0$ (3)

Loop 4: $\frac{-j}{\omega C_2}(I_4 - I_3) + Z_D(I_4 - I_1) + \frac{-j}{\omega C_1}(I_4 - I_5) = 0$ (4)

Loop 5: $R(I_5 - I_2) + R(I_5 - I_3) + \frac{-j}{\omega C_1}(I_5 - I_4) + \frac{-j}{\omega C_s} I_5 = (1 - S)\frac{E}{2}$. (5)

A final condition on the bridge is that there is no current flowing through the detector at balance. This can be expressed in terms of the loop currents of Figure 1B as

$$I_1 - I_4 = 0. \tag{6}$$

Equation (6) may be used to simplify equations (1) and (4) since only the conditions at balance are of interest to this development. This simplification has the added advantage of removing from consideration the impedance associated with the detector.

Equations (1) through (5) may be expressed in terms of the loop currents as

$$Z_u I_1 = \frac{E}{2} \tag{7}$$

$$(R - \frac{j}{\omega C_T}) I_2 + \frac{j}{\omega C_T} I_3 - RI_5 = S \frac{E}{2} \tag{8}$$

$$\frac{j}{\omega C_T} I_2 + (R - \frac{j}{\omega C_T} - \frac{j}{\omega C_2}) I_3 + \frac{j}{\omega C_2} I_4 - RI_5 = 0 \tag{9}$$

$$\frac{j}{\omega C_2} I_3 - (\frac{j}{\omega C_2} + \frac{j}{\omega C_1}) I_4 + \frac{j}{\omega C_1} I_5 = 0 \tag{10}$$

$$- RI_2 - RI_3 + \frac{j}{\omega C_1} I_4 + (2R - \frac{j}{\omega C_1} - \frac{j}{\omega C_s}) I_5 = (1 - S) \frac{E}{2}. \tag{11}$$

Because the currents I_1 and I_4 are the only currents in the expression for the condition of the bridge at balance, it is necessary to find an expression for these two currents in terms of the known parameters in order to derive the bridge balance conditions. A convenient method of finding these currents is the use of Cramer's rule for the solution of a set of simultaneous equations by determinants.

Equation (7) is the only equation that is a function of I_1. Because it expresses I_1 as a function of the parameters that all of the other currents will be expressed in, it need not be used to find the other currents.

Thus, I_4 is the only current that need be found by Cramer's rule. By Cramer's rule

$$I_4 = \frac{\begin{vmatrix} R - \frac{j}{\omega C_T} & \frac{j}{\omega C_T} & S\frac{E}{2} & -R \\ \frac{j}{\omega C_T} & R - \frac{j}{\omega C_T} - \frac{j}{\omega C_2} & 0 & -R \\ 0 & \frac{j}{\omega C_2} & 0 & \frac{j}{\omega C_1} \\ -R & -R & (1-S)\frac{E}{2} & 2R - \frac{j}{\omega C_1} - \frac{j}{\omega C_s} \end{vmatrix}}{\begin{vmatrix} R - \frac{j}{\omega C_T} & \frac{j}{\omega C_T} & 0 & -R \\ \frac{j}{\omega C_T} & R - \frac{j}{\omega C_T} - \frac{j}{\omega C_2} & \frac{j}{\omega C_2} & -R \\ 0 & \frac{j}{\omega C_2} & -\frac{j}{\omega C_2} - \frac{j}{\omega C_1} & \frac{j}{\omega C_1} \\ -R & -R & \frac{j}{\omega C_1} & 2R - \frac{j}{\omega C_1} - \frac{j}{\omega C_s} \end{vmatrix}} \quad (12)$$

The values of these two determinants can be found by expansion by minors and then simplified to

$$I_4 = \frac{\frac{js\frac{E}{2}}{\omega^3 C_2 C_s C_T} - \frac{E}{2}\left(\frac{2R}{\omega^2 C_1 C_T} + \frac{2R}{\omega^2 C_2 C_T} + \frac{R}{\omega^2 C_1 C_2}\right) + \frac{E}{2}j\left(\frac{R^2}{\omega C_1} + \frac{R^2}{\omega C_2} - \frac{1}{\omega^3 C_1 C_2 C_T}\right)}{-\frac{R^2}{\omega^2 C_1 C_s} - \frac{R^2}{\omega^2 C_2 C_s} + \frac{1}{\omega^4 C_1 C_2 C_s C_T} + j\left(\frac{2R}{\omega^3 C_1 C_s C_T} + \frac{2R}{\omega^3 C_2 C_s C_T} + \frac{R}{\omega^3 C_1 C_2 C_s}\right)} \quad (13)$$

Rationalization and collections of terms yields

$$I_4 = \frac{S\omega^2 C_1 R[2(C_1 + C_2) + C_T]\frac{E}{2}}{[1 - R^2\omega^2 C_T(C_1 + C_2)]^2 + R^2\omega^2[2(C_1 + C_2) + C_T]^2}$$

$$+ j\frac{E}{2}\left[\frac{\omega C_s[1 - R^2\omega^2 C_T(C_1 + C_2)]^2 + R^2\omega^2[2(C_1 + C_2) + C_T]^2}{[1 - R^2\omega^2 C_T(C_1 + C_2)]^2 + R^2\omega^2[2(C_1 + C_2) + C_T]^2}\right] \tag{14}$$

$$+ j\frac{E}{2}\left[\frac{S\omega C_1[1 - R^2\omega^2 C_T(C_1 + C_2)]}{[1 - R^2\omega^2 C_T(C_1 + C_2)]^2 + R^2\omega^2[2(C_1 + C_2) + C_T]^2}\right]$$

If Z_u is assumed to be a parallel combination of a resistor and a capacitor, then from equation (7)

$$I_1 = (\frac{E}{2})(\frac{1}{Z_u}) = \frac{E}{2}(\frac{1}{R} + j\omega C_u). \tag{15}$$

Setting I_1 equal to I_4 and dividing through by $\frac{E}{2}$ yields the balance condition

$$\frac{1}{R} + j\omega C_u = \frac{S\omega^2 C_1 R[2(C_1 + C_2) + C_T]}{[1 - R^2\omega^2 C_T(C_1 + C_2)]^2 + R^2\omega^2[2(C_1 + C_2) + C_T]^2} \tag{16}$$

$$+ j\omega C_s + \frac{jS\omega C_1[1 - R^2\omega^2 C_T(C_1 + C_2)]}{[1 - R^2\omega^2 C_T(C_1 + C_2)]^2 + R^2\omega^2[2(C_1 + C_2) + C_T]^2}$$

In order for the equality to be true, the real parts of the equation must be equal and the imaginary parts must be equal. Thus, the

two balance conditions are

$$\frac{1}{R_u} = \frac{S\omega^2 C_1 R[2(C_1 + C_2) + C_T]}{[1 - R^2\omega^2 C_T(C_1 + C_2)]^2 + R^2\omega^2[2(C_1 + C_2) + C_T]^2} \tag{17}$$

$$C_u = C_s + \frac{SC_1[1 - R^2\omega^2 C_T(C_1 + C_2)]}{[1 - R^2\omega^2 C_T(C_1 + C_2)]^2 + R^2\omega^2[2(C_1 + C_2) + C_T]^2} \tag{18}$$

From equations (17) and (18) it can be seen that C_2 appears only in the balance conditions as a sum with C_1. Thus, it is necessary to know which value of C_1 is switched into the measuring circuit only for the multiplication factor. Only S, C_1, and C_s are variable and they are used to determine the balance conditions at a constant frequency.

If the values for R, $C_1 + C_2$, C_T and ω are substituted into equations (17) and (18) the balance conditions when $R = 5.00 \times 10^4\ \Omega$, $C_1 + C_2 = 1.111 \times 10^{-7}$ f, $C_T = 1.02 \times 10^{-10}$ f, and $\omega = 6.283 \times 10^3$ radians/second are

$$R_u = \frac{1.124 \times 10^{10}}{SC_1} \tag{19}$$

$$C_u = C_s - 2.440 \times 10^{-5}\, SC_1 \tag{20}$$

where C_1, C_u, and C_s in equations (19) and (20) have the units of picofarads and R_u has the unit of ohms. S is the fraction read

directly from the transformer.

By changing the value of C_1 by a special switching circuit it is possible to change the decade over which R_u is being measured. For all but one value of C_1 the second term in equation (20) is negligible and if S is less than 10^{-2} for the largest value of C_1, then the second term is negligible also.

The bridge is independent of the voltage impressed across the transformer as far as the balance conditions are concerned. However, due to Joule heating in some of the components, there is a definite voltage dependence.

There is also a frequency dependence inherent in the balance conditions. It is particularly pronounced at high frequencies. Around 1000 cycles per second, a small change in the frequency has little effect.